The Effect of Sea Level Rise on the Operations of the MOSE Barrier in Venice

An Analysis Using the Rosner and an Adapted Framework for Adaptation

Robin Oomens

Hydraulic Structures and Flood Risk
Delft University of Technology
The Netherlands

6 July 2023

Preface

This report is the Master's thesis in Civil Engineering by Robin Oomens. The thesis was written at the Delft University of Technology (TU Delft) and Deltares, a leading research institute for water and soil.

I would like to express my gratitude and thanks to Dr. Elisa Ragno, Dr. ir. Ferdinand Diermanse, and Dr. ir. Alessandro Antonini for their invaluable help during the thesis. They provided useful advice during our frequent meetings and were always available to answer questions and discuss ideas.
My time at Deltares was very enjoyable, and I would like to thank my colleagues for making me feel like a part of the team from the beginning. I always looked forward to going to the office.
I would also like to thank my family and friends for their mental support during the year. They helped me stay relaxed, which allowed me to enjoy the thesis from beginning to end.

Delft, June 2023
Robin Oomens

Abstract

Coastal cities and communities are threatened by Sea Level Rise (SLR). Designing adaptations to protect against the rising sea requires a novel approach. With changing conditions, a broader approach considering multiple climate scenarios is required. A city facing an increasing threat from sea levels is Venice, one of the UNESCO world heritage sites. To protect the historic Italian city against floods, the MOSE barrier was constructed by the Italian government.
In 2020, the MOSE barrier was used for the first time. The mobile barrier closes when high water levels are foreseen in the city, preventing floods. Due to SLR, it is anticipated that the barrier will have to close more in the future, leading to questions about the functionality of the barrier when water levels rise. This might require adaptations or alternatives for the MOSE barrier but assessing these options is challenging due to the uncertain sea level future scenarios.

The main objective of this thesis is to explore the potential of the framework proposed by Rosner et al. (2014) to evaluate the economic feasibility of an adaptation strategy against sea level rise in the city of Venice.
This framework assesses the potential regrets (monetary losses) on the decision to invest in an adaptation strategy accounting for errors in the evaluation of the level of sea level in the future. The framework incorporates trends based on historical sea level observations, including the uncertainties around these trends.

First, different methods of calculating design values under varying conditions are compared. This comparison is focused on different non-stationary Extreme Value Analysis (EVA) distributions. Due to SLR, a stationary and thus constant situation is not valid for Venice. This leads to the choice of the Rosner framework since it evaluates the feasibility of adaptations under varying conditions.

The regret of adapting or not adapting to a trend or SLR scenario is calculated from the damages associated with that scenario and the costs of the adaptation. The damages are computed by calculating the number of MOSE barrier closures for the different scenarios and multiplying this number by the costs that are related to a closure event. The adaptation that was chosen for evaluation is raising the entire city by 30 cm. This is accomplished by injecting seawater into a deep soil layer underneath the city.

The analyses resulted in smaller expected regrets when the choice is made to adapt. This was the case for all SLR scenarios, the difference between the adapt and not adapt regrets is larger for higher levels of SLR. This includes a higher SLR scenario due to a trend with large uncertainty. This is under the assumption that the adaptation, lifting the city, will work, the technical feasibility of this method was not investigated in this thesis.
A more precise calculation of the number of closures is advised. However, it is evident that adaptations are required to keep the MOSE barrier functional and the city of Venice safe from high waters. Raising the city will allow more time to evaluate which alternative to the MOSE barrier is best suited for the future.

Contents

1 Introduction

1.1 Trends in extremes

The Intergovernmental Panel on Climate Change (IPCC) projects that sea-level rise (SLR) will increase in the coming decades. The main processes causing SLR are thermal expansion of the oceans and melting of the land-based ice (Glavovic et al., 2022). Thermal expansion means that water increases in volume as it heats up. Even if the global mean temperature stabilizes, sea levels will continue to rise since the main contributors to sea-level rise (oceans, glaciers, and ice sheets) respond to climate change on timescales ranging from decades to millennia (Nauels et al., 2019). Even if global temperatures will stabilise, the high heat capacity of the water will result in a continuation of thermal expansion. This highlights the need to investigate adaptation strategies against sea level rise to protect cities and communities near the sea.

To choose the right adaptation strategy, water levels that could occur in the future need to be quantified. Analysing extreme events from the past can give an indication of water levels that can be expected in the future.

To develop an adaptation strategy such as coastal protection systems, a characterisation of the sea level in its extreme conditions need to be assessed. To assess the probabilities of extreme events, Extreme Value Analysis (EVA) is used. Specifically, EVA allows estimating from past observations the statistical characteristics of the event of interest, e.g., extreme sea level. Then, from these characteristics, inference can be made on events with an extremely low probability of occurrence, often outside of the range of observation, which will be used for the design of infrastructures (Coles, 2001). For example, EVA is used to determine how high a dike must be to prevent floods expected from a storm that is expected to occur, on average, once in a thousand years. This value is not known from measurements since the data has not been available for 1000 years (Coles and Pericchi, 2006), i.e., return period. Other applications include predicting extreme wind pressures when designing wind turbines (Gumbel et al., 2009), estimating extreme wave conditions for offshore structures (Melchers, 2010), and predicting extreme conditions for water management applications (Katz et al., 2002).

To infer events from historical observations requires that EVA be conducted under the stationary assumption that the observations are independent and identically distributed (iid). This assumption means that the extreme events should not contain trends (Coles, 2001). However, water level observations present a statistically significant trend over time, because of the rising global temperature. This implies that the statistical characteristics of extremes, and so the distribution modelling such extremes, are not constant over time, and traditional approaches to inference are not possible. (Milly et al., 2008) argues that stationarity is dead because the assumption that natural systems fluctuate in an unchanging envelope of variability is not valid anymore. This is caused by the changing climate and human interference with natural systems. Hence, methods to conduct EVA under the nonstationary assumption should be explored.
One option is to remove the trend from the extremes to transform the observations in iid variables and the EVA distribution of choice is fitted on the detrended extremes. After statistical inferences are made from iid variables, the expected effect of the trend can be added.
Another option is to model the characteristics of the distributions, i.e., the parameters of the distribution, as a function of time. This results in a distribution with a higher number of parameters to be estimated from the observations. This option will be referred to as NEVA approach hereafter. The extremes do not have the trend removed for this analysis as the distribution has parameters that should account for the trend.
Sea water level data is likely to contain a trend, the data is not stationary, and a non-stationary approach is the model option of choice. Different NEVA model variations can be applied and compared. The different models used in this thesis are introduced in Section 2.1.

When a NEVA distribution is used for estimating extremes in the future, it is important to know why the trend is there. The NEVA will assume the trend to continue, if the trend is caused by a temporal event, for example human activity induced land-subsidence, it is not correct to assume this trend continuing.
(Luke et al., 2017) has argued that a stationary method with trend removal is nearly always better than a non-stationary method. In an example, they use half of a dataset that appears to be having a trend. When a stationary analysis is applied, the results match up better with the measurements than the non-stationary method, which continues this trend, while in the measured data the trend does not continue in the future.

In stationary analysis the design value that is linked to a return period is constant. The design values resulting from non-stationary analysis are not constant over time. As mentioned, the statistical properties of the EVA distribution change over time and so does the design value. This leads to an extra choice for determining the design value for your protective measure: which year in the future is used for calculating the design value? This reference year could for example be the last year of the design lifetime of the structure so that it, in theory, is fulfilling the safety standards throughout its lifetime. It will be over-designed in all years prior to that reference year.

1.2 Risk-based decision making

Design choices are often made using a decision tree based on cost-benefit analysis. In this situation, the cost-benefit analysis yields a score for every decision path after which the highest-scoring adaptation is chosen. Design values used for the different decision paths are taken as a constant value if the observations are treated as stationary. If the data is non-stationary, these design values will not be constant over time. Non-stationarity in the observations is identified using a trend test and when there is no significant trend found, a stationary situation is assumed for all different adaptation options (Rosner et al., 2014). Statistical tests might fail to capture a trend due to the quantity and quality of the observations or to the strength of the trend itself. In hypothesis testing, the null hypothesis can be rejected in favour of an alternative hypothesis is there is enough evidence to do so. The rejected hypothesis is not considered in the decision process hereafter. To overcome the limitations of hypothesis tests, especially when a trend is expected due to prior knowledge of physical processes involved, (Rosner et al., 2014) proposed a framework (hereafter referred to as the Rosner framework) to account for errors in trend detection when developing an adaptation strategy. The proposed framework introduces the concept of *regret* to quantify in monetary terms the consequences of a false result of a hypothesis test.

The Rosner framework introduces a novel approach in risk management and cost-benefit analysis since it accounts for errors in the results of a hypothesis test. In the context of adaptation to a changing climate, this framework provides insight into the effects of such an error, which can be significant and can result in loss of lives and large damages due to unpreparedness. This framework can inform policy makers on the risks associated with opting for a particular adaptation strategy.

In this study, the framework developed by (Rosner et al., 2014) is applied to the city of Venice. Venice has experienced SLR for as long as measurements have been taken, and measures must be taken to prevent future damages. The city is unique in the fact that it consists of many important historical buildings that need protecting. The location inside the lagoon leads to high waters inside the city on a frequent basis. Projections for the next 100 years predict even faster SLR for Venice. This makes Venice an interesting case study for applying the Rosner framework.

1.3 Case study: Venice

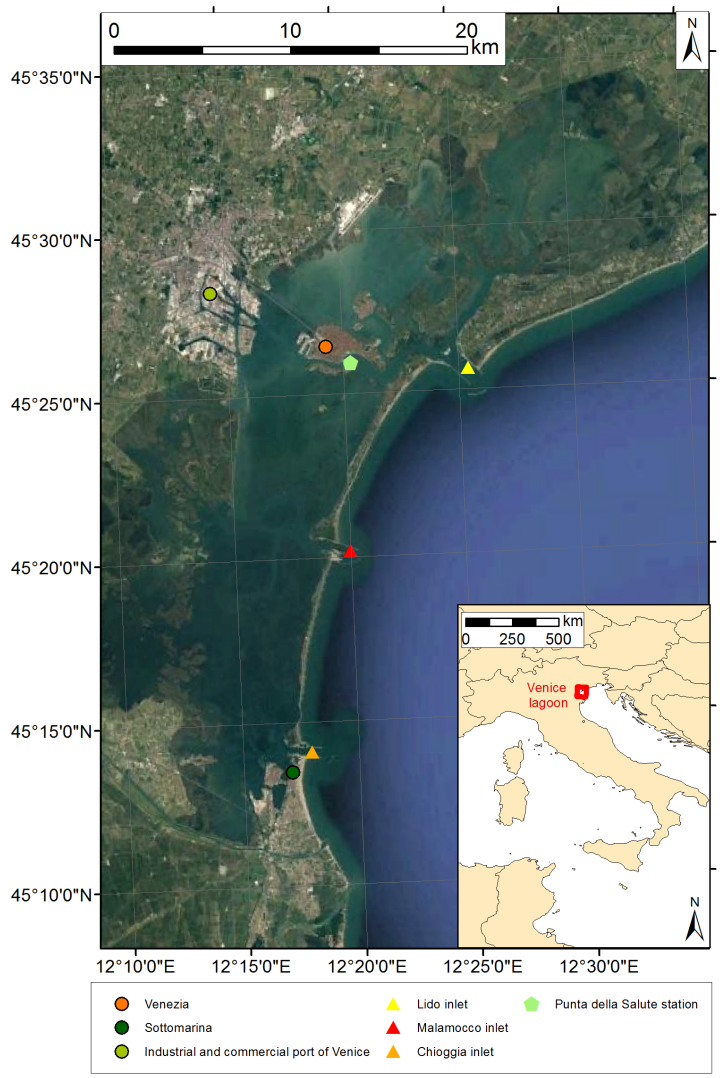

Figure 1.1: Overview of the Venice lagoon with the three inlets (Cavallaro et al., 2017).

Venice, a city of islands, canals, and bridges, has a complex relationship with floods. Located in the Venetian Lagoon along the Adriatic Sea, the city has a long history of flooding caused by a combination of factors, including high tides, storm surges, and precipitation. Coping with floods is a constant challenge posed by the city's unique location and historical status. The city and the lagoon are a UNESCO world heritage site that needs protecting. The Venice Lagoon, which is one of the most important ecosystems in Europe, covers a total surface area of around 550 km^2. It is in the northern part of the Adriatic Sea, which is part of the Mediterranean basin, and is connected to the sea by three inlets: Lido, Malamocco, and Chioggia. An overview of the lagoon is displayed in Figure 1.1.

The tide and storm surge play a significant role in flooding in Venice. High tide events occur frequently in the city, primarily in autumn and winter. The Scirocco winds blow over the Adriatic Sea and creates wave set-up towards the northern parts of the Sea causing higher water levels in the Venice lagoon.

Due to the shallowness of both the Adriatic Sea and the lagoon, wind set-up effects are larger than in deeper seas like the Mediterranean Sea, resulting in significant water level variations inside the lagoon. When set-up and high tide coincide, the water levels in Venice lead to floods.

Land subsidence, which refers to the sinking of the land surface, is a significant contributor to the vulnerability of Venice. The city sits on a layer of soft sediment, including clay and silt, which is gradually compacting under its weight, causing the ground level to sink. Moreover, land subsidence is exacerbated by groundwater extraction for industrial and domestic purposes. (Zanchettin et al., 2021) found that land subsidence is an important part of relative sea-level rise (RSL) in Venice. The amounts of vertical land movement (VLM) differ for various decades of data, and the VLM should be removed from the sea-level data to show the rise in sea level that can be projected into the future.

As a result of land subsidence and high-water levels, Venice has implemented several measures over the centuries to mitigate flooding, including the construction of raised walkways and the installation of pumps to remove water. In November 1966, Venice was hit by an unprecedented flood that submerged much of the city under more than 1.5 meters of water. This flood damaged countless buildings, including many historic landmarks and artworks. The water levels are expressed as height above the reference level for the gauge station: Zero Mareografico Punta della Salute (ZMPS). The most recent flooding event occurred in November 2019 where the combination of high tides and fierce winds let the water up to 187 cm + ZMPS. The floodwaters inundated a large part of Venice's most iconic locations, including St. Mark's Square and the Doge's Palace, prompting renewed calls for action to protect the city from future flooding.

Discussions on flood prevention measures have been ongoing for a long time, the plans to build a storm surge barrier started after the 1966 flood which reached water levels of 194 cm + ZMPS (Cavallaro et al., 2017). After being approved in the early 2000s, the city has built the Experimental Electromechanical Module (MOSE) to prevent flooding. The next section will explain the workings of the barrier.

1.4 The MOSE barrier system

The MOSE barrier's purpose is to protect Venice from storm surges. It closes when high surge levels are forecast and remains open during normal conditions. The barrier is situated across the three lagoon's inlets, namely Lido, Malamocco, and Chioggia. It comprises gates that are located on the inlet bed, allowing water and ships to pass over them. This is important for maintaining efficient ship traffic and the ecological balance of the lagoon. The barrier enables salt water from the Adriatic Sea to enter and exit the lagoon with the tides.

When the barrier is closed, the tidal flow is temporarily halted, which can threaten the ecological system of the lagoon. To facilitate shipping in and out of Venice, locks have been installed at each inlet, with the Malamocco lock specifically designed to accommodate larger vessels and provide access to the port. Smaller pleasure and fishing boats can pass through the locks at the other two inlets. An overview of the Venice lagoon with its three inlets can be seen in Figure 1.1, which shows the distribution of the 78 gates that make up the MOSE barrier. The Lido inlet features an artificial island in the middle, reducing the overall span of the barrier. The northern and southern barriers each comprise 21 and 20 gates, respectively, while the Malamocco and Chioggia barriers have 19 and 18 gates. A closer look at each inlet can be seen in Figure 1.2. (Cavallaro et al., 2017)

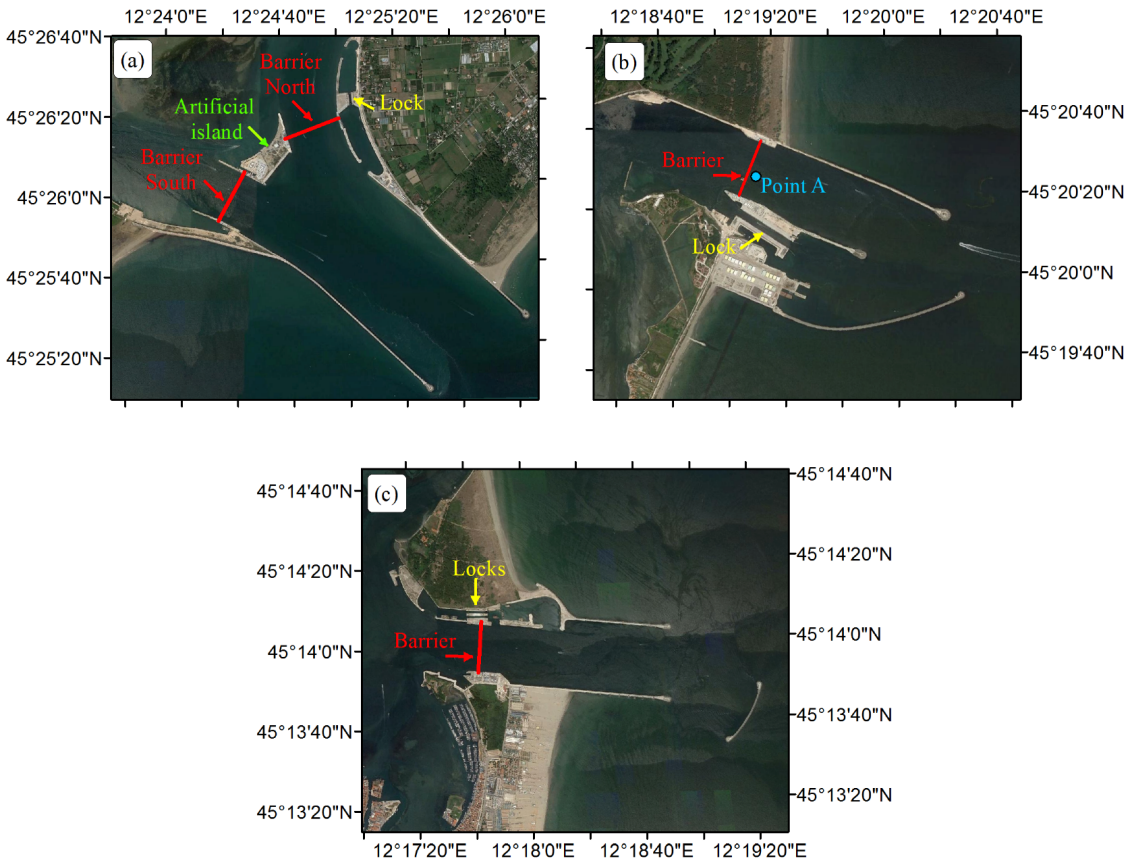

Figure 1.2: Barrier and lock location per inlet: a) Lido, b) Malamocco and c) Chioggia (Cavallaro et al., 2017).

The gates lie in caissons when they are not in use. This way, they are not visible, which minimizes interference with the landscape (Kolbus, 2019). When the gates must be raised, they are filled with air, which causes them to tilt up. The gates are 20-30 meters long and 20 meters wide (Buckley, 2022). They can withstand a maximum water level of 3 meters above the mean sea level. A cross-view of a gate is shown in Figure 1.3. The caisson (3) is located entirely within the seabed. Uplift is prevented through the foundation (5), and the gate is in the open position (1). When in this position, the gate is lying down on the caisson to allow water to flow freely over the entire structure. The hinge (2) can be reached through the maintenance chamber (4). This design conforms to the demand that the barrier is not visible from above the water level. The lagoon is located on the left side of the figure, and the Adriatic Sea is on the right side.

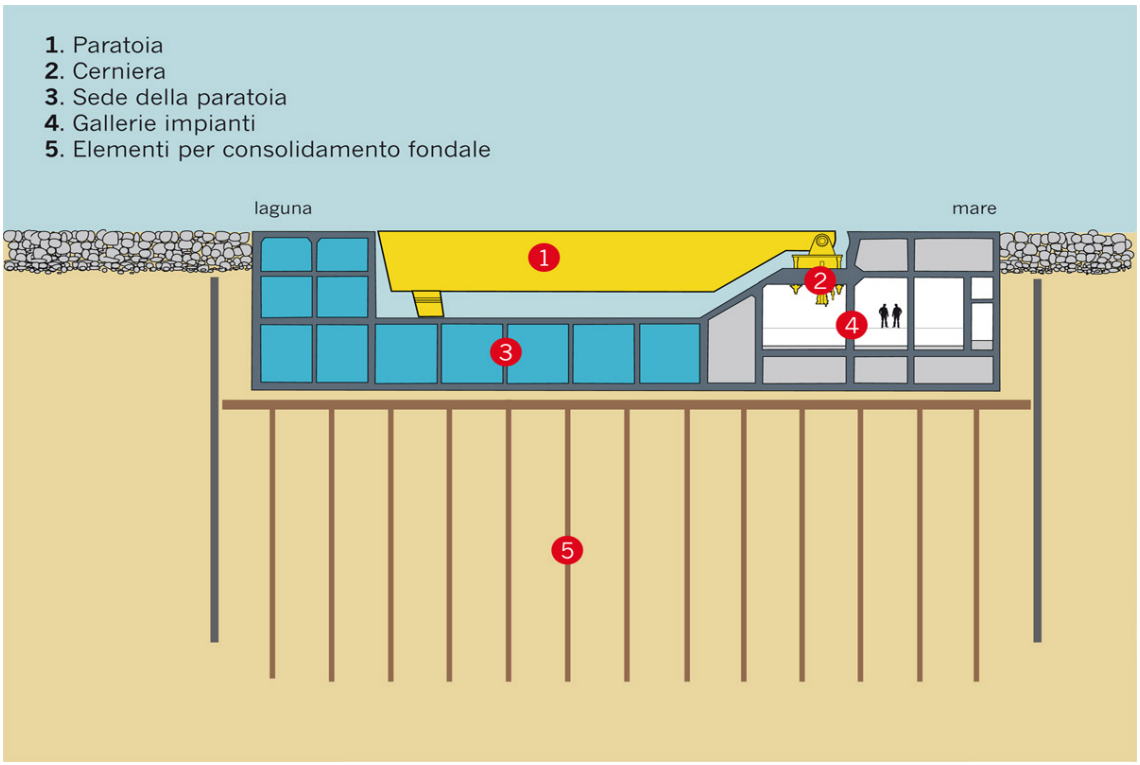

Figure 1.3: Cross-view of the barrier gate (Kolbus, 2019)

The gates close when the water level in the measuring station in Venice is forecast to exceed 110 cm + ZMPS. The closure is based on a forecast. This forecast system will not be used in this thesis because the technique used to calculate number of MOSE barrier closures is based on water level data from the past only. An explanation of the closure system is provided in Appendix A.

The closure is performed for all barriers in all inlets. The current program does not allow for partial closure. The water level is measured in the city, and the projection for the closure level is also provided for the city. However, the water level inside the lagoon can vary up to 60 cm + ZMPS. Opening the barrier is done if the water level on the lagoon side of all barriers is lower than the water level at the seaside, and the predicted water level should not exceed the threshold again within four hours (Umgiesser and Matticchio, 2006).

The average duration of barrier closure is expected to be around four to five hours (MOSEVenezia, 2022). This time includes the opening and closing of the gates themselves. However, the duration of surges is expected to increase in the future (Jordà et al., 2011), which could lead to longer closure times in the future.

If the frequency of closures increases, a solution could be to increase the safeguarding threshold. In (Fontinia et al., 2010), the costs and benefits are evaluated for different scenarios. The scenarios consist of a barrier closing height combined with a safeguard level. This safeguard level is considered due to the uncertainty in predicting the water level to close the barrier, as discussed earlier. These scenarios are then evaluated for various levels of sea-level rise, leading to frequencies of tides that determine the frequency of closure and benefits. Benefits are the avoided costs of repairs to buildings, taking care of children and the elderly who must stay indoors and missed tourist spending. The avoided damages are large compared to the economic losses of the harbour, leading to the conclusion that increasing the threshold for closure is less beneficial. This is also valid for sea-level rise, although the difference

between the benefits for the different thresholds decreases. Increasing the threshold is not a viable option, as the benefits decrease because fewer costs are being avoided, while costs increase due to higher damages from floods up to the higher threshold.

1.5 Future of MOSE

According to a study by (Umgiesser, 2020), it is inevitable that the MOSE barrier will have to close more frequently in the future. If sea-level rise reaches 60 cm + ZMPS, the barrier will have to be closed year-round. This is caused by the high tides exceeding the threshold for closure of 110 cm + ZMPS.

If the barrier must be closed all the time, it will no longer function as a barrier but more like a permanent flood wall. The barrier was not designed for this purpose, and therefore other adaptation measures are being considered. The IPCC report (Glavovic et al., 2022) discusses several types of adaptation strategies that cities can use to cope with the effects of SLR.

The first type of measure is structural measures, which are usually built from concrete or steel and include storm surge barriers and weirs. The MOSE barrier is an example of a structural measure. They are built to protect existing land so that the city does not need to move. Structural measures are highly effective in the short term, but they bring the risk of failure and should therefore be combined with other measures such as spatial planning or warning systems.

Nature-based measures have a similar function to structural measures as they protect the city from the water without the need for the city to move or adapt otherwise. The difference is in the materials used and usually space required. To implement nature-based solutions, space must be available to raise dunes and dikes. When dunes or dikes are raised, their footprint increases as well due to their slopes. They, therefore, require more space than a structural solution with the same height. The advantage is lower maintenance and failure probabilities since the system interacts with the sea and sand naturally available. Nature-based engineering is easier adaptable, but sand availability can become a problem in the future. Nature-based measures are remarkably effective and sustainable, but quantifying the protection can be difficult, which complicates calculations.

Accommodation of the built environment is beneficial for small sea-level rise. It will provide protection when hard solutions are not yet completed or can be an alternative when hard solutions are not possible due to space or financial limitations. It is limited to small sea-level rise and can be an issue in the historic city of Venice.

Advance strategy is suitable for large sea-level rise and can offer great benefits. In this strategy, land is created in front of the coast to push back the coastline. It is expensive and can have a negative impact on the present ecosystem. It also requires a lot of materials.

The retreat strategy requires the people of the city to move away from the coast. The retreat strategy is highly effective and is becoming increasingly inevitable. However, it is a drastic measure, both culturally and financially. Land must be available as well. (Glavovic et al., 2022)

The last strategy would be the ultimate strategy to save the inhabitants, as it would mean that the historic city of Venice would be abandoned.

Venice is chosen for implementing the Rosner framework since SLR is an issue the city has faced for a long time and will continue and increase in the future. An adaptation is built in the form of MOSE, but novel solutions are needed if SLR increases. The city's unique status as UNESCO world heritage requires a solution for protecting its historical buildings. The lagoon itself is protected as well creating a conflict in adaptation measures since most adaptations to protect the historical city will harm the lagoons ecosystem.

This leads to the main research question on how to implement the Rosner framework for Venice. Within the framework the effects of SLR on the operations of the MOSE barrier are determined and include the frequency of closures for different SLR scenarios as well as costs related to these closures. SLR scenarios are based on historic trends and on projections for different climate scenarios. Expected regrets from the framework are used to compare different strategies. Different methods of (N)EVA are applied to the water level maxima and compared based on goodness of fit scores.

1.6 Research Question

1.6.1 Main research question

How to assess adaptation measures for sea-level rise in Venice?

1.6.2 Sub questions

- How do stationary and non-stationary extreme value analyses results compare when applied to historical water level data in Venice?
- How does sea-level rise affect the operation of the existing MOSE barrier?
  - How many times does the barrier have to close in the future due to sea-level rise?
    - What is the effect of the trend in historical mean sea-level rise on the number of closures per year?
    - What is the effect of a trend in maximum sea-levels after correcting them for mean sea-level rise on the number of closures per year?
    - What is the effect of future projections on the number of closures per year?
  - Which costs are related to the more frequent and longer closures?
  - Is the MOSE barrier the right adaptation if sea-level rise increases?
    - Which alternatives are there?
- How can the (Rosner et al., 2014) framework be applied to the MOSE barrier?
  - How large are the damages for the different scenarios?
  - What are the regrets for the different scenarios?
- What conclusions can be drawn from the framework?

Different EVA techniques will be investigated to compare their performance on historical SLR data in Venice. The effects of different SLR scenarios on the number of closures of the MOSE will be addressed through counting the number of closures in the past if mean sea level would be at the level of the SLR scenario in question. Different processes contributing to the cost of a closure event are investigated after which the Rosner framework is used to compare regrets for different adaptation scenarios.

1.7 Thesis Outline

Section 2 elaborates on different methods and techniques used for this thesis, previous applications, and the theory behind them. The results on extreme water levels in Venice, including the comparison between different EVA techniques is shown in Section 3. Section 4 compares the number of expected closures for different SLR scenarios. These results are then integrated into the Rosner framework and an adapted variant for a risk-based approach in Section 5. The results and methods used are discussed in Section 6. The research questions are answered in Section 7 and recommendations are provided in Section 8.

2 Literature study

In this chapter, methods and tools used in this thesis are described. The definition and use of different extreme value analysis methods are discussed in Section 2.1. Background on the (Rosner et al., 2014) framework is given in Section 2.2, the damage model used for computing the damages in the city of Venice is introduced in Section 2.3. Costs of a closure event are described in Section 2.4. The adaptation to be assessed is introduced in Section 2.5. The SLR scenarios used in the study are described in Section 2.6.

2.1 Extreme value analysis

As mentioned in Section 1.1, Extreme Value Analysis (EVA) distributions are used to estimate probabilities of extreme events that have never been recorded. This is used for design purposes; a few examples were given in Section 1.1. The EVA distribution is used to model the extremes observed after which the distribution can be used to infer return values for return periods beyond the length of the dataset. To conduct an EVA on the water level data of Venice, it is important to determine which types of EVA distributions are commonly used and what their advantages and drawbacks are.

First, extreme values need to be obtained. To conduct any EVA, the extremes selected must be independent (Coles, 2001). This means the extreme events need to be unique and should not be correlated to one another.

The Fisher-Tippet-Gnedenko theorem states that maxima in any form, if they are independent and identically distributed, will converge into one of three distributions: Gumbel, Fréchet or Weibull (Coles, 2001). From this theorem, EVA distributions were computed that can be used for several types of maxima. The two distributions that are commonly used for EVA are the Generalized Extreme Value distribution (GEV) and the Generalized Pareto distribution (GP), which use different extreme values obtained by different methods.
Non-stationary Extreme Value Analysis (NEVA) distributions change over time. They are applied to maxima that are not detrended and add time varying parameter(s) in the distribution. Non-stationary methods have been applied for the design of coastal protection structures (Haigh et al., 2014), river flood defences (Renard et al., 2016) and bridges (Li et al., 2020) where a changing climate was the reason to choose for a non-stationary EVA approach.

Methods for stationary analysis are described in Section 2.1.1 and Section 2.1.2 where the GEV and GP are discussed, respectively. For the GEV method, the non-stationary application is elaborated on in Section 2.1.3. An alternative non-stationary method called the Transformed Stationary method (TS) is introduced in Section 2.1.4.

2.1.1 Stationary GEV

First, the GEV distribution is explained. The GEV distribution is used to model extremes sampled via the block maxima approach. One maximum is the maximum value within a predefined temporal window, i.e., block. Usually, the block size is set to one year. By obtaining annual maxima (AM), seasonal effects that yield larger extremes during certain months of the year are removed. The extreme events are considered independent because of the long time between them. An underlying trend can still be present leading to the extremes to not be identically distributed. If this is the case, the trend must be removed first before the GEV distribution is used to model the extremes. The cumulative density function of the GEV distribution is described by:

$$G(z) = exp\left(-\left[1+\xi\left(\frac{z-\mu}{\sigma}\right)\right]^{-1/\xi}\right) \tag{2.1}$$

Where:
μ = location parameter
ξ = shape parameter
σ = scale parameter
z = annual maxima

The model has three parameters: the location, scale, and shape parameter. The location parameter describes the shift of the function. When this parameter is changed, the entire function will shift left or right while the shape of the function remains the same. If all data points are raised by the same value, the location parameter will also increase with this value while the scale and shape parameter do not change. The scale parameter describes the spread of the distribution. For larger values, the distribution will be more spread out. The shape parameter influences the tail of the distribution. The sub-families of the GEV distribution, Gumbel, Fréchet and Weibull, have different tail behaviours and the shape factors $\xi = 0$, $\xi > 0$ and $\xi < 0$ correspond, respectively, to these sub-families. The Gumbel distribution has no upper or lower limit, the Fréchet distribution has a lower limit but no upper limit while the Weibull distribution has an upper limit but no lower limit.

The Maximum Likelihood Estimation method is one way of estimating the parameters of the GEV distribution. Here, the log-likelihood is used since it has some benefits compared to the standard likelihood function. The likelihood function involves multiplication of many numbers, which often leads to exceedingly small values that require many decimal places. When converted to a log-likelihood function, it becomes a summation function, which is easier for numerical tools to maximize (Coles, 2001).

$$l(\mu, \sigma, \xi) = -m \cdot log(\sigma) - (1 + 1/\xi) \sum_{i=1}^{m} log \left[1 + \xi \left(\frac{z_i - \mu}{\sigma}\right)\right] - \sum_{i=1}^{m} \left[1 + \xi \left(\frac{z_i - \mu}{\sigma}\right)\right]^{-1/\xi} \tag{2.2}$$

Where:
m = number of extremes
z_i = value of the extreme

Confidence ranges of the fitted parameters are calculated from the standard errors of that parameter. These are obtained from the variance-covariance matrix. The covariance between the different parameters, for example X and Y, is calculated as:

$$Cov(X, Y) = \int_{-\infty}^{\infty} \int_{-\infty}^{\infty} [x - E(X)] [y - E(Y)] f_{X,Y}(x, y) dx dy \tag{2.3}$$

Where:
$E(X), E(Y)$ = expectation of X and or Y, this is the mean value
$f_{X,Y}$ = joint density function

Once the parameters are known, the model can be used to estimate return periods beyond the length of the dataset. It can also assess return values for return periods within the length of the dataset, although this is usually not relevant for design purposes. The downside of the AM method is that its results are sensitive to the number of extremes it is modelled on. Information on longer return periods is weaker if less extreme points are available (Coles, 2001). For AM, only one extreme per year is used. This means that many available data points are not used. An alternative is the Peak Over Threshold (POT) method.

2.1.2 Stationary GP

The GP distribution is fitted to extremes obtained through the POT method, which selects peaks that exceed a certain threshold. This allows for more extreme data points per year. The threshold needs to be selected carefully, as it influences the results from the GP. One way to select a threshold for the POT method is by observing the mean residual life plot, in which the mean excesses are plotted as a function of the selected threshold. If linear behaviour, increase in threshold leads to increase in mean excess, is observed from a certain threshold in the plot, that threshold may be well suited. Another method is assessing the stability of parameters. The shape and modified scale parameter are plotted for the different thresholds. If the parameters stabilise, the threshold is suited for the POT method (Coles, 2001). To include as many peaks as possible, the lowest threshold value from which linear behaviour is observed or the parameters stabilise, should be chosen. To ensure that the extreme events are independent, there should be a minimum spacing between the peaks to ensure that they are individual events. The cumulative density distribution of the GP is:

$$H(y) = 1 - \left(1 + \frac{\xi y}{\sigma + \xi\,(u - \mu)}\right)^{-1/\xi} \tag{2.4}$$

Where:
$y = z - u$ = excess over threshold
z = peak
u = threshold
μ = location parameter
σ = scale parameter
ξ = shape parameter

The parameters are estimated similarly as with the GEV model. The log-likelihood of the GP distribution is:

$$l(\sigma, \xi) = -k \cdot log(\sigma) - (1 + 1/\xi) \sum_{i=1}^{k} log\,(1 + \xi y_i/\sigma) \tag{2.5}$$

Where:
y = excess over threshold
σ = scale parameter
ξ = shape parameter
k = number of excesses of threshold

When computing return periods, it is important to note that the number of extremes is not necessarily equal to the number of years, as is the case when using AM. Therefore, a computation is needed to obtain return periods per year. The N year return level can be computed by: (Coles, 2001)

$$z_N = u + \frac{\sigma}{\xi}\left[(N n_y)^{\xi} - 1\right] \tag{2.6}$$

Where:
z_N = N year return level
n_y = number of observations per year
u = threshold
σ = scale parameter
ξ = shape parameter

2.1.3 Non-stationary GEV

For the non-stationary analysis, the GEV distribution parameter(s) are modified to include a varying component. The distribution is therefore changing for every time step and thus not stationary anymore. All three parameters can be modified (location, scale, and shape) and the varying component can be time or any other covariate, for example temperature or CO_2. Maximizing the log-likelihood estimates the parameters. The time varying modification of the parameters can be linear, quadratic, or even higher order, depending on the parameter. However, adding more parameters makes the model more complex, which is undesirable for the principle of parsimony. To determine if the extra information coming from more parameters is worth the increased complexity, the Akaike Information Criterion (AIC) is calculated. The AIC value is used to compare the maximum likelihoods from different parameter fits, it penalizes the use of more parameters (Coles, 2001). Its formula is given as:

$$AIC = 2(K) - 2(L)$$

Where:
K = Number of independent parameters
L = Log-likelihood estimate

Lower values of AIC lead to a preferred choice of distribution. It checks if the increase in likelihood is greater than the penalty applied for extra parameters.

The formula for the GEV with time varying location parameter is:

$$G(z(t)) = exp\left(-\left[1+\xi\left(\frac{z-(\mu_0+\mu_1*t)}{\sigma}\right)\right]^{-1/\xi}\right) \tag{2.7}$$

Where:
μ_0 = location intercept parameter
μ_1 = location trend parameter
ξ = shape parameter
σ = scale parameter
z = annual maxima

2.1.4 Non-stationary transformed stationary

The transformed stationary method (TS) removes the trend from the data, performs a maxima log-likelihood analysis on the data, and then adds the trend to the estimated parameters. This way, the maximization of the data is done for fewer parameters and should, therefore, have a lower AIC value and decreased complexity (Mentaschi et al., 2016). The AIC value includes a penalty that raises the value if more parameters are used, as is explained in Section 2.1.3. A lower AIC value means the model is preferred over the higher AIC model. (Luke et al., 2017) has argued that a stationary method with trend removal is nearly always better than a non-stationary method. They have also concluded that fitting a stationary distribution on detrended data gave better results.

The non-stationary GEV distribution with a linear time-dependent parameter in the location parameter is defined as:

$$G(z) = exp\left(-\left[1+\xi_{non-st}\left(\frac{x(t)-\mu_{non-st}}{\sigma_{non-st}}\right)\right]^{-1/\xi_{non-st}}\right) \tag{2.8}$$

Where:
$\xi_{non-st} = \xi_{st}$
$\sigma_{non-st} = S_y(t) \cdot \sigma_{st}$
$\mu_{non-st} = S_y(t) \cdot \mu_{st} + T_y(t)$
$x(t)$ = Stationary series

The stationary time series is calculated from the original data by, with notations from (Mentaschi et al., 2016):

$$x(t) = \frac{y(t) - T_y(t)}{S_y(t)} \tag{2.9}$$

Where:
$x(t)$ = Stationary series
$y(t)$ = Original non-stationary data set
$T_y(t)$ = Trend in the series
$S_y(t)$ = Long-term varying standard deviation of $y(t)$

Instead of fitting this distribution to the original dataset with the trend still present, the data is detrended, and the original, stationary GEV is fitted. This way, only three parameters must be fitted instead of four, as is the case with this non-stationary GEV, leading to less uncertainty in the three parameters. After this, the trend that was removed is introduced as the β_1 parameter and will vary over time. The distribution now varies over time and has become non-stationary.

2.2 Rosner framework

In this study, the framework developed by (Rosner et al., 2014) will be used to assess flood risk for the city of Venice. The framework, shown in Figure 2.2, is a decision tree designed for adaptation to sea level rise where the decision to adapt is weighted by the results of a test of hypothesis on the significance of the trend in the observations. Here, the concept of *expected regret* is introduced to quantify the consequences of false results in the output of a test of hypothesis, i.e., adapting when the trend is not present or not adapting when there is a trend. The different hypothesis and errors are shown in Figure 2.1.

The null hypothesis (H_0) states that there is no trend in the data, the alternative hypothesis (H_A) is that a trend is present in the data (Rosner et al., 2014). A type I error relates to falsely disregarding the null hypothesis, meaning a trend is reported when there is no trend present. The type II error relates to a false disregarding of the alternative hypothesis, meaning a trend is reported to not be present when there is a trend present. The probabilities of these errors are expressed by α and β for a type I and type II error, respectively. The hypotheses and errors are visually displayed in Figure 2.1.

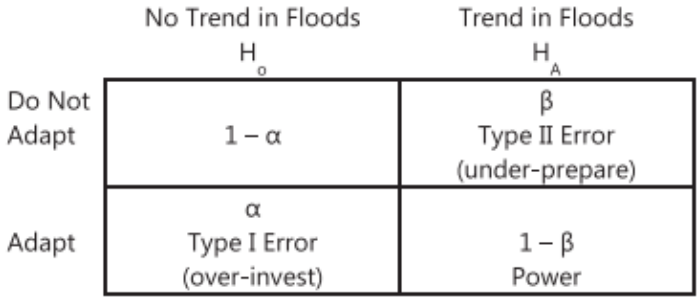

Figure 2.1: Decision matrix with definitions of type I and II errors (Rosner et al., 2014)

The Mann-Kendall test is used to assess if there is a significant trend in the dataset. This test checks if there is a monotonic trend, meaning consistently increasing or decreasing. The test statistic S is set to 0 indicating no trend. When a data point is higher than a data point from an earlier time, 1 is added to S. If a data point is lower than the previous one, 1 is subtracted from S. For an increasing trend, S will be large. In order to quantify how significant the trend is, S has to be compared to the variance in S.

The normalized test statistic Z (standard score) is calculated from this data as follows:

$$Z = \frac{S - 1}{\sqrt{Var(S)}}$$

$$p(Z) = \frac{1}{\sqrt{2\pi}} e^{-\frac{Z^2}{2}}$$

The significance of this trend is expressed by the p-value. The trend is considered significant if the p-value is smaller than 0.05 (Rosner et al., 2014).

The H_0 hypothesis is rejected if α is lower than 0.05, this means that a trend is wrongly reported less than 5% of the time (Rosner et al., 2014).

An alternative to calculate the type I error probability α is:

$$\alpha = 1 - F[t]$$

Where:

F = Cumulative distribution of Student's t variable T_{n-2}

n = Number of data points

The trend slope b_1 and the standard deviation of the trend slope s_{b1} together estimate the t value for the Student's t test: $t = \frac{b_1}{s_{b1}}$. Reading this t value from a Student's t table provides the $F[t]$ value, after which the α can be calculated.

The β that describes the type II error probability can be calculated directly from the α value. With the correlation coefficient between x (year) and y (water level) values known (ρ), the type II error probability is expressed as:

$$\beta = F(t_{1-\alpha,n-2} - \delta\sqrt{n}) \tag{2.10}$$

Where:

$t_{1-\alpha,n-2}$ = The value of the Student's t random variable with non-exceedance probability $1-\alpha$
$\delta = \frac{1}{\sqrt{\frac{1}{\rho^2}-1}}$

As can be seen in Figure 2.2, there are four scenarios. They are:

- Adapting when a trend present.
  In this scenario the adaptation is constructed, and the trend is present. This leads to damage cost D1.
- Adapting when no trend is present.
  This scenario relates to the type I error and leads to an over-investment. The adaptation is built to prevent damages caused by the trend. However, the trend is not present leading to a regret. The damages for this scenario are referred to as D2.
- Not adapting when a trend is present.
  This scenario relates a type II error, under-preparedness. The adaptation is not built while the trend is present, leading to potentially large damages, D3.
- Not adapting when no trend is present.
  The adaptation is not built, and the trend is not present, leading to damage D4.

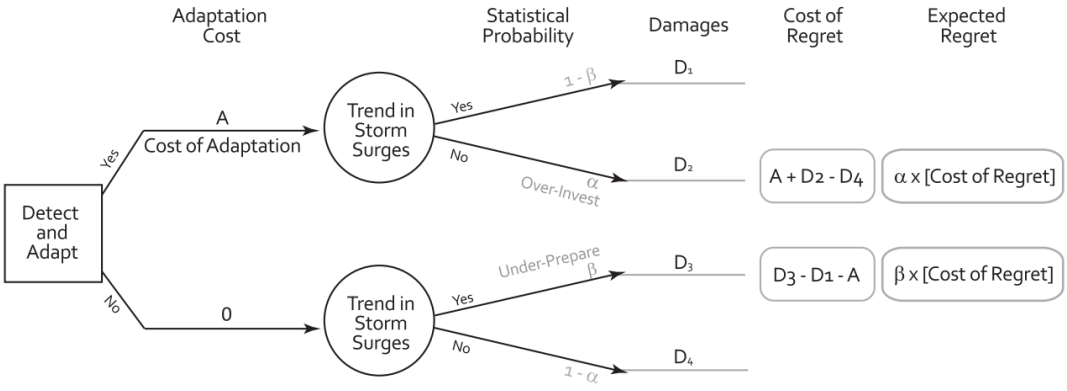

Figure 2.2: (Rosner et al., 2014) framework

The four damages are used to calculate the cost of regret for each type of error. The damages are accumulated over the years that the adaptation is assessed. In this step, the cost of regret for the type I error leading to over-investment is calculated by:

$$A + D2 - D4$$

Where:

A = Cost of the adaptation

D2 = Cumulative damages from storm levels without a trend present but with the adaptation in place
D4 = Cumulative damages from storm levels without a trend and adaptation present

The cost of regret from a type II error leading to under-preparedness is calculated by:

$$D3 - D1 - A$$

Where:
A = Cost of the adaptation
D3 = Cumulative damages from storm levels with a trend present but without the adaptation in place
D1 = Cumulative damages from storm levels with a trend and adaptation present

Now, the regret values are known for both error types; however, they are not scaled for their probability of occurrence. This is done by multiplying the costs of regret by the probability of the error.

Type I error expected regret:

$$\alpha \cdot [Cost \quad of \quad regret]$$

Type II error expected regret:

$$\beta \cdot [Cost \quad of \quad regret]$$

The two values of expected regret can be compared to assess whether adapting for the trend leads to less regret than not adapting, making it the preferred option. This way, the effects of the two types of errors are evaluated instead of disregarding the trend when it is deemed statistically insignificant.

2.3 Damage model

To estimate the damages for the four scenarios in the Rosner framework, the INSYDE (In-depth Synthetic Model for Flood Damage Estimation) model proposed by (Schlumberger et al., 2022) for the city of Venice is used. INSYDE estimates the damages on buildings only, hence, additional costs need to be added to account for the operations of the MOSE barrier itself.

(Schlumberger et al., 2022) applied the INSYDE damage model for the city of Venice. The INSYDE model calculates the damages of different components of a structure based on the water level. The different components are shown in Figure 2.3. Each component has a maximum damage value depending on the size of the building and the year of construction. Fragility curves for each component determine how much of this maximum damage value is assigned per component based on the water level. Some components use the water level outside of the building while others require the water level inside the building. Inundation maps of the city are modelled using a bathtub approach, i.e., the water level is assumed to be at the same height everywhere in the city. This is a simplification of the actual flooding process where water will pass through the canals at different velocities, creating slightly different flood heights in various places across the city. To calculate this kind of flow, complex hydrodynamic models are needed that consider wind, river, and tidal processes.

	Sub-component		Sub-component
Cleanup	C1 – Pumping C2 – Waste disposal C3 – Cleaning C4 – Dehumidification	Structural	S1 – Soil consolidation *S2 – Local repair* *S3 – Pillar repair*
Removal	R1 – Screed *R2 – Pavement* R3 – Skirting R4 – Partition walls R5 – Plasterboard R6 – External plaster	Finishing	F1 – External plaster replacement F2 – Internal plaster replacement F3 – External painting F4 – Internal painting *F5 – Pavement replacement* F6 – Skirting replacement
	R7 – Internal plaster R8 – Doors R9 – Windows R10 – Boiler	Windows and doors	W1 – Door replacements W2 – Window replacements
Non-structural	N1 – Partition replacements N2 – Screed replacement N3 – Plasterboard replacement	Building systems	P1 – Boiler replacement P2 – Radiator painting *P3 – Underfl. heating replacement* P4 – Electrical system replacement P5 – Plumbing system replacement

Figure 2.3: Different damage components that are evaluated for every building

The maximum damages per component are based on insurance claims from past flooding events (Schlumberger et al., 2022). The different components describe structural damages, except for cleaning costs. Damages due to missed income from tourism and costs of extra help for the elderly are not included in the model.

2.4 Costs of closing MOSE

The extra costs per closure of the MOSE barrier due to other components than damage from the 110 cm + ZMPS water level in the city during a closure event are the direct costs of closing the MOSE. These costs are estimated at 300,000 euros per closure event, as staff needs to be transported to the barrier to operate and check it. The cost of the staff itself, as well as other operational costs such as power, are also included.

The costs of closing the MOSE barrier range from 350,000 to 1.3 million euros per year (Vergano et al., 2010). This number is due to the decreased port activity caused by waiting times caused by the locks. In high wave conditions, the locks cannot be used, leading to a complete closure of the port. The broad range of the cost is due to economic and barrier closure projections that come with uncertainty. The 350,000 euro figure is the cost estimation for the current mean sea level in Venice. The article concludes that the costs are minor compared to the damages that come from a flood. Therefore, the economic damage of MOSE on port and harbour activities is acceptable because much larger damages due to floods are avoided.

2.5 Lifting Venice

The MOSE barrier is an essential device for protecting Venice. Without anything in place to seal off the lagoon, damages due to high flood events would drastically increase in the future due to sea-level rise. The barrier is not designed to close frequently, and it should only close at rare water levels where the city would sustain a lot of damage. The water level for closure was selected at 110 cm + ZMPS, with infrequent closing in mind.

Sea-level rise leads to an increase in the number of closures. The MOSE barrier will require more maintenance due to the more frequent closing, and if the trend in the annual maximum water level continues, the barrier will have to close even more times per year. An adaptation is needed to keep the MOSE barrier functional.

Scientists believe that it is possible to inject water into the clay layers underneath Venice, which would make the city rise (Handwerk, 2012). However, it is not precisely known how much the city will rise, but an increase of as much as 30 cm is possible. In a study conducted by (Teatini et al., 2010), a heterogeneous ground layer could result in irregular uplift in the city. These irregularities fall within the allowable legal limits for building safety and are also smaller than the settlements that occurred in the 1960s due to groundwater extraction. The costs for this adaptation are estimated to be between 200-300 million Euros. The barrier closes when a water level of 110 cm + ZMPS is projected for Punta Della Salute.

2.6 Sea level rise scenarios

Projections of sea level rise for various scenarios are provided by the NASA tool (NASA, 2022). The tool estimates sea level rise for many locations worldwide, including the Venice Lagoon, based on different Representative Concentration Pathway (RCP) scenarios that relate to varying greenhouse gas concentration scenarios. The different pathways are related to various emission and global warming scenarios. RCP1.9 relates to global warming being limited to 1.5 °C, while RCP8.5 relates to a scenario where emissions keep rising through this century (Glavovic et al., 2022).

The effects and probabilities of the different scenarios are highly uncertain, and their occurrence is highly dependent on human behaviour, including factors such as fuel types used, population growth, and economic growth. The different RCP scenarios are therefore coupled to a Shared Socioeconomic Pathway (SSP). These pathways relate to human behaviour and can be coupled to expected CO_2 levels and, thus, the RCP scenarios. How the SSP and RCP scenarios relate is not exactly known but has been visualized in a model. Figure 2.4 shows how many runs of a certain SSP scenario can reach a certain RCP scenario, leading to some RCP scenarios not likely to happen for certain SSP pathways.

The SLR projection tool couples RCP1.9 and RCP2.6 to SSP1, SSP2 to RCP4.5, SSP3 to RCP7.0, and SSP5 to RCP8.5. This means that a certain level of CO2 might be expected when the world follows the coupled SSP. The five SSP scenarios are explained in more detail (Hausfather, 2018):

SSP1 - Sustainability
The world develops towards lower energy and resource use. Welfare is distributed more equally over the world and within countries themselves. This includes education, healthcare, and economic development.

SSP2 - Middle of the Road
Paths do not deviate from current and historical patterns. Inequality between countries remains and grows further. Less resources are used, the overall population stabilizes, and small progress in sustainability is made.

SSP3 - Regional Rivalry
Countries focus on their own regional issues like security, energy, and food supply, leading to greater

environmental damage. Inter-regional goals are not a priority, and there will be less investment in technology and education.

SSP4 - Inequality
Inequalities increase both between and within countries. Higher-educated communities use less fossil fuels and are shifting towards sustainable energy sources, while lower-educated communities remain reliant on fossil fuels and have less investment in education and technology.

SSP5 - Fossil-fuelled Development
The world develops rapidly on all fronts: technological, educational, and in healthcare. To achieve this, all available fossil fuels are used without limit. This will lead to an energy-intensive lifestyle. The idea is that increased development should lead to sustainable solutions.

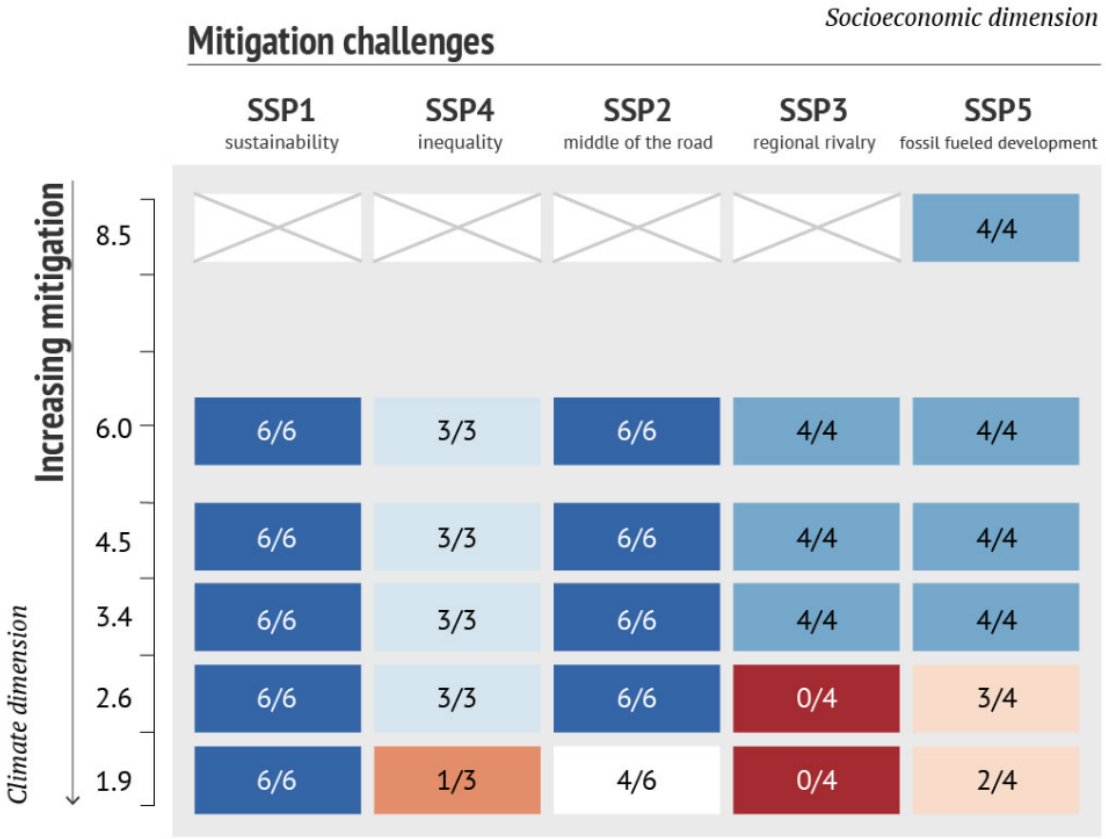

Figure 2.4: Combination of SSP and RCP model runs (Rogelj et al., 2018)

The elevated level of uncertainty makes it challenging to plan measures for mitigating climate change induced SLR. Therefore, a framework that addresses uncertain trends is becoming increasingly important for developing effective adaptation strategies.

3 Characterizing Extreme Water Levels in Venice

To make the series stationary, the mean sea level reference should be the same for every year. To achieve this, the water levels are detrended. The water level in Venice differs for every moment of the day, this happens because the water level contains different components: mean sea level, astronomical tide, meteorological induced components, and the relative height of the measurement gauge (Zanchettin et al., 2021). On a short timescale, a day for example, the mean sea level and relative height of the gauge station are deterministic, meaning they do not vary. The astronomical tide is made up of different components that together induce a predictable water elevation change. Meteorological conditions like wind, rain, temperature, and atmospheric pressure can lead to varying water elevations.

A way of detecting long term variations, is comparing the annual mean water levels. Changes in the annual mean water levels can be attributed to slow changing processes like sea level rise and land-subsidence (Zanchettin et al., 2021). When the water levels are detrended through annual means, the deterministic components are removed and only the stochastic components of the water levels remain.

The results are displayed in Section 3.1. The spread of the extreme water levels throughout the year is shown in Section 3.2.

3.1 Data detrending

The dataset of water levels from the Punta Della Salute gauge station in Venice is shown in Figure 3.1. The gauge station is in the city centre near the Basilica di Santa Maria della Salute. The water level is measured currently measured 24 times a day, before 1983, this was done only 4 times a day. To create a data set of equal number of measurements per day from 1924 till 2020, data points were inferred between the measured values leading to a water level data point being available for every 15 minutes. While the water levels in 2020 are available, MOSE was operational during that year, compromising the statistics of extreme water levels. Therefore, 2020 was removed from the analysis.

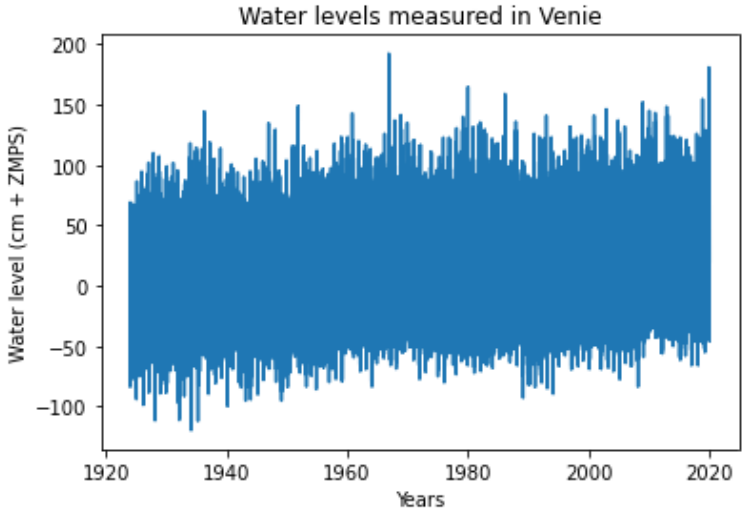

Figure 3.1: Water levels measured in Venice from 1924 till 2020

The data is detrended using the annual mean sea level, which contains long-term trends such as sea-

level rise and the effects of land subsidence. To detrend the data, the annual mean of each year is subtracted from all data points in the corresponding year. The resulting annual means are plotted in Figure 3.2a, providing a detrended data set of water levels between 1924 and 2020 in Figure 3.2b. This set is then adjusted to the 2020 reference level.

In 1924, the mean sea level was 6.24 cm + ZMPS. Over the following years, the mean sea level rose by 2.76 mm per year, resulting in an annual mean water level of $(2020 - 1924) * 0.276 + 6.24 = 96 * 0.276 + 6.24 = 26.50 + 6.24 = 32.74$ cm + ZMPS in 2020.

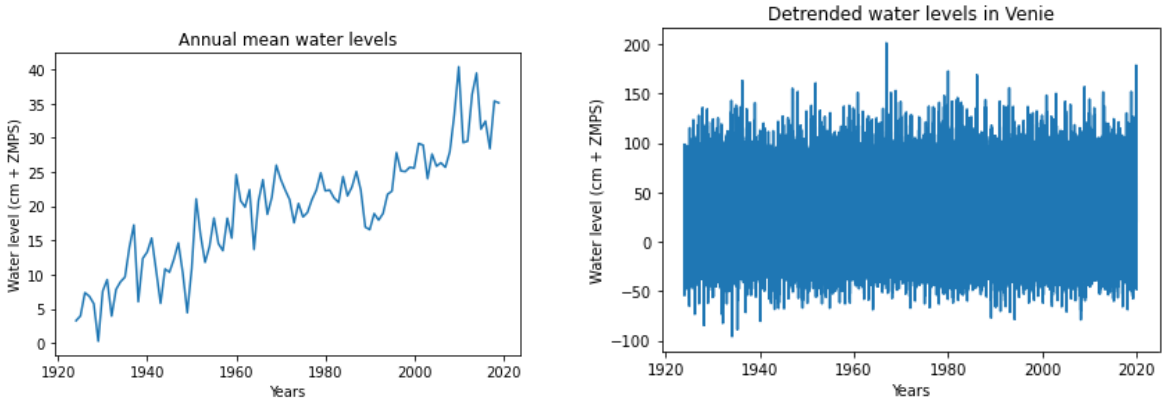

(a) Annual mean sea-level

(b) Detrended water levels in Venice

Figure 3.2: Annual mean and detrended water levels

3.2 Seasonality

Sea level will continue to rise in the future, the level of increase is depending on the SLR scenario and is therefore uncertain.

The closures over the last 96 years are summed by month to give insight in the distribution of closures over the year. Figure 3.3 displays the average peaks per month for various levels of sea level rise.

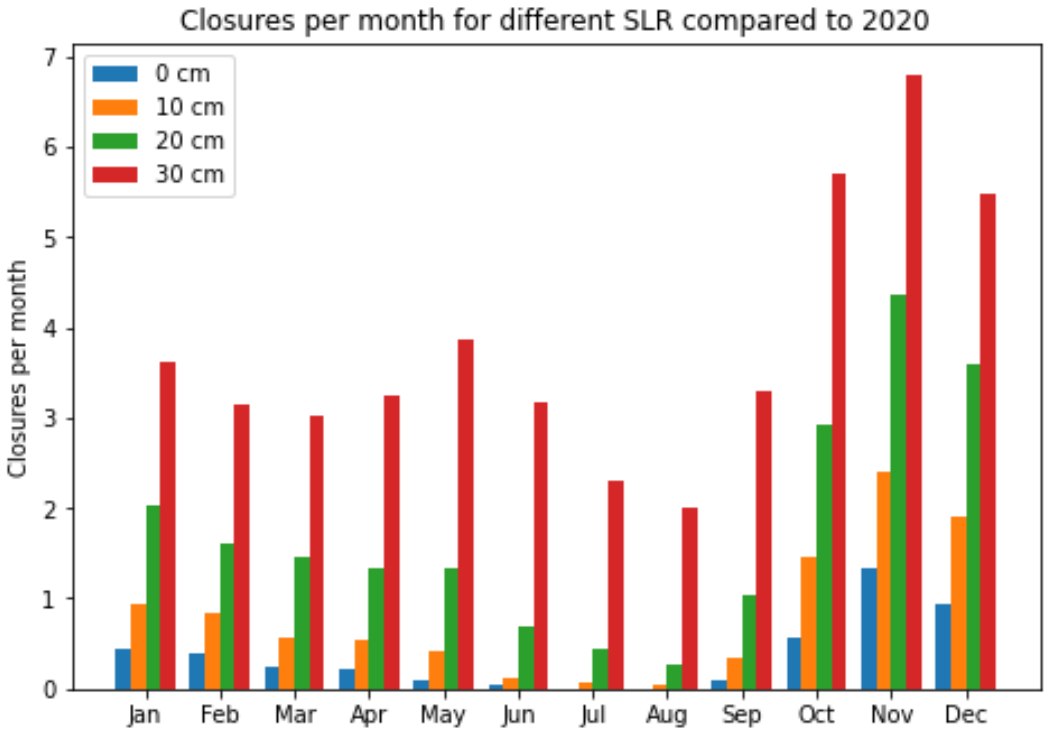

Figure 3.3: Peaks per month for different SLR values

The monthly closures for 2020 mean sea level (no sea level rise) are blue in Figure 3.3. Most peaks are in November and December while the summer has no peaks at all. There is thus a clear seasonal effect in the floods. With 10 cm of SLR, there are close to zero peaks expected for summer and with 20 cm SLR the number of expected peaks in June, July and August is still below 1. From 30 cm SLR, the floods are expected throughout the entire year. The barrier will then have to be closed half of the time from October till December.

3.3 Extreme Value Analysis

To protect Venice against high waters in the future, extreme water levels need to be estimated so designs can be adapted for water heights not yet seen in the past. EVA is used to infer these extreme events. Since the water levels in Venice are not stationary due to sea level rise and land subsidence, analysing the extremes requires dealing with a trend in the data. This thesis will compare different EVA techniques under a non-stationary assumption. The data can be detrend to perform a stationary extreme value analysis (EVA). This will provide a distribution that is only representing the conditions in one year. The removed trend is extrapolated into the future and added back into the data, leading to a distribution that represents conditions in the future. A non-stationary distribution changes over time where the distribution will shift with the trend and can be extrapolated for future years to give insight in the changes of the return periods and values.

To demonstrate the effect of the stationary and non-stationary method on the data in Venice, the GEV distribution is fitted for a stationary case where the annual maxima are detrended, and for a non-stationary situation where the annual maxima are not detrended and the location parameter of the GEV distribution can vary over time. The formulas for these two distributions can be found in Section 2.1. The Mann-Kendall trend test is conducted to evaluate if a trend is present. When there

is no significant trend present, a stationary GEV will be applied. For comparison, the non-stationary GEV will also be fitted to the detrended annual maxima.

The different fits are compared using the Akaike Information Criterion (AIC) value. This value compares the goodness of the fit, (log-likelihood value), and the number of parameters to be estimated.

The transformed stationary method (TS) is applied to the annual maxima as well. This method removes the trend from the data, fits three parameters, and then reintroduces the trend in the location parameter. This way the fit of the three parameters is more precise and the error should be smaller than the error when fitting four parameters, which is done for fitting a non-stationary GEV distribution. The modified GEV equation used is Equation (2.8). The trend is removed with Equation (2.9).

In Section 3.4, the results of a stationary fit of the GEV distribution are shown. Different non-stationary methods are used, and their results are found in Section 3.5. The results of the different methods are compared in Section 3.6.

3.4 Stationary analysis

First, the block maxima approach was applied to detrended hourly data of observed water level. Then, the Generalized Extreme Value (GEV) distribution was fitted to the annual maxima. The cumulative density distribution of the GEV function is given as:

$$G(z) = exp\left(-\left[1+\xi\left(\frac{z-\mu}{\sigma}\right)\right]^{-1/\xi}\right)$$

The return levels resulting from this GEV, and the data points it was fitted to is shown in Figure 3.4. Visually the trend looks well fitted for most points except one. This event is the extreme high-water event in 1966. In Appendix F the QQ and PP plot are displayed, these are also visual checks to assess the goodness of fit for the distribution. The parameters fitted are:

$\xi = 0.0768$
$\sigma = 13.9681$
$\mu = 127.2997$

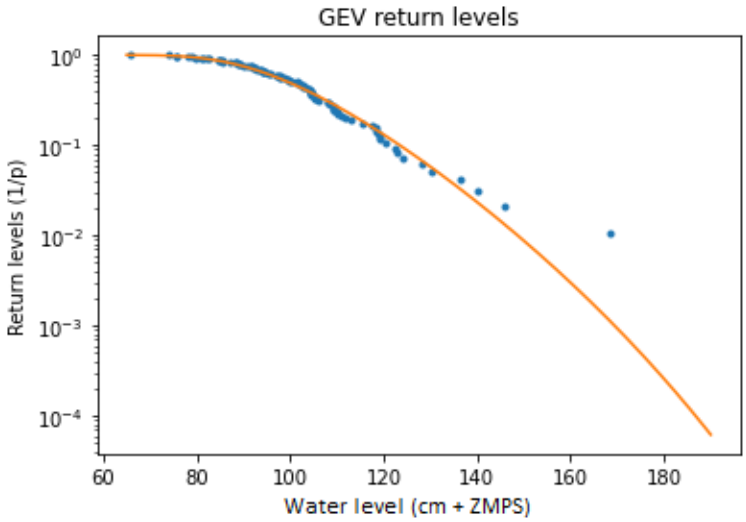

Figure 3.4: GEV return levels for detrended AM

3.5 Non-stationary analysis

Since a trend is present in the original data, shown in Section 3.1, a non-stationary approach is used. Four models are compared to one another. These four models are described by the following distributions and parameters:

- Model A: Stationary fit with added trend in mean sea-level

  $G(z) = exp\left(-\left[1+\xi\left(\frac{z-\mu(t)}{\sigma}\right)\right]^{-1/\xi}\right)$

  Where:

  $\xi = \xi, \quad \sigma = \sigma \quad \text{and} \quad \mu(t) = \mu + t * SLR_{peryear}$

- Model B: Non-stationary fit on original maxima

  $G(z(t)) = exp\left(-\left[1+\xi\left(\frac{z-\mu(t)}{\sigma}\right)\right]^{-1/\xi}\right)$

  Where:

  $\xi = \xi, \quad \sigma = \sigma$ and $\mu(t) = \mu_0 + \mu_1 * t$
  μ_0 = location intercept parameter
  μ_1 = location trend parameter

- Model C: Transformed Stationary approach

  The TS method uses a unique way of detrending the data set before fitting the GEV distribution. The formula for detrending the data is given:

  $x(t) = \frac{y(t)-T_y(t)}{S_y(t)}$

  Where:
  $x(t)$ = Stationary series
  $y(t)$ = Original non-stationary data set
  $T_y(t)$ = Trend in the series
  $S_y(t)$ = Long-term varying standard deviation of $y(t)$

  After detrending, the GEV distribution is fitted:

  $G(z(t)) = exp\left(-\left[1+\xi\left(\frac{z-\mu(t)}{\sigma(t)}\right)\right]^{-1/\xi}\right)$

  Where:

  $\xi = \xi$
  $\sigma(t) = S_y(t) \cdot \sigma$
  $\mu(t) = S_y(t) \cdot \mu + T_y(t)$

- Model D: Non-stationary fit on detrended maxima

  The distribution is fitted on detrended annual maxima after which mean sea level rise is added for every year, similarly to model A.

  $G(z(t)) = exp\left(-\left[1+\xi\left(\frac{z-\mu(t)}{\sigma}\right)\right]^{-1/\xi}\right)$

  Where:

$\xi = \xi, \quad \sigma = \sigma$ and $\mu(t) = \mu_0 + \mu_1 * t + SLR_{peryear}$
μ_0 = location intercept parameter
μ_1 = location trend parameter

3.5.1 Model A: Stationary fit with added trend in mean sea-level

Model A fits a stationary GEV as described in Section 3.4 for the annual maxima detrended towards 1924 mean sea level. In the location parameter, the trend in mean sea level rise of 2.76 cm per year is added.

The return value of the 100-year return period from 1924 till 2020 is plotted in Figure 3.5. The parameters fitted for the distribution are:

$\xi = 0.0768$
$\sigma = 13.9681$
$\mu = 100.5797$

Their 95% confidence bounds are:

CI Bounds:
ξ = [0.1832,-0.0296]
σ = [12.0102,16.2452]
μ = [97.5236,103.6357]

Log-likelihood: -399.4749

AIC: 804.9595

Return level 1924: 154.71 cm
Return level 2020: 181.01 cm

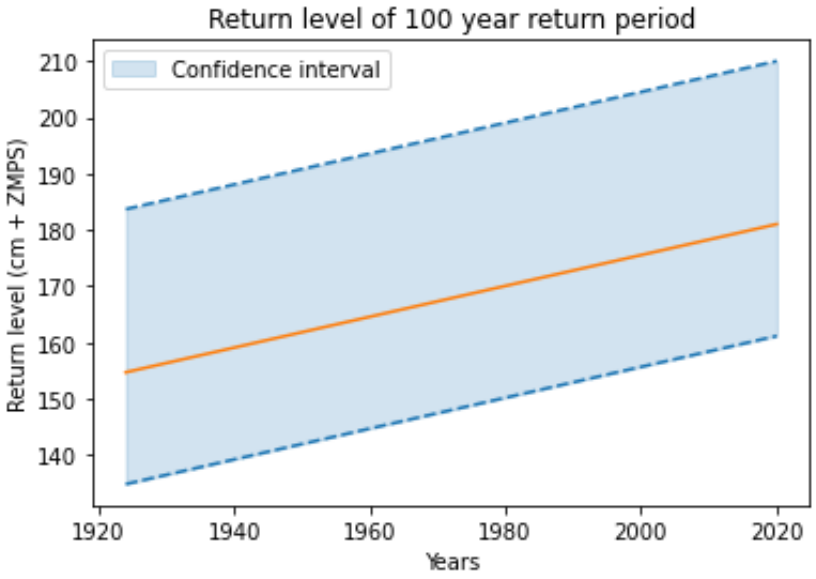

Figure 3.5: Return level for 100-year period over time for shifting mean sea level

3.5.2 Model B: Non-stationary fit on original maxima

For the GEV distribution, the location parameter is selected to shift with the level of SLR over time. The shape and scale parameter remain the same. Allowing more parameters to change over time increases complexity and thus uncertainty in the distribution. The new and parameters for Equation (2.7) are:

Stationary fit parameters:
$\xi = -0.0304$
$\sigma = 14.2954$
$\mu_0 = 94.9226$
$\mu_1 = 0.3786$

CI Bounds:
ξ = [0.0454,-0.1381]
σ = [13.1763,16.6872]
μ = [88.410,99.1135]

log-likelihood = -404.21

AIC: 816.4204

Return level 1924: 165.88 cm
Return level 2020: 201.85 cm

Fitting for higher order non-stationary, where the time-varying parameter is exponential, results in a higher AIC value. The linear time-varying parameter is therefore the better fit.

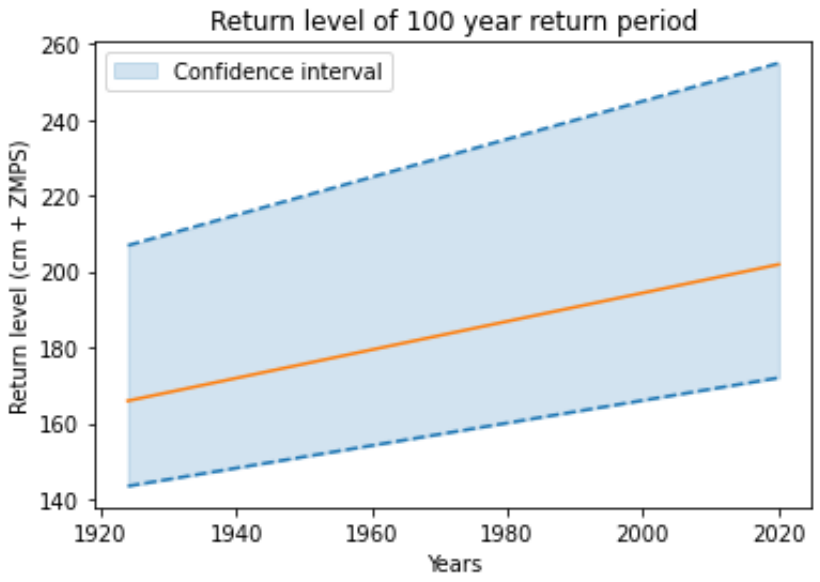

Figure 3.6: Return level for 100-year period over time non-stationary fit

3.5.3 Model C: Transformed stationary (TS) approach

This method was proposed by: (Mentaschi et al., 2016). After detrending the data, the parameters found for the stationary fit are:

Stationary fit parameters:
$\xi = 0.0488$
$\sigma = 0.5530$
$\mu = 3.8043$

CI Bounds:
$\xi = [0.1704, -0.0729]$
$\sigma = [0.4732, 0.6462]$
$\mu = [3.6820, 3.9265]$

Log-likelihood: -91.4531

AIC: 188.9063

Return level 1924: 139.89 cm
Return level 2020: 206.36 cm

Since this method moves the distribution of the data to a mean of zero and a standard deviation of one, the AIC values are not comparable with the other methods.

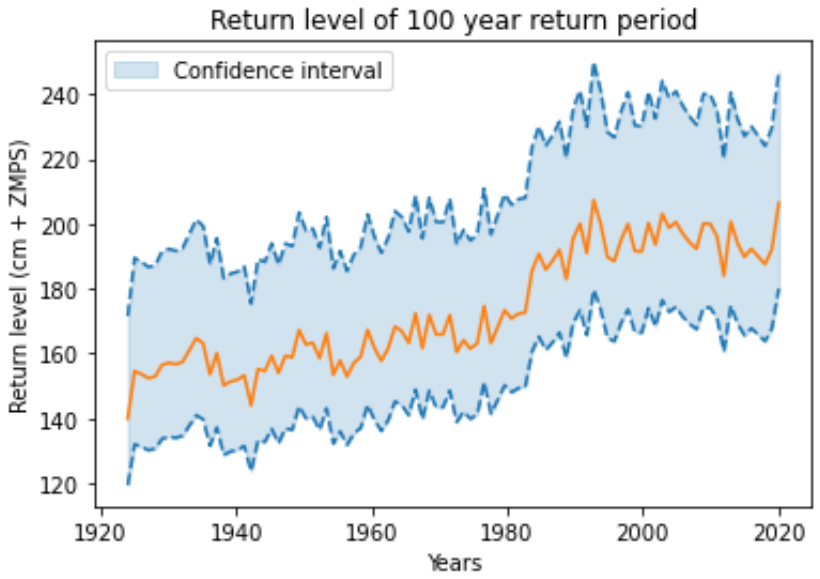

Figure 3.7: Return level for 100-year period over time for TS method

3.5.4 Model D: Non-stationary fit on detrended maxima

The data is detrended for mean sea level. For comparison, a non-stationary EVA is applied on the detrended residuals (annual maxima) to compare the return values and AIC values between stationary and non-stationary methods. For the GEV distribution, the location parameter is selected to shift with the level of SLR over time. The shape and scale parameter remain the same. Allowing more parameters to change over time increases complexity and thus uncertainty in the distribution. The new parameters for Equation (2.7) are:

Stationary fit parameters:
$\xi = -0.0337$
$\sigma = 13.5312$

$\mu_0 = 121.9518$
$\mu_1 = 0.1091$

CI Bounds:
ξ = [0.0666,-0.1288]
σ = [12.2192,15.4492]
μ = [118.5532,127.0803]

log-likelihood = -397.30

AIC: 802.595

Return level 1924: 162.81 cm
Return level 2020: 199.48 cm

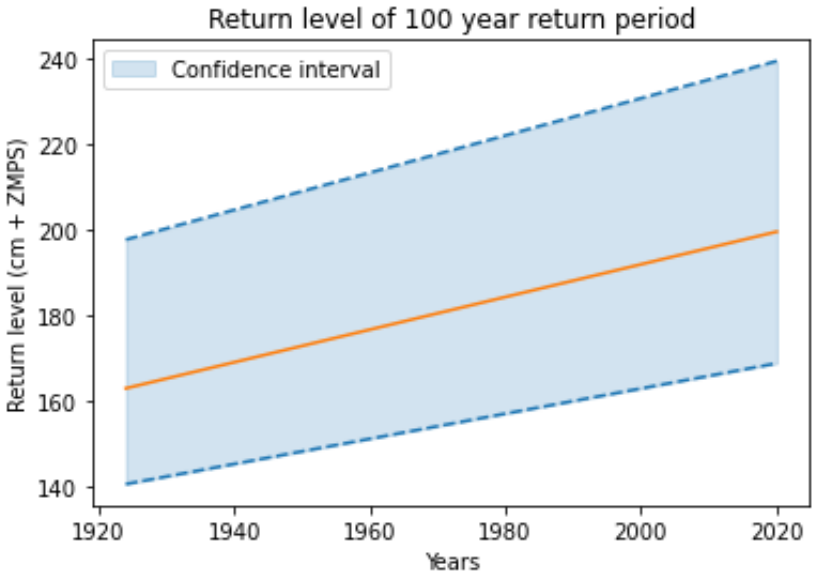

Figure 3.8: Return level for 100-year period over time non-stationary fit on detrended maxima

3.6 Comparison

After evaluating the four methods, the method with the lowest AIC value is preferred due to the largest log-likelihood and the least number of parameters. The AIC values and its composition can be seen in Table 3.1. The highest log-likelihood is found for model C, this value is not comparable due to the standardisation that is used before fitting the distribution. The maxima are standardised to lower values by dividing over the standard deviation of each year. The AIC values that can be compared are those of models A, B and D. Where model D has the highest log-likelihood. This is the model where the non-stationary fit is applied on detrended data. The high log-likelihood is expected because the extra parameter is likely to improve the likelihood of the distribution parameter fit. The AIC value includes a penalty for the use of more parameters, this penalty is higher for the non-stationary fit due to its extra parameter, this implies the gain in likelihood is worth the extra complexity induced by using more parameters.

The change of the return level of a 100-year return period event are plotted for all methods in Figure 3.9. The results of the non-stationary fits (models B and D) are closely matched even though their AIC values are quite different (818.42 for model B and 802.56 for model D). Model C oscillates around the

stationary line until 1981 and then jumps to the non-stationary values until 2020. The reason for the jump is identified and can be explained from the way the data is post-processed, further analyses on this is given in Appendix D. The annual maxima or other extreme values used for this thesis are not affected by this post-processing.

Model	Log-Likelihood	Penalty	AIC
A	-799.0	6	805.0
B	-808.4	8	816.4
C	-182.9	6	188.9
D	-794.6	8	802.6

Table 3.1: AIC composition and comparison between the different models

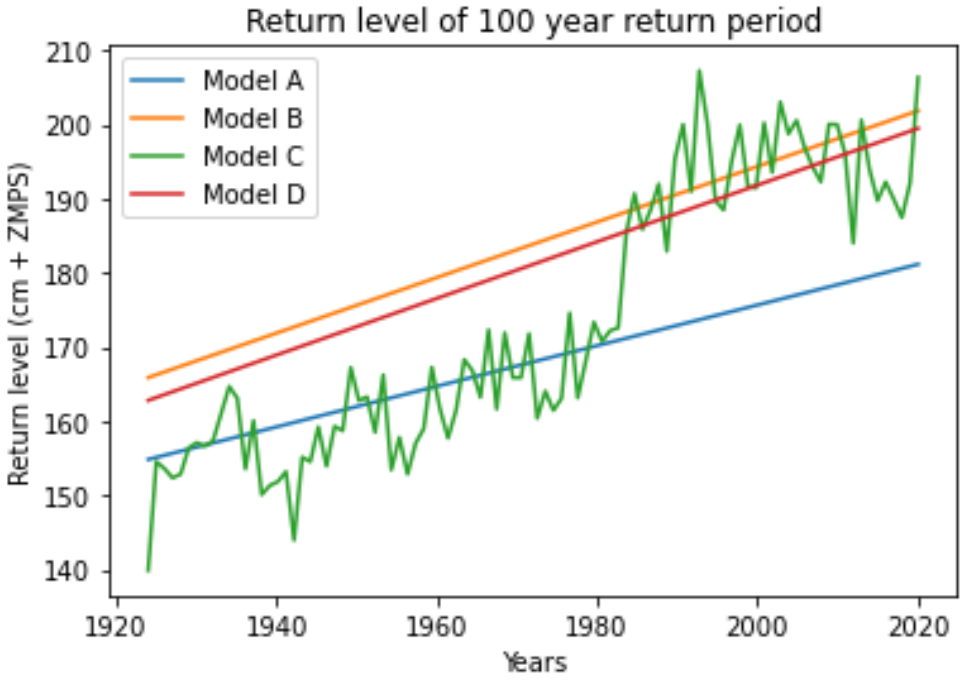

Figure 3.9: The results from the different non-stationary methods compared

The return levels of the distributions as well as the return levels that result from different SLR scenarios in 2100 are plotted in Figure 3.10. Model C is extrapolated by using the trend in the standard deviations used for this method in Section 3.5. The non-stationary methods reach return levels that are similar to the expected return level in scenarios RCP4.5 till RCP8.5.

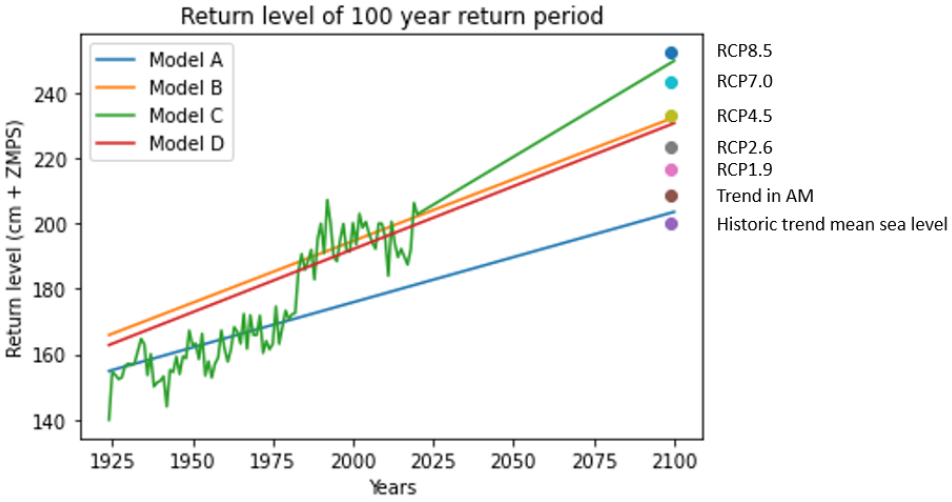

Figure 3.10: The results from the different non-stationary methods compared with the different scenarios till 2100

4 Investigating MOSE closure for different sea level rise scenarios

In this chapter, the framework proposed by (Rosner et al., 2014) is applied to the city of Venice to evaluate future adaptation strategies. Damages caused by high sea water levels comprise costs related to the MOSE closure and maintenance (Section 4.1) and damages to buildings. These are the number of closures for different trend scenarios, displayed in and the damages (Section 5.1.1). Uncertainties are introduced in Section 5.2 and implemented in the framework in Section 5.3.

4.1 Number of closures due to extrapolating historic trends

The number of closures per year is based on the rise in mean sea-level. In this analysis, the frequency of storms is assumed constant. Thus, if the mean sea-level is stable, the number of high-water events per year is stable as well. This can be checked when the mean sea-level is removed from the water levels. If there are more high-water events in later years, this can indicate a trend in frequency. The check will be done in Section 4.1.1 of the results.

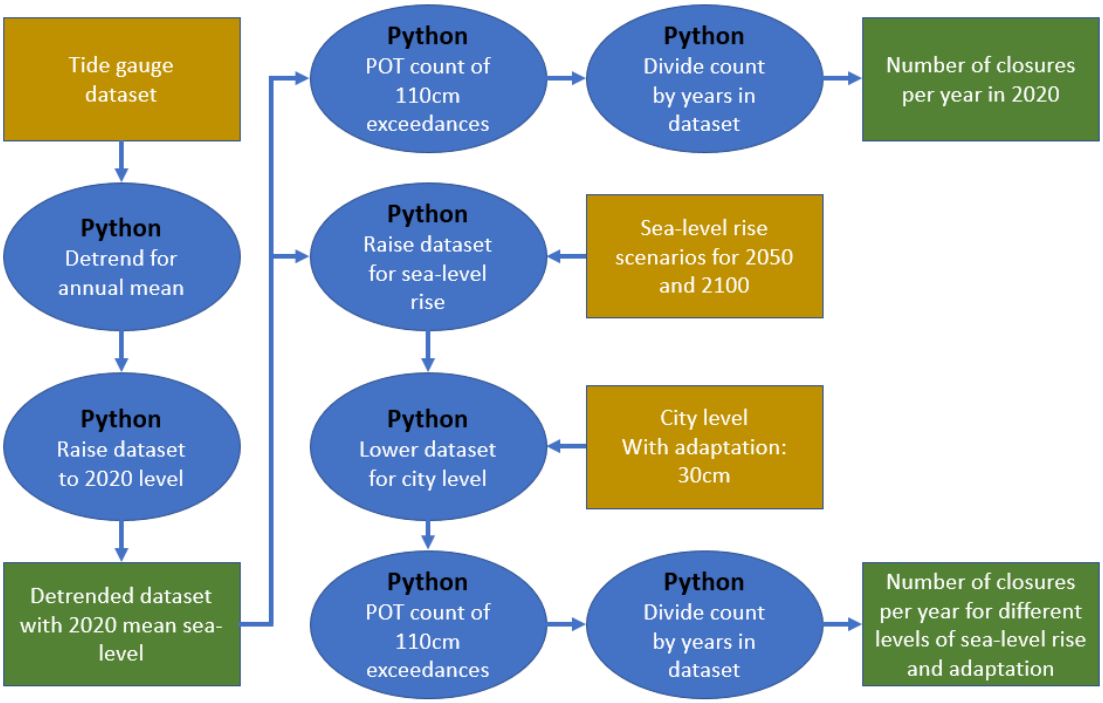

Figure 4.1: Flowchart for the process of calculating the number of closures

Figure 4.1 presents the flowchart for calculating the number of closures. The input is a dataset containing all measured water levels in Venice from 1924 to 2021. Since the barrier started operating in 2020, the last year is not used. The first step is to remove the trend in the dataset. To do this, the annual mean water level is calculated, and this annual mean is then removed from all water levels, leading to the entire water level dataset being detrended through the annual means. To adjust this dataset to the mean sea level of 2020, the dataset is raised with the mean sea-level for 2020. Now the dataset is detrended to the 2020 reference level.

If the exceedances of 110cm + ZMPS are counted, the total number of closures is known if the mean sea-level would be at the 2020 level for the entire time. The barrier can close every 12 hours; therefore, the peaks must be separated by at least 12 hours. To calculate an average number of closures per year, the number of peaks is divided by the number of years that the dataset consists of, resulting in the average number of closures per year if the mean sea-level would be at the 2020 level.

The level of sea-level rise can be specified for 2050 and 2100. The sea-level rise for the years between 2020, 2050, and 2100 is taken as a linear function. For each year, the number of closures is calculated for that year's level of sea-level rise.

This method describes the calculation of the number of closures if no adaptation is made. The effect of the adaptation is the city rising 30cm, which takes ten years. The closures after adaptation are calculated by lowering the dataset by 30cm.

This way, the choice to adapt and the choice of sea-level rise levels for 2050 and 2100 lead to a number of closures for every year from 2020 to 2100.

The different processes for causing more closures in the future are compared in Section 4.1.1. In Section 4.1.2, the trends in the historic water level data set are identified. These trends are: land subsidence, annual mean sea level rise and a trend in the annual maxima present after removing the annual mean sea level. Two scenarios are then created where different trends are extrapolated into the future. The expected number of closures from 2020 till 2100 resulting from extrapolating historical trends are shown in Section 4.1.3.

4.1.1 Dominant processes affecting the frequency of closures

For this analysis, closures are calculated by raising the peaks of water levels for new mean sea levels in the future. This assumes that the closures are most influenced by the rising mean sea level. However, possible historical trends in storms are not considered this way. To check this presumption, the number of high-water events per year from the detrended observations is plotted to see if there is a trend in the number of events over the years. A high-water event is classified as such when the water level reaches 110 cm + ZMPS. The events must be 48 hours apart so they can be assumed separate events.

The closures per year and the assumed linear trend are displayed in Figure 4.2a. The Mann-Kendall trend test had a value of $p = 0.24$, this means the trend is considered not significant since it is higher than $p = 0.05$. For comparison, the linear trend in the annual means is plotted in Figure 4.2b. The hypothesized linear trend in storm events has a slope equal to 0.025 closures per year, meaning that additional 2.5 closures per year extra in 100 years are expected. On the other hand, an increase in the mean sea level could lead to an increase of 10-600 closures per year (Umgiesser, 2020).

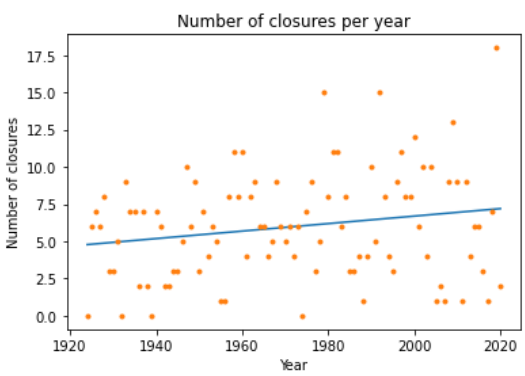

(a) Frequency of closures after detrending

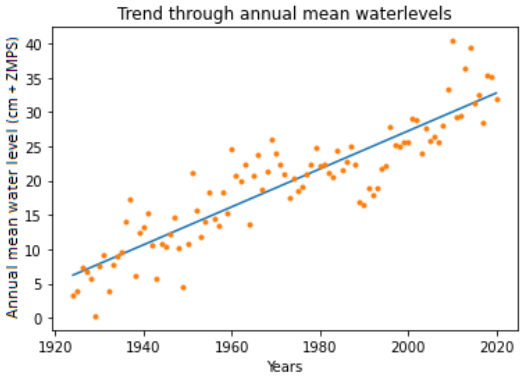

(b) Annual mean sea-level with trend

Figure 4.2

4.1.2 Sea-level rise trend extrapolation

For extrapolation of the historic trend in the future, the trend that can be attributed to sea-level rise has to be established from the data. The trend in the annual means is influenced by land subsidence (Zanchettin et al., 2021). Therefore, the land subsidence needs to be removed from the data to obtain the trend in sea-level rise instead of relative sea-level rise. (Zanchettin et al., 2021) has been able to apply a correction factor for land subsidence. The correction factor can be seen in Figure 4.3a. The annual means without land subsidence can be seen in Figure 4.3b. The trend in these means can be fitted with a trend line. The trend line can be linear or be a higher order polynomial. Higher order fittings that fit the data more closely may not be suited for extrapolating, since the complexity in the fit increases and the uncertainties increase. The linear fit indicates a sea-level rise of 1.38 mm per year. The land subsidence is estimated to be 1 mm per year for the future. This value is estimated for the city, since the subsidence near the newly constructed barrier inlets is higher due to expected soil settling (Zanchettin et al., 2021). The total annual rise from historic data is therefore 2.38 mm per year.

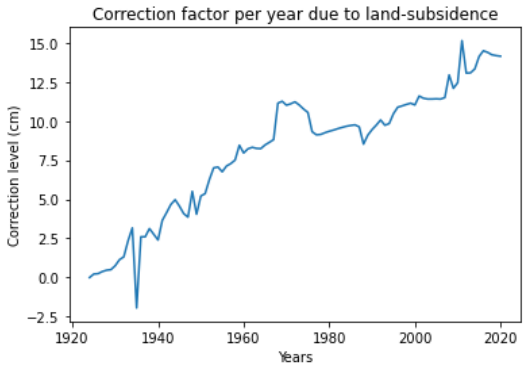

(a) Correction factor for land-subsidence per year.

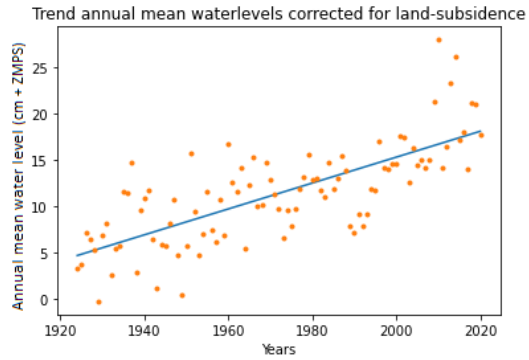

(b) Annual means corrected for land-subsidence.

Figure 4.3: Land-subsidence correction

The annual maximum values also exhibit a trend. Figure 4.4 displays the detrended AM values with their trend line fitted. The trend is 1.02 mm per year, which is similar in magnitude to sea-level rise. However, the significance of the trend could be different. The significance is determined by the

probability of falsely assuming that a trend is present when it is not (type I error), which will be calculated in Section 5.1.3.

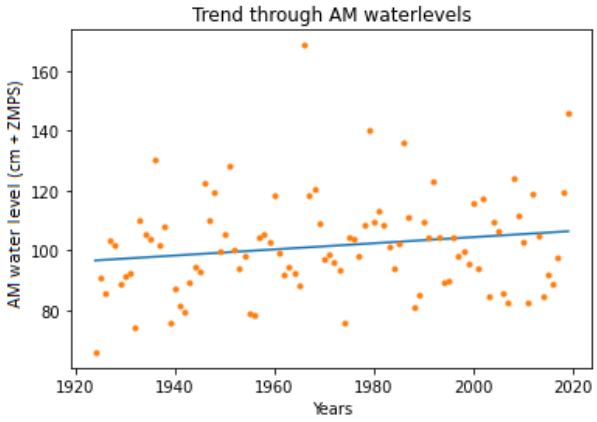

Figure 4.4: Detrended Annual Maxima (AM) with line fitted

4.1.3 Number of closures

The barrier is closed when a high-water peak reaches at least 110cm + ZMPS. The number of times this would have happened if 2020 mean water level had prevailed is counted. The peaks must be at least 12 hours apart to count as two separate closures. Figure 4.5 shows the exceedances for 2020 mean water level. There are 579 closures over the 96-year period. The average number of closures per year is:

$$Closures = \frac{579}{96} = 6.0$$

The expected number of closures for 2020 is therefore 6.

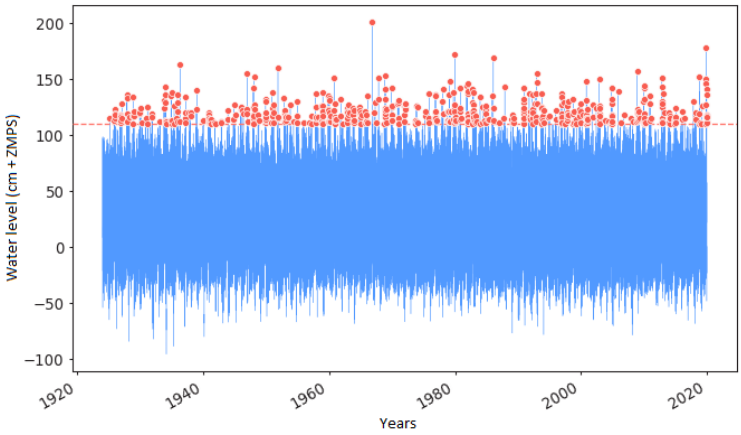

Figure 4.5: Exceedance of 110cm + ZMPS in the past

The expected closures per year as well as their percentile increase compared to 2020 are shown in Table 4.1.

If the city is raised by 30cm, the water levels should be lowered by 30cm before counting the exceedances of 110cm + ZMPS. This results in only 0.8 closures per year for 2050.

City level	Sea-level rise (cm)	Year	Closures per year	Increase to 2020 (%)
0	0	2020	5.8	0
0	7.1	2050	11.8	103.4
30	7.1	2050	0.8	-86.2

Table 4.1: Closures per year due to historical water level means

The trend in the annual maxima, corrected for mean sea-level rise, is statistically insignificant. However, the effect of this trend will be evaluated in the (Rosner et al., 2014) framework. The annual increase in water levels will be a combination of the trend in the maxima of 1.02 mm per year and, the trend from SLR and expected land-subsidence of 2.38 mm per year. This means that water levels will have to be raised by $30 \cdot 0.34 = 10.2$ cm compared to 2020. Table 4.2 displays the results of this trend on the number of closures per year.

If the city is raised by 30cm, the water level data set should be adjusted by lowering it by 30cm before counting the exceedances of 110cm + ZMPS.

City level (cm)	Sea-level rise (cm)	Year	Closures per year	Increase to historical trend (Table 4.1) (%)
0	0	2020	5.8	0
0	10.2	2050	15.3	29.7
30	10.2	2050	1.0	25.0

Table 4.2: Closures per year due to added trend from annual maxima

4.2 Number of closures due to sea level rise projections

Sea-level rise projections for different RCP scenarios are provided by (NASA, 2022). Estimates of sea-level rise for the centre of Venice are given for various scenarios from 2020 to 2100 in Figure 4.6.

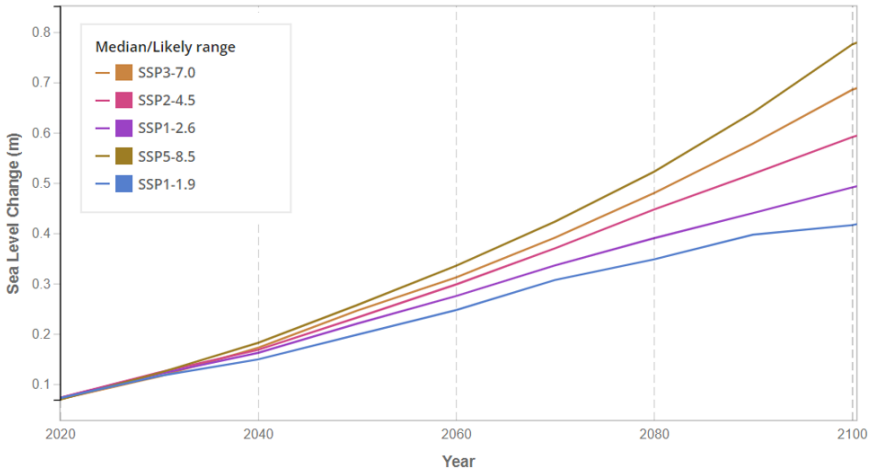

Figure 4.6: SLR projections for Punta Della Salute

The IPCC presents different scenarios for sea-level rise, which will lead to a rise in water level. To estimate the levels of sea-level rise in Venice for each scenario, the sea level projection tool developed by (NASA, 2022) is utilized. The number of MOSE closures is then calculated for each scenario

and year using the median value of sea-level rise. As projections extend further into the future, the associated uncertainties increase, resulting in larger ranges of plausible outcomes. The resulting number of closures per year is presented in Table 4.3.

City level (cm)	Scenario	year	Sea-level rise (cm)	Closure per year
0	RCP2.6	2050	15	24
		2100	42	209
	RCP4.5	2050	16	26
		2100	52	308
	RCP7.0	2050	17	28
		2100	59	353
30	RCP2.6	2050	15	1.5
		2100	42	18
	RCP4.5	2050	16	1.7
		2100	52	44
	RCP7.0	2050	17	1.8
		2100	59	82

Table 4.3: Closures per year due to sea-level rise projections

When sea levels rise by more than 10cm, the MOSE barrier must close for the largest tides of the year, including regular high tides. As sea levels continue to rise, the barrier will eventually have to close for regular tides higher than 110cm + ZMPS, losing its function as a storm surge barrier. This is expected to occur before 2050 for all climate scenarios without adaptations.

To determine the impact of rising sea levels on the number of closures, the dataset of water levels is raised, and the number of closures for different mean water levels is counted. Projections for how much the mean water level will rise are based on different RCP scenarios and extrapolations of existing trends. To adapt to these rising sea levels, the lifting of Venice, as discussed in Section 2.5, will be utilized as the adaptation strategy for the (Rosner et al., 2014) framework. Figure 4.7 displays the number of closures for sea level rises from 0 cm to 90 cm. The blue line represents the number of closures with no adaptation applied, while the orange line indicates the number of closures with a 30 cm lifting of the city. The vertical lines indicate the levels of sea level rise projected for different scenarios (numbered 1 to 7) in 2050 (blue) and 2100 (orange).

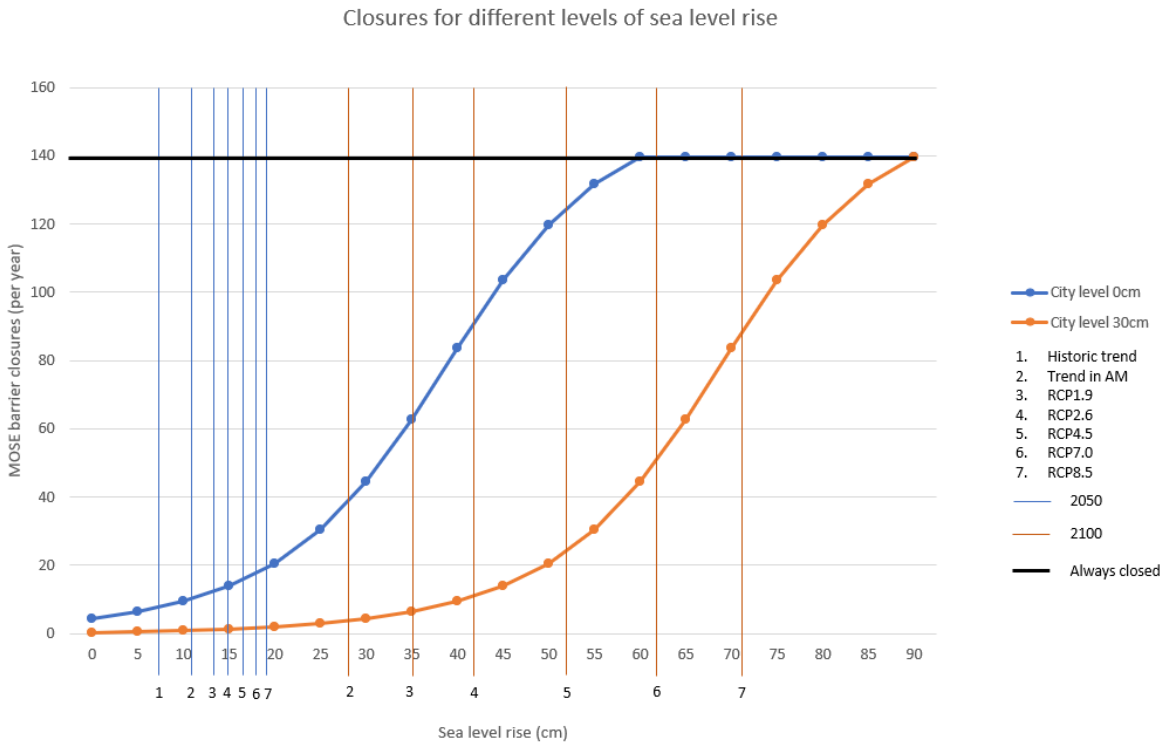

Figure 4.7: Number of closures for amount of sea level rise

Raising the water level data set above 50cm renders the number of closures unreliable for several reasons. Firstly, many data points will be above the threshold of 110cm + ZMPS, resulting in peaks occurring every 48 hours in succession. Eventually, the number of closures will approach a maximum where there is a peak every 12 hours, leading to prolonged periods of closure. Secondly, it may not be feasible to close the MOSE barrier so often. If the barrier is closed every day, it will lose its function as a storm surge barrier, which is to remain open most of the time and only close for extreme water levels. For this reason, the maximum number of closures is chosen as 140 per year, hence the horizontal line for number of closures in Figure 4.7.

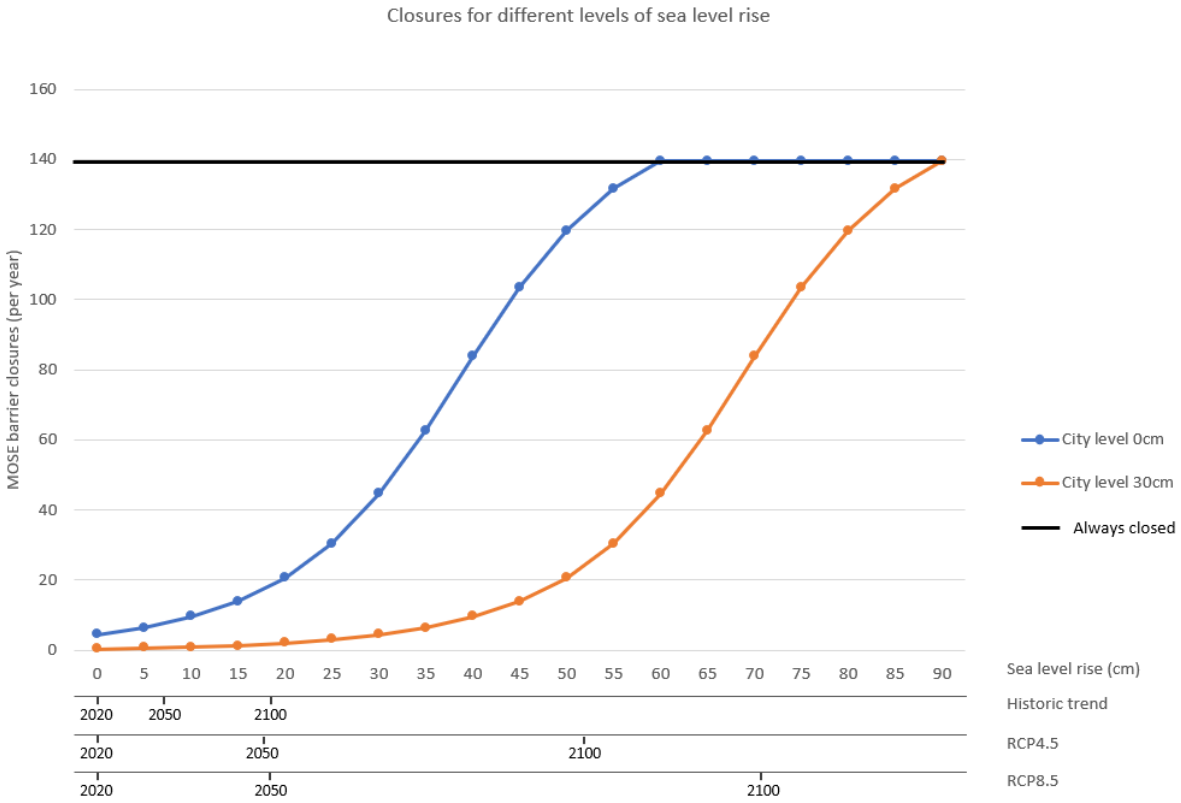

Figure 4.8: Number of closures for amount of sea level rise with time axes

5 Risk-based approach to flood management in Venice

5.1 Rosner framework applied for historic trends

The framework proposed by (Rosner et al., 2014) aims to evaluate the feasibility of an adaptation strategy considering errors in the detection of trends in the magnitude of high-water levels by quantifying the regret associated with different decisions. To calculate the regret, four damage scenarios resulting from the four possible adaptation pathways must be known, as well as the cost of the adaptation. Comparing the damages between the adapted and non-adapted scenarios can also provide insight into the benefits of adaptation and the optimal timing for implementation. Two pathways lead to a scenario where the sea level rise trend is absent. In addition to trends, this setup can also be used to compare different sea level rise projections. A higher sea level rise scenario can be modelled as a trend, with a lower sea level rise scenario serving as an alternative if the trend were not present. To calculate the expected regret, the probability of errors must be known, which can be calculated for the trend in the annual maxima. However, this is not known for sea level rise projections. Instead, a weight of expectation can be assigned to different projections, but the results are subject to human behaviour in the future and thus highly uncertain.

5.1.1 Damages

The damages for each scenario within the framework are calculated by multiplying the number of closures by the amount of damage per closure. The damage per closure includes the direct costs of closing the MOSE, which involves sending operators to the MOSE and lost harbour income due to the lagoon being less accessible, as well as the damage caused by the water level inside the city reaching 110cm + ZMPS above the reference level. Although this only causes minor flooding, it still causes damage.

As shown in Figure 5.1, the flowchart illustrates how the damage per flood event is calculated. The water level in the city will be 110cm + ZMPS during closure since higher water is blocked by the MOSE. A data set containing various information about structures in Venice is used to calculate the damage per structure. The water level at the level of the building is calculated by subtracting the flood depth from the building elevation, resulting in the inundation depth of the structure. INSYDE does this for all structures, resulting in a list of inundated structures. These structures are then evaluated in the INSYDE model to compute the damage per structure.

INSYDE returns the damages per component per structure. The total damage is obtained by adding the different components per structure and then adding the damages of all structures. The list of different damage components was already shown in Figure 2.3. Each component has a fragility function that indicates the height for which the component has damage. Some components will have damage from lesser amounts of water, while others might only result in damage when high water levels are reached. The model considers the doorstep to determine if, and if so, how much water has entered the interior of the building.

The total damage per flood is the sum of the direct costs of closing the barrier and the costs of the 110cm + ZMPS flood.

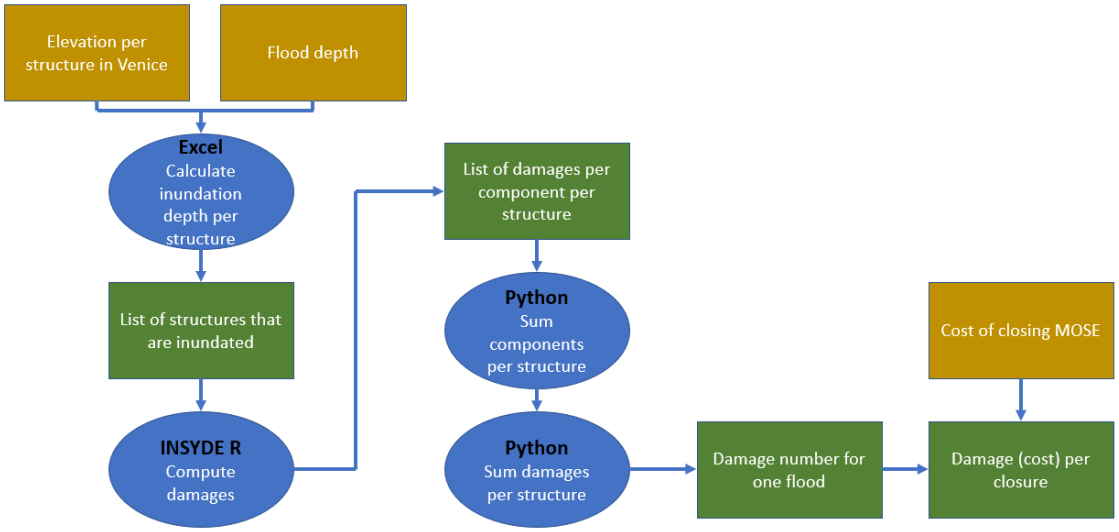

Figure 5.1: Flowchart for process of calculating damages

Damages due to high sea levels are categorized into two types: flood damage and closing costs. Flood damage includes damages due to water levels of 110cm + ZMPS in the city, leading to clean-up costs and minor damages to structures. Income loss due to less tourist activity, costs due to children having to stay home, and elderly inhabitants needing extra help are minor for floods up to 110cm + ZMPS. In general, the damages are deemed acceptable since the closing limit is chosen for this water level.

The damage to buildings is calculated with the INSYDE model (Schlumberger et al., 2022). A bathtub model is used which simulates a constant water level inside the city. The model contains information on many structures in Venice. First, the model must determine which buildings are inundated and, if so, to what extent. A water level of 110 cm + ZMPS is simulated in the city, and buildings that are inundated can be seen in Figure 5.2.

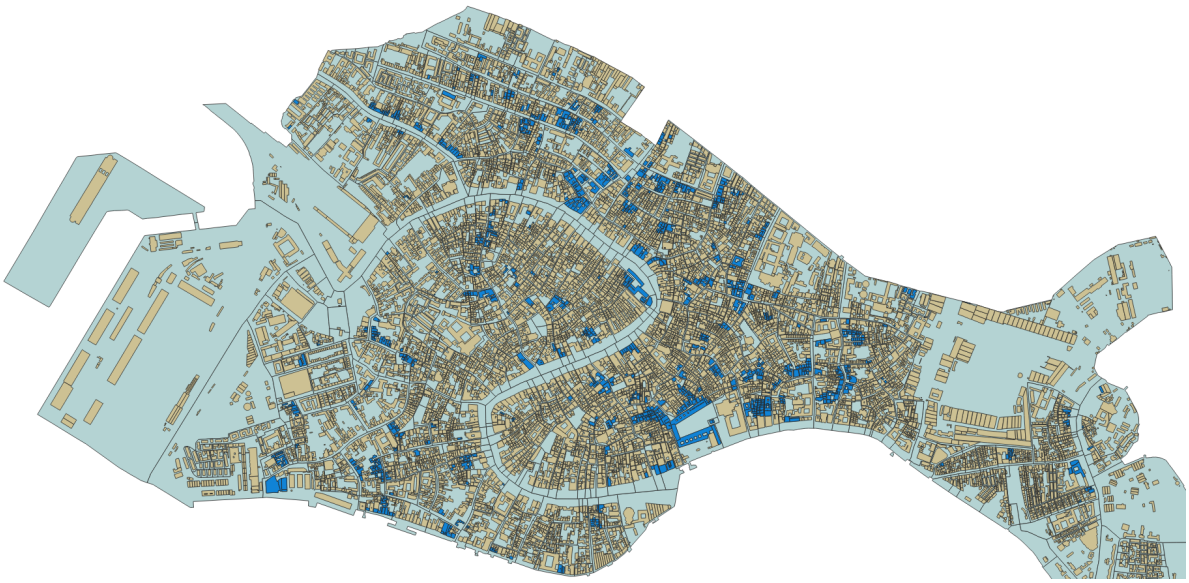

Figure 5.2: Structures flooded at 110cm + ZMPS water level in dark blue

The INSYDE model is comprised of different damage components, and the total damage figure for a building is the sum of these components. Each component has a fragility curve that shows the level of damage for different flood levels. In the case of a 110cm + ZMPS water level in the city, the inundation of buildings is minor, typically only a few centimetres, rather than tens of centimetres. The model considers both the water level inside and outside of the building, as well as the dimensions and costs of each component.

Because each closure of MOSE causes the city to flood up to 110cm + ZMPS, the costs per component are added up for all buildings, resulting in a total damage figure. This figure is displayed in Figure 5.3, where it can be seen that most components do not result in any damage due to the low water level. This is expected, as the small inundations are unlikely to enter the interior of most buildings. In total, the sum of the components shown in Figure 5.3 results in a total damage figure of 602,700 Euro.

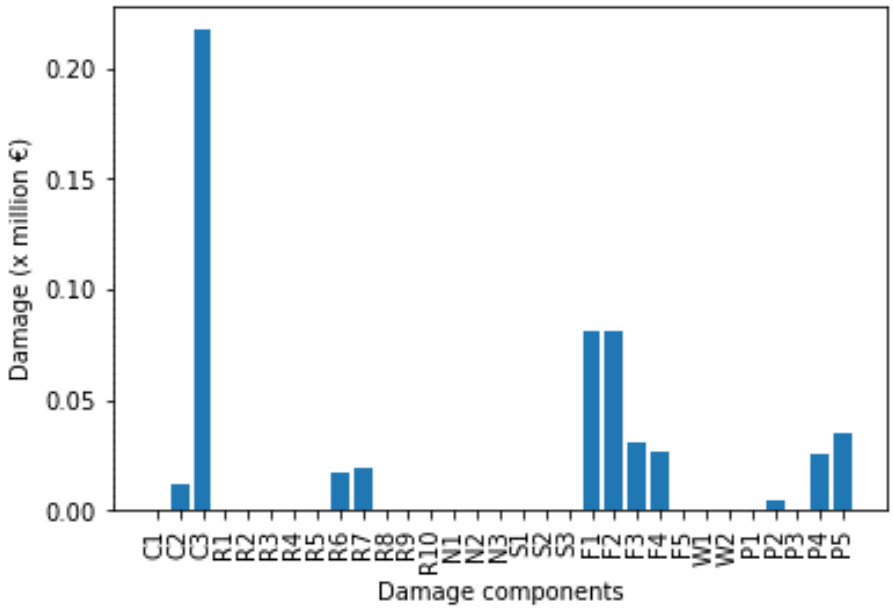

Figure 5.3: Total cost per component for a 110cm + ZMPS flood

To put the damages for the 110cm + ZMPS flood into perspective, a damage curve is drawn to display the costs of different flood heights. The damage curve as well as a zoomed version can be seen in Figure 5.4 and Figure 5.5.

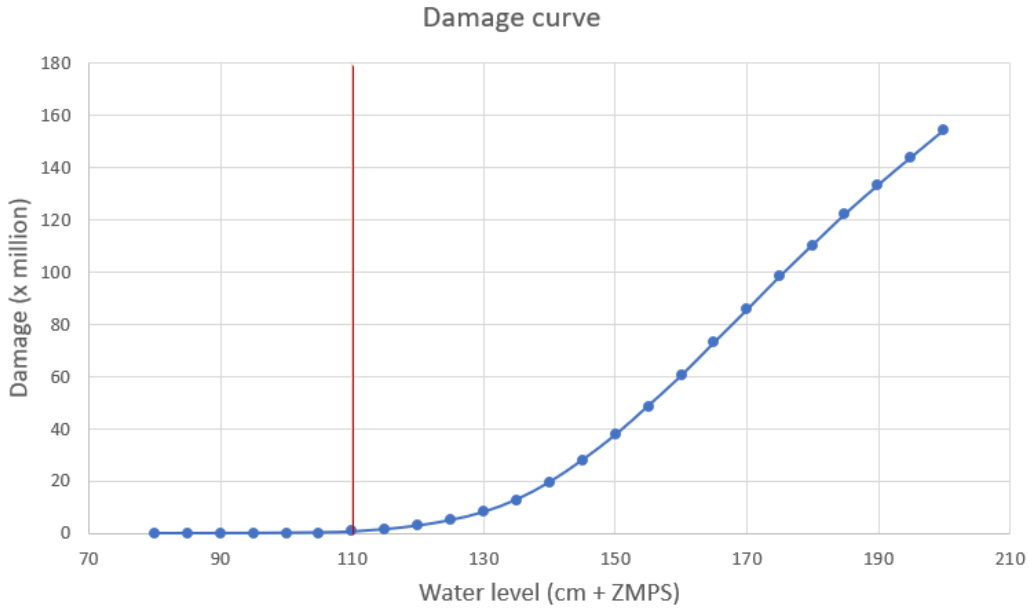

Figure 5.4: Damage curve city of Venice for different water levels without MOSE

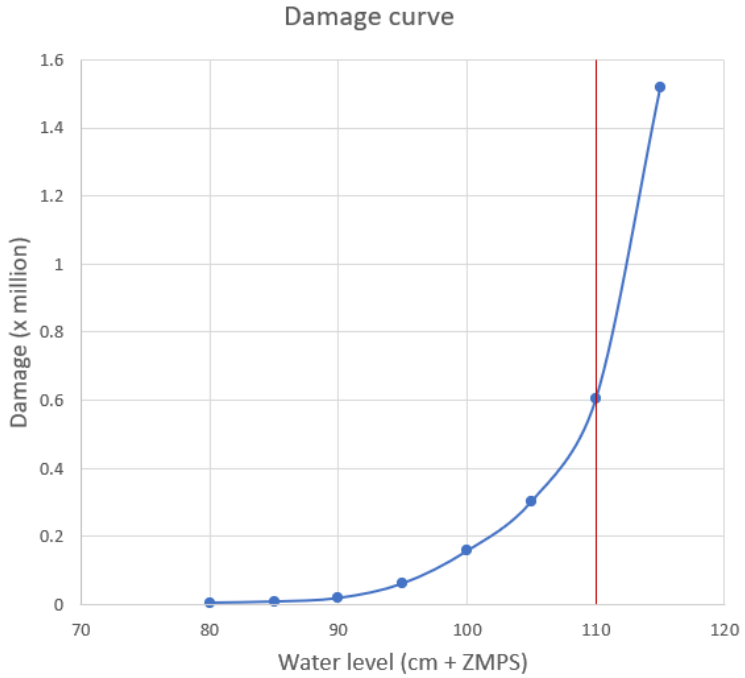

Figure 5.5: Damage curve zoomed in

The damage curves highlight the necessity of the MOSE. Damages from floods above 110cm + ZMPS increase exponentially to 20 million euros of damage per flood for a water level of 140cm + ZMPS. For floods above 140cm + ZMPS, the damage increase is linear.

Closing costs relate to the costs of closing the barrier. Personnel must be moved to the barrier islands to oversee the closing and patrol boats are needed to hold off marine traffic (Harlan and Pitrelli, 2022). These costs are estimated at 300,000 Euros per closure. More frequent closures also lead to a higher maintenance load. To conduct maintenance, the gates are transported to a dry dock. Many closures per year leaves less time to conduct this maintenance since the period over which the barrier closes are extended. Yearly maintenance costs are estimated at 80 million Euros per year (Carbonaro, 2019). There are no exact numbers on extra costs due to more closures per year. These costs will increase for more closures leading to higher costs each year. The port activities are also hindered for every closure as the ships must use locks to enter or leave the lagoon, taking up more time. For high tides, these locks cannot be used either, leading to a complete shut-down of port activities. These indirect costs are estimated at 350,000 to 1.3 million Euros per year, depending on the number of closures and the economic development rate (Vergano et al., 2010). The total damage per high water event is a sum of these components and is shown in Table 5.1. The yearly costs depend on the number of closures. When the barrier closes more often, the maintenance costs will be higher. It is difficult to estimate how much higher they will be.

Damage components	Damage (Euros)
Standard closing costs	300,000
Port activity damage	70,000
Damage from 110cm + ZMPS flood	602,700
Total damage per flood	972,700

Table 5.1: Total damage per flood

The damage per year is calculated by multiplying the number of closures per year with the cost of one closure. The damages are then added cumulatively until 2100.

The damages over time are calculated for the scenario where the trend in the annual maxima is real (D1 and D3 in the framework). The difference between the damages is due to the adaptation. The model will calculate the total damages up to 2100 twice, by changing the year of adapting to see the effect on the total damage. The SLR in 2050 and 2100 is calculated from the trend in annual maxima, which was found to be 1.02mm per year. This trend will be added on top of the historic trend in relative SLR of 2.38mm per year.

The total rate of sea level rise will be $0.102 + 0.238 = 0.340cm$ per year. Compared to 2020, this will lead to $0.34 * (2050 - 2020) = 10.2cm$ SLR in 2050 and $0.34 * (2100 - 2020) = 27.2cm$ in 2100. The year of adapting is chosen as 2025, and it will take the city 10 years to lift 30cm.

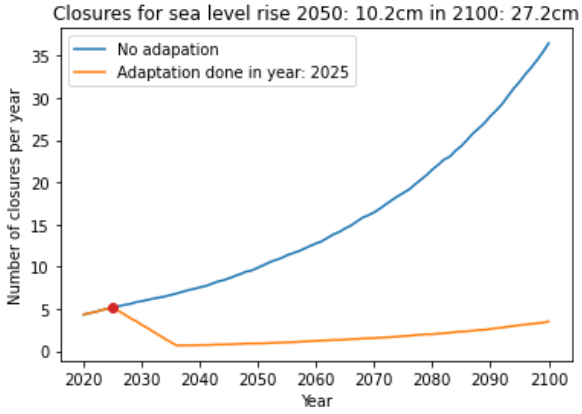

(a) Closures per year

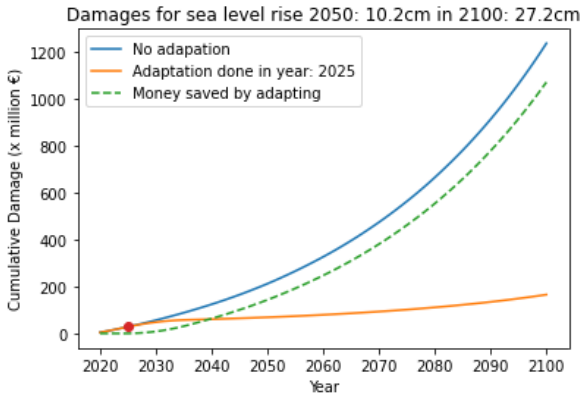

(b) Cumulative damage per year

Figure 5.6: Closures and damages for trend in annual maxima with adaptation in 2025

The difference between the damages is shown by a dashed green line, which indicates the amount of money saved by opting for the adaptation. If the cost of adaptation is below this line, the benefits outweigh the costs. However, this analysis does not consider the potential regret that would result from the scenario not occurring. For comparison, the same plot was generated with the adaptation year set to 2060 (see Figure 5.7). Although the total amount of money saved is still considerable, as the budget for adaptation is around 200-300 million euros for 2020 value, adapting in 2060 would result in approximately 500 million euros more in damages compared to adapting in 2025.

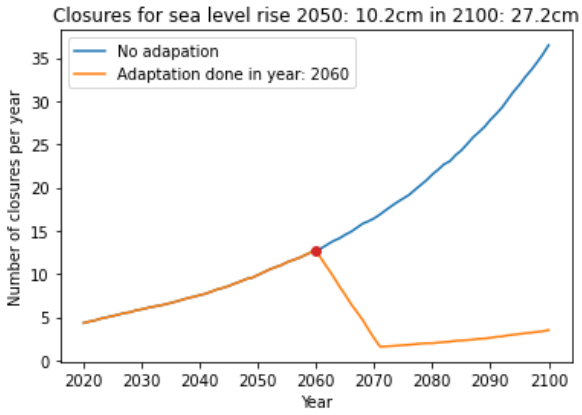

(a) Closures per year

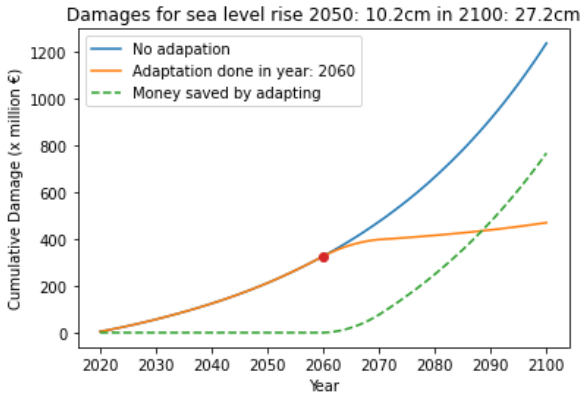

(b) Cumulative damage per year

Figure 5.7: Closures and damages for trend in annual maxima with adaptation in 2060

5.1.2 Regrets

The results from the previous sections are used to calculate annual expected damages and the regret associated with over-investment or under-preparedness. The steps for combining all the information to calculate damages and regret from 2020 to 2100 are shown in Figure 5.8.

The model calculates the number of closures per year. The number of closures for the selected sea-level rise scenario is plotted. From these closures, the damages can be directly calculated, and the

cumulative damages are plotted over the years to provide insight into the total damage from 2020 to 2100.

Over-investment regret occurs when the choice was made to adapt, but the expected trend does not occur. Under-preparedness regret occurs when the choice was made not to adapt, but the trend does occur. The equations for calculating these regrets are:

$$OverInvest = A + D2 - D4$$

$$Under - Prepare = D3 - D1 - A$$

To calculate the regret from over-investment, the damages of the alternative hypothesis where the trend does not occur need to be known. The model provides an option to specify the sea-level rise scenario used to calculate the damages for this alternative hypothesis.

To give probabilities to the errors leading to regret, alpha and beta factors can be specified. These factors are used to calculate the expected regret.

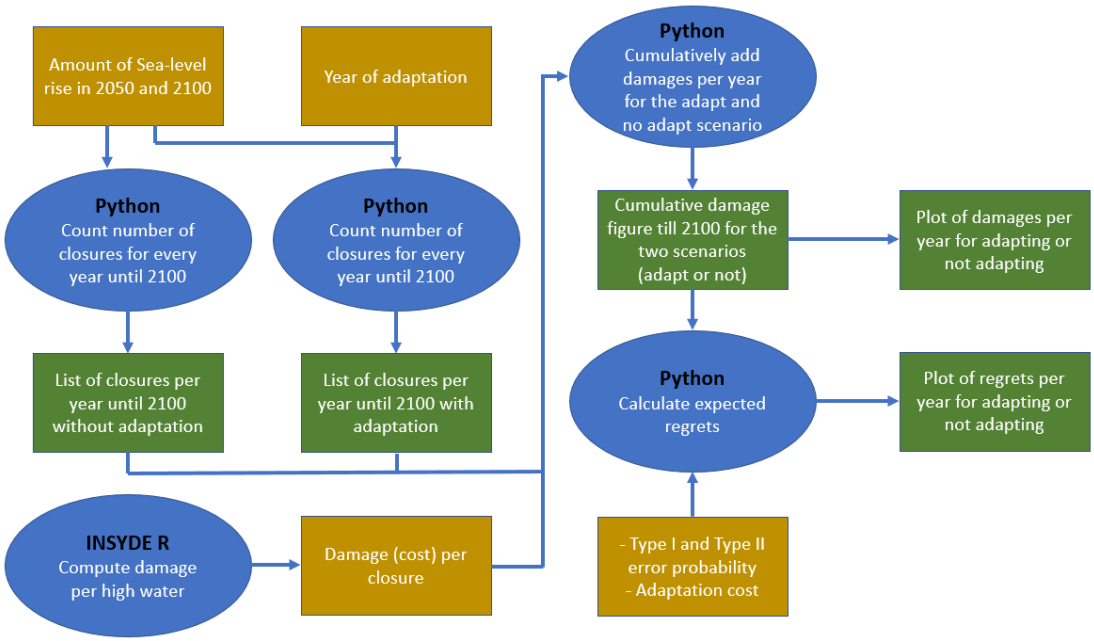

Figure 5.8: Flowchart for plotting the results of the framework

The regrets that arise from over-investing and under-preparing are calculated using the damages from Section 5.1.1. In addition to the damages associated with the chosen scenario, damages resulting from the alternative scenario are also considered. In the alternative scenario the extra trend in the extremes is not present. In Figure 2.2, these damages are referred to as D2 and D4. The cost of adaptation is also considered from now on.

To evaluate the regret in the scenario of the trend in the annual maxima, the same information is used as in Section 5.1.1. For the scenario without the extra trend in the extremes, the situation with only SLR from historic data is chosen. In this scenario, there is no additional SLR due to a trend in the annual maxima. Figure 5.9 displays the regrets over time. If the adaptation budget is higher, it will take longer for the adaptation scenario to have a smaller regret than the no adaptation

scenario. The adaptation budget can also be high enough that the regret never falls below the no adaptation regret, meaning that the adaptation is too expensive for the effect it brings over the years considered. However, this graph does not consider the uncertainties related to the trends, which can have a significant impact on the regret figure. In the next section, this will be added to the graph.

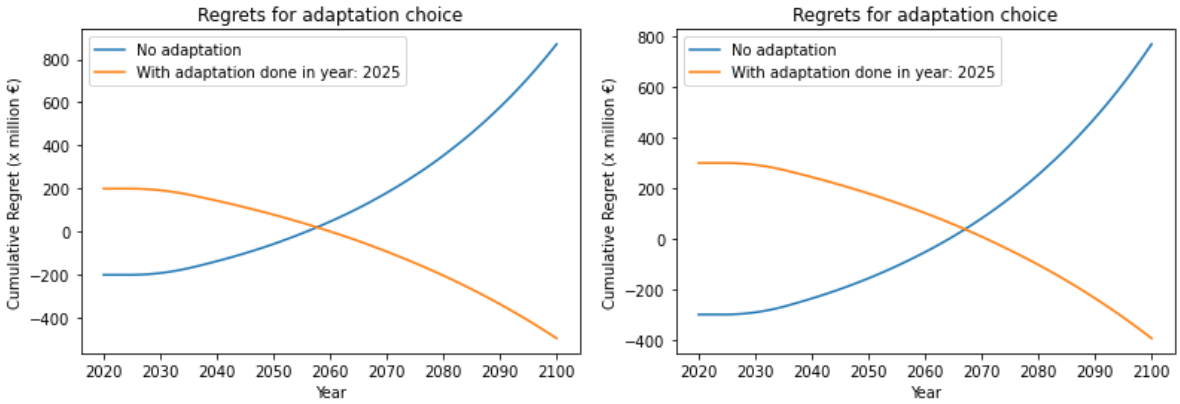

(a) Regrets with adaptation budget of 200 million (b) Regrets with an adaptation budget of 300 million

Figure 5.9: Regrets over the years for different adaptation budgets when additional trend in AM is considered as SLR scenario

5.1.3 Expected regrets

The Mann-Kendall test is used to assess if there is a significant trend in the dataset. This test checks if there is a long-term trend.

The significance of this trend is expressed by the p-value. The trend is considered significant if the p-value is smaller than 0.05 (Rosner et al., 2014). For the trend in the mean water levels, the p-value equals $4.4 * 10^{-16}$. The trend is therefore significant and should be taken into consideration. The trend in the annual maxima after detrending has $S = 530$. The variance $\sigma = 99813.33$ as calculated by the Mann-Kendall tool in Python. The standard score can be calculated:

$$Z = \frac{S-1}{\sqrt{\sigma}} = \frac{529}{\sqrt{99813.3}} = 1.674$$

The p value resulting from this Z score is:

$$p(Z) = \frac{1}{\sqrt{2\pi}} e^{-\frac{Z^2}{2}} = \frac{1}{\sqrt{2\pi}} e^{-\frac{1.674^2}{2}} = 0.094$$

So, the type I error probability is $\alpha = 0.094$.

The type II error probability is expressed as β and is calculated with Equation (2.10). This equation is filled in with:
$n = 96$
$t_{1-\alpha,n-2} = t_{0.906,94} = 1.326$
$\delta = \frac{1}{\sqrt{\frac{1}{0.174^2}-1}} = 0.177$

Resulting in: $\beta = P(T_{94} \leq 0.405) = 0.343$

The regret value from Section 5.1.2 is then multiplied by the error probability and yields the expected regret. In Figure 5.10, the same parameters were used as in Figure 5.9, but now the regrets are multiplied by the error probabilities.

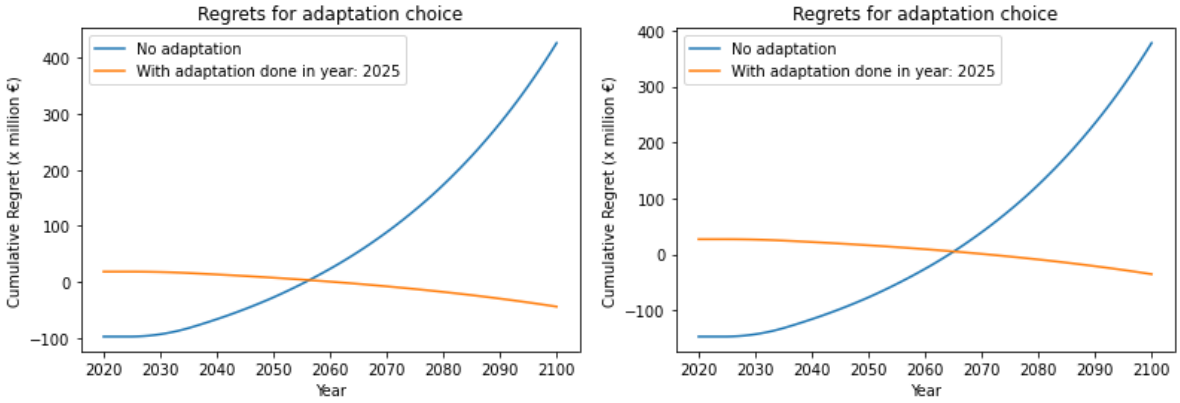

(a) Expected regrets with adaptation budget of 200 million

(b) Expected regrets with an adaptation budget of 300 million

Figure 5.10: Expected regrets over the years for different adaptation budgets when additional trend in AM is considered as SLR scenario

5.2 Randomness and uncertainties

The model has been developed based on values without uncertainties included. However, there are uncertainties associated with most of the numbers used in the model. This section aims to quantify some of these uncertainties to determine how much the results from the framework could vary.

To account for randomness, the number of peaks will be varied to see how much variability there is in the number of barrier closures. Inflation bounds will be added to the damages to account for the changing value of money over time.

5.2.1 Randomness in number of closures

The model calculates closures by lifting detrended data according to a chosen mean sea level. However, the same peaks are counted every time the dataset is lifted higher, while the peaks themselves are random. Nevertheless, the peaks for every year between 2020 and 2100 are not random. To evaluate the effect of randomness on the closures per year, peaks can be generated randomly.

If the water level dataset is adjusted for sea level rise, the number of peaks will increase. The rising of the dataset introduces new peaks. However, the peaks are always the same, and there is no variability in the number of peaks for a given amount of sea level rise. To introduce variance in the number of peaks per year, a randomizing process is added to the counting method.

The method involves drawing 80 years of water levels from the original dataset. First, the detrended water levels from the original dataset are split into 96 groups, grouping the water levels per year (1924-2019 is 96 years of data). Next, 80 years are randomly selected to represent 2020 until 2100. Each year has the data raised with the modelled level of sea level rise for that year. This results in 80 years of data with sea level rise present. Now the peaks are counted for each year, leading to 80 sums of peaks. This process is then repeated 500 times to create 500 different numbers of peaks per year. The process is displayed in a flow chart in Figure 5.11. For every year, the median, mean, and standard deviation are calculated. The 95% confidence interval is then calculated using the formula:

Confidence intervals:

$$CI(x) = \mu(x) \pm 1.96 \cdot \sigma(x)$$

Where:
$\mu(x)$ = Mean closure for year x
$\sigma(x)$ = Standard deviation of year x

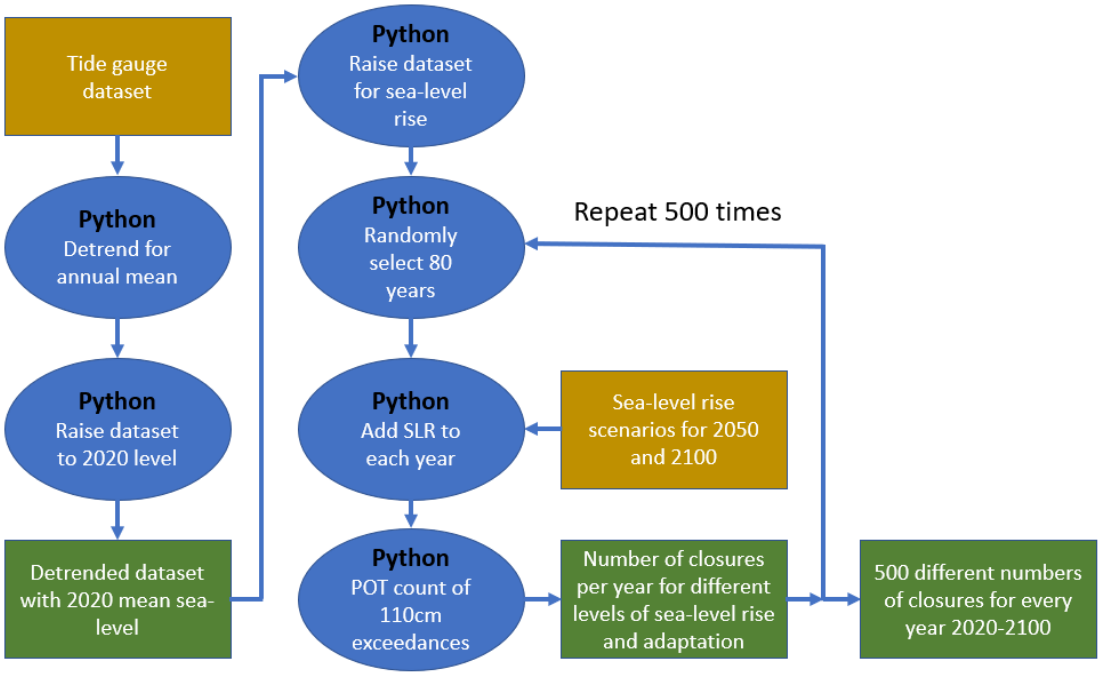

Figure 5.11: Flowchart for process of calculating number of closures with randomness

For each year, the median and standard deviation are calculated. The median and the 95% confidence intervals, generated from the standard deviation, are plotted in Figure 5.12 together with the closures calculated from the previous method.

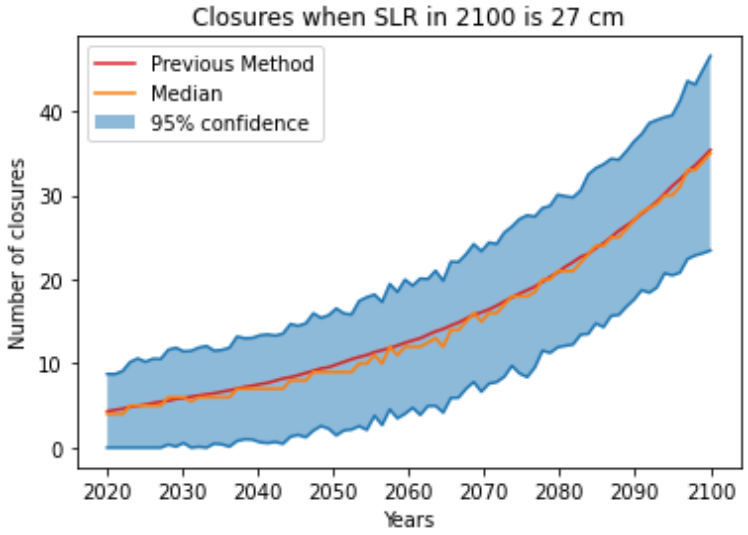

Figure 5.12: Results with randomness included compared to method without randomness

The result is a more realistic estimate of the number of closures. It is important to note that the number of closures does not necessarily need to increase every year, as there may be years with fewer closures. This variability is visible in the confidence interval, where the number of closures can even be zero between 2020 and around 2035.

5.2.2 Economic uncertainties

Due to inflation, the value of 100 million euros of damage in 2020 is not the same as 100 million euros in 2050 or 2100. Inflation reduces the purchasing power of money, meaning that future damages will cost more to repair in today's value due to higher prices. It is difficult to predict the inflation rate as global events such as economic crises, wars, and interest rates set by the European Central Bank can have a significant impact. The median expectation for inflation in the Euro zone is projected to be 2% until 2027 (O'Neill, 2023). However, inflation in the Euro zone has fluctuated between 4% and 0% since the introduction of the Euro (Bank, 2023), so these values will be used as the variability range. The possibility of no inflation is very unlikely due to the reinstated interest. This inflation factor also affects the adaptation costs as their costs are also impacted by inflation.

5.3 Rosner framework with uncertainties

The framework is filled in again, once for the trend in AM that is added and compared to the trend in the historic data, this is done in Section 5.3.1. In Section 5.3.2, the trend in the AM is assumed to be the only trend present and is compared to there being no trend in the data after 2020.

5.3.1 Trend in annual maxima

After introducing randomness in the number of closures, the confidence bounds can be plotted for the damages and regret as well. The results are depicted in Figure 5.13 and 5.14. The figures reveal that the regret associated with over-adapting in 2100 falls within the uncertainty bounds of the regret associated with under-preparedness.

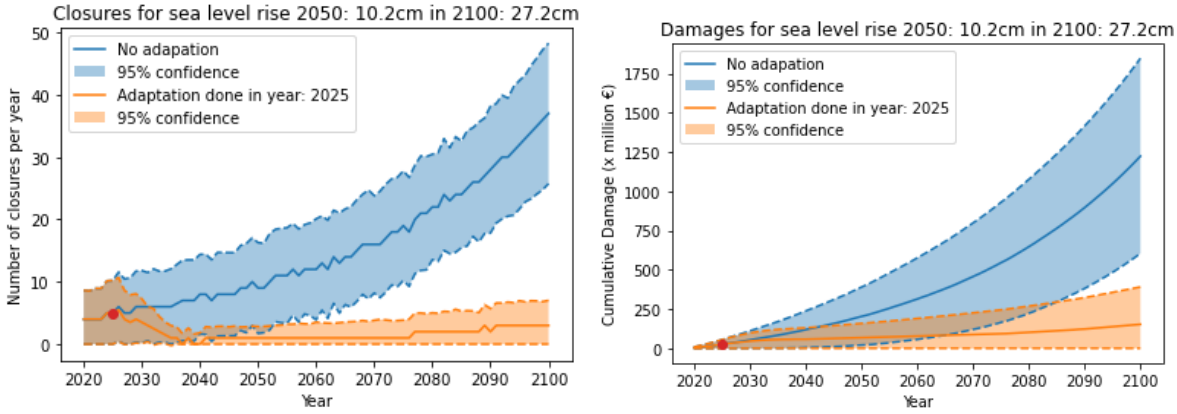

(a) Closures per year

(b) Cumulative damages

Figure 5.13: Closures and damages for trend in annual maxima with uncertainty bounds

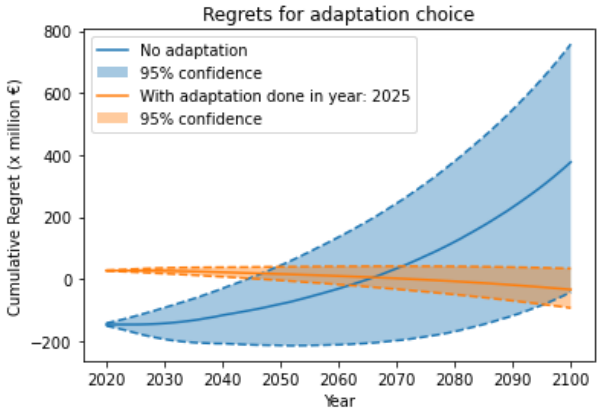

Figure 5.14: Regrets for trend in annual maxima

The same process is repeated for economic uncertainties. The results are shown in Figure 5.15 and Figure 5.16. The uncertainty is large for the damages in case of no adaptation. They vary from 1 billion to 4 billion depending on the inflation rate. The uncertainty grows over the years, rendering damage estimations more precise in the near future.

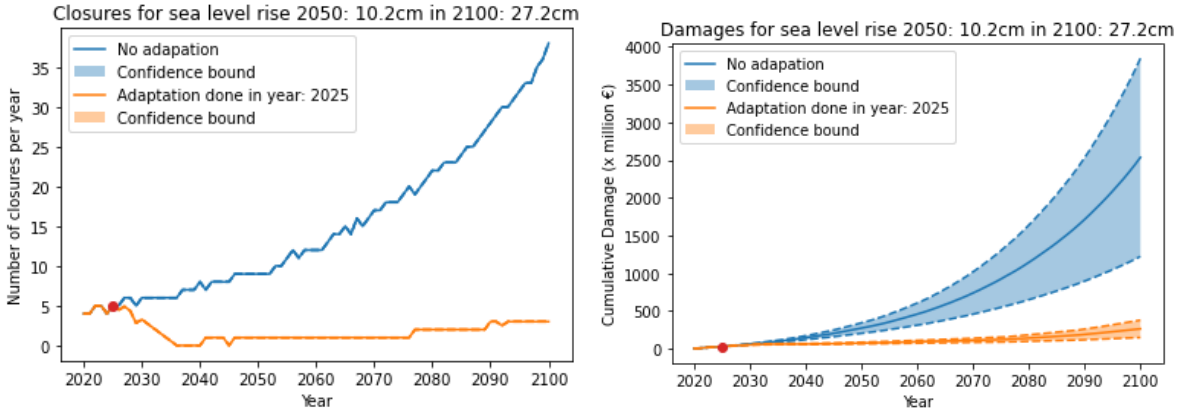

(a) Closures per year

(b) Cumulative damages

Figure 5.15: Closures and damages for trend in annual maxima with uncertainty bounds

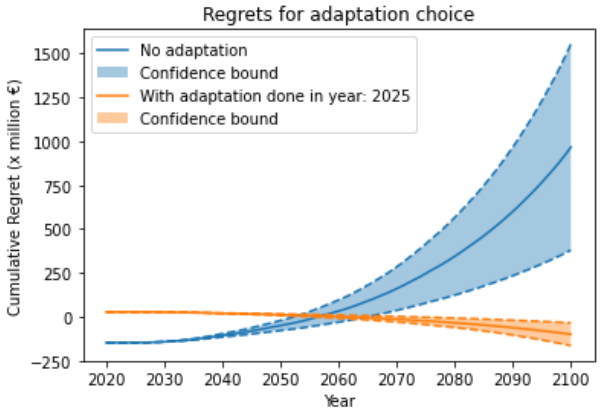

Figure 5.16: Regrets for trend in annual maxima

Combining the two uncertainty contributors by adding the 95% confidence bounds from the random closures with the positive and negative scenarios for inflation results in a wider spread area of confidence. The edges of the bounds represent a worst-case scenario at the top, combining both a negative inflation scenario with the highest number of closures, and a best-case scenario with no inflation and the lowest number of closures. The result is shown in Figure 5.17 and Figure 5.18.

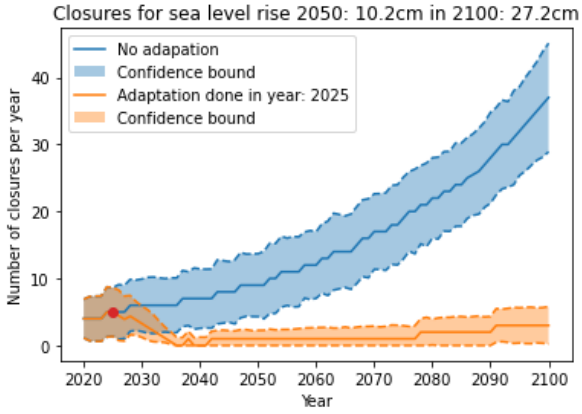

(a) Closures per year

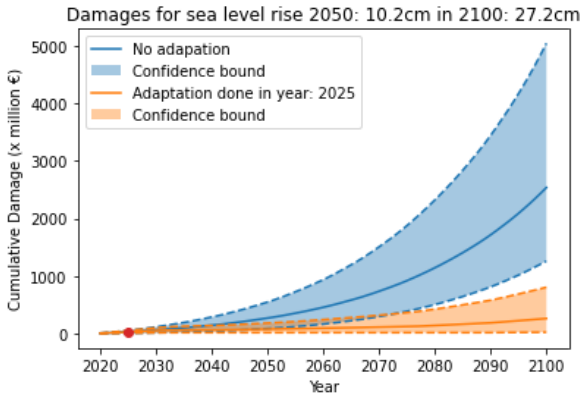

(b) Cumulative damages

Figure 5.17: Closures and damages for trend in annual maxima with uncertainty bounds

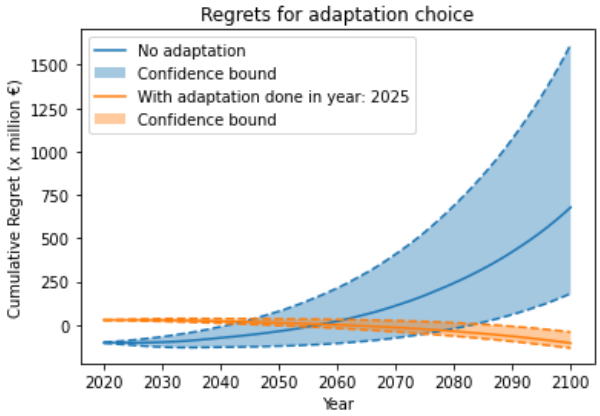

Figure 5.18: Regrets for trend in annual maxima

The resulting median damages and regrets are displayed in Table 5.2. The benefit for adapting in regret is around 860 million euros.

Scenario	Damage (mil. euros)	Regret (mil. euros)
No adaptation	2538	681
Adaptation	266	-104
Benefit	2272	785

Table 5.2: Resulting damages and regrets in 2100 for trend in annual maxima

5.3.2 Trend in annual maxima without historic SLR

The trend found in the annual maxima (AM) after detrending for mean sea level rise is analysed as an added trend on top of the rise in mean sea levels. This is realistic since mean sea level rise is significant and cannot be assumed to stop. However, it makes it difficult to see the effect of the trend in the AM in number of added closures and damages. To analyse this, the trend in the AM alone is used as input for the model. The closures and damages resulting from this analysis are shown in Figure 5.19.

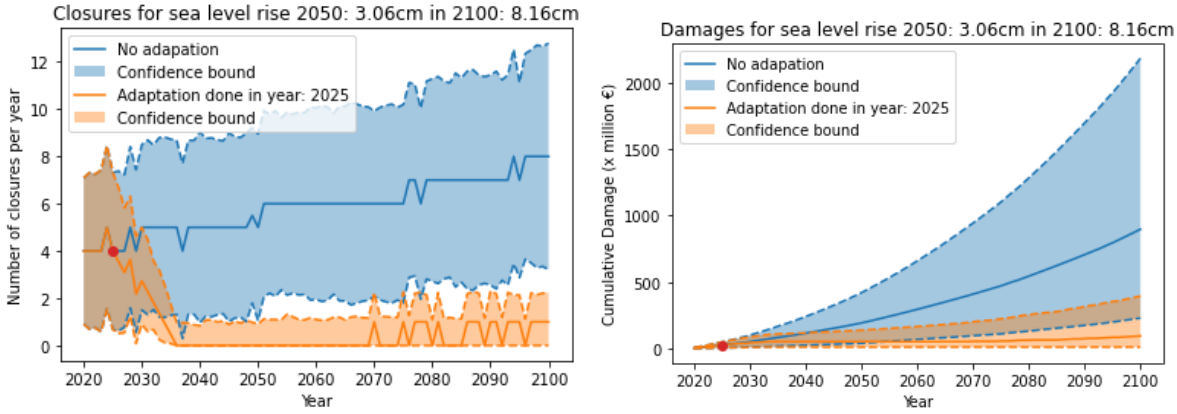

(a) Closures per year (b) Cumulative damages

Figure 5.19: Closures and damages for trend in annual maxima alone

The median increase in closures from this trend alone is 4 more closures per year in 2100 than in 2020. Even though this number of increases is minor compared to the increases due to mean sea level rise, the damages over the years still accumulate to hundreds of millions. To see if the adaptation is worthwhile, the regrets are calculated for two different adaptation budget scenarios. In Figure 5.20a, the regrets due to an adaptation budget of 300 million euros are shown. Even though the effect of this trend is small, and the barrier is still able to function normally with 8 closures per year, the adaptation strategy will lead to lower regret. This means the profits from nearly never having to close are larger than the costs of the adaptation. If due to economic circumstances or wrong estimations of cost the adaptation budget required would reach higher values, for example 800 million euros. The regrets for building the adaptation are not clearly lower and thus beneficial, as is shown in Figure 5.20b.

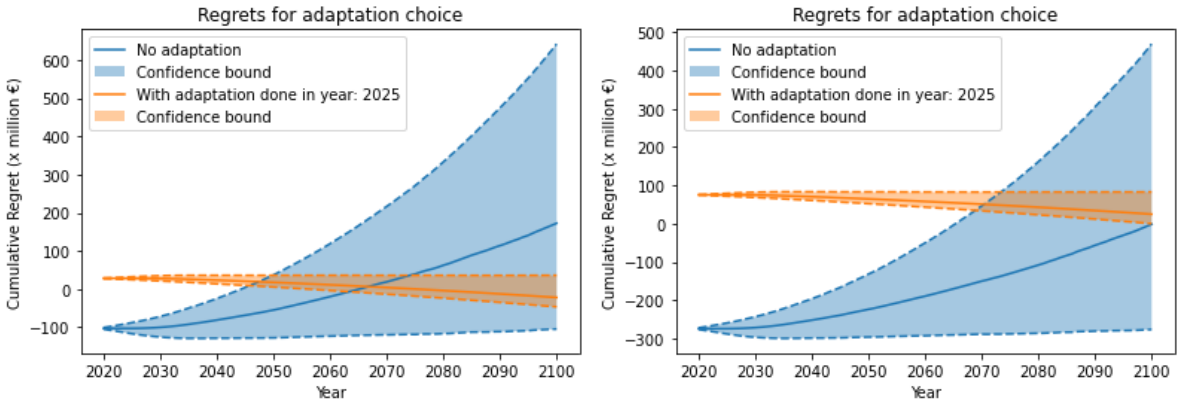

(a) Regrets for 300 million euros adaptation budget (b) Regrets for 800 million euros adaptation budget

Figure 5.20: Regrets for adapting to the trend in AM alone for different adaptation budgets

In Table 5.3, the damages and regrets for 2100 are compared for two adaptation costs. The adaptation path is beneficial when the costs of the adaptation are 300 million euros, 225 million euros benefit. However, when the costs are higher, in this case 800 million euro, the benefits are -26.2 million euros. This means the adaptation pathway leads to a regret that is 26.2 million euros higher than the regret that is obtained when no adaptation is made.

Scenario	Damage (mil. euros)	Regret Costs: 300 mil. (mil. euros)	Regret Costs: 800 mil. (mil. euros)
No adaptation	903	177	-1.5
Adaptation	87	-22	24.7
Benefit	816	199	-26.2

Table 5.3: Damages and regrets in 2100 from the trend in annual maxima alone

5.4 Modified Rosner framework applied for future SLR projections

The process of counting closures and computing damages is the same as the method used for the unmodified framework. The difference lies in calculating the expected regret, which cannot be done using error probabilities since these are calculated from historical data trends, which are not available for projections. To assign some probabilities to the scenarios, the probability of the scenario not occurring can be used instead of the error probability.

For different RCP scenarios, a comparison will be made between the scenario being likely or unlikely. When the scenario is likely, the regret over over-investing is multiplied by a small probability because the trend of this scenario is perceived as likely, and thus the chance of the trend not occurring is small. The regret for under-preparedness is multiplied by a large probability since the assumption is made that the scenario is likely. For the unlikely scenario, the process is repeated, but the probabilities are reversed. The formulas for the expected regret are:

Expected regret over-investment **likely** RCP scenario = Regret over-investment·0.15

Expected regret under-preparedness **likely** RCP scenario = Regret over-investment·0.85

Expected regret over-investment **unlikely** RCP scenario = Regret over-investment·0.85
Expected regret under-preparedness **unlikely** RCP scenario = Regret under-preparedness·0.15

The filled in frameworks for RCP4.5 and RCP8.5 are shown in this section. The number of closures for different SLR projections are shown in Section 4.2. The damages, regrets and expected regrets for these scenarios are shown in Section 5.4.1, Section 5.4.2 and Section 5.4.3, respectively. Uncertainty is then added to the number of closures as well as the damages, results from this analysis can be seen in Section 5.4.4.

5.4.1 Damage pathways

The same process used for the historic framework can be applied to the SLR projections, using the projected SLR for 2050 and 2100 as input for the model. The values for these projections can be found in Section 4.1.2. The number of closures for the 4.5 scenario is shown in Figure 5.21a. Without adaptation, the number of closures will exceed 150 per year before 2080. With the adaptation, the number of closures in 2100 is around 50, which would still make the barrier usable.

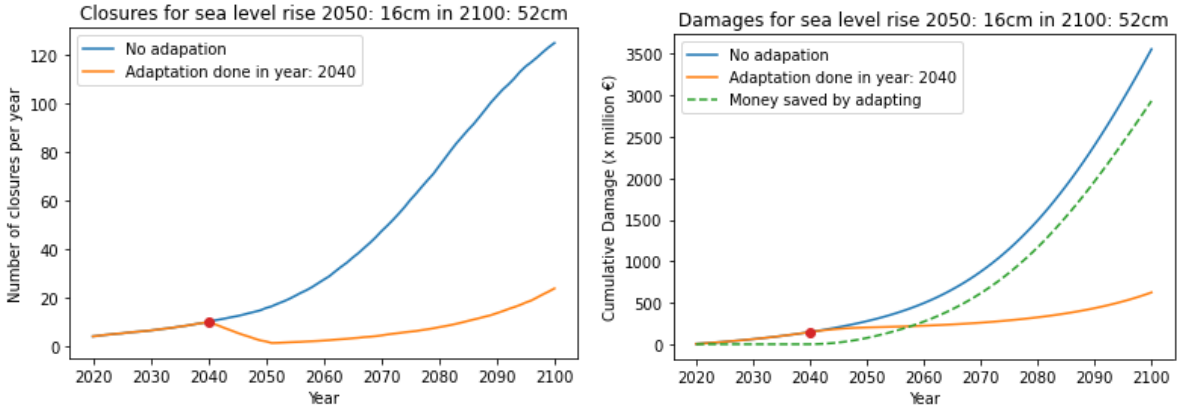

(a) Closures per year

(b) Cumulative damage per year

Figure 5.21: Closures and damages for RCP 4.5 scenario with adaptation in 2040

The extreme 8.5 scenario renders both the adaptation and no adaptation strategies ineffective, making the barrier unusable. However, building the adaptation provides more time before the barrier becomes obsolete, and it also results in cost savings due to reduced damages during the time that an alternative solution is sought.

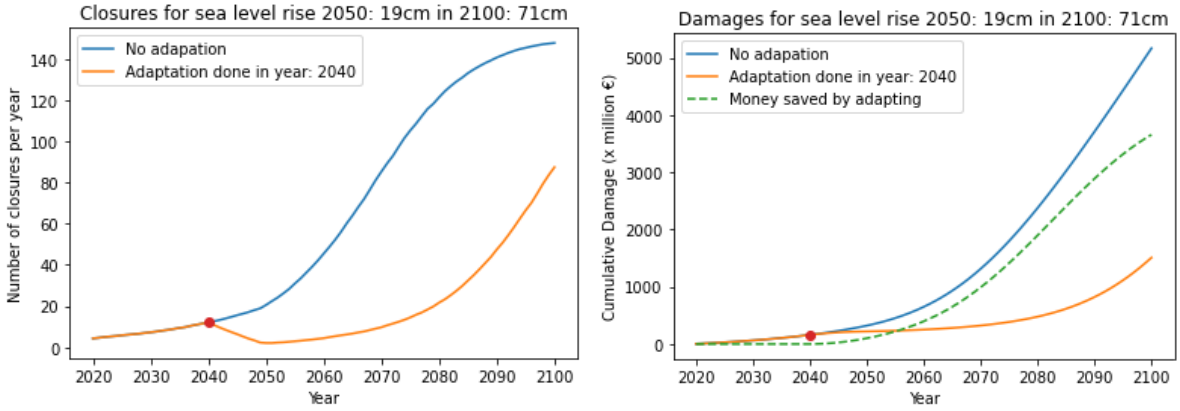

(a) Closures per year

(b) Cumulative damage per year

Figure 5.22: Closures and damages for RCP 8.5 scenario with adaptation in 2040

5.4.2 Regrets

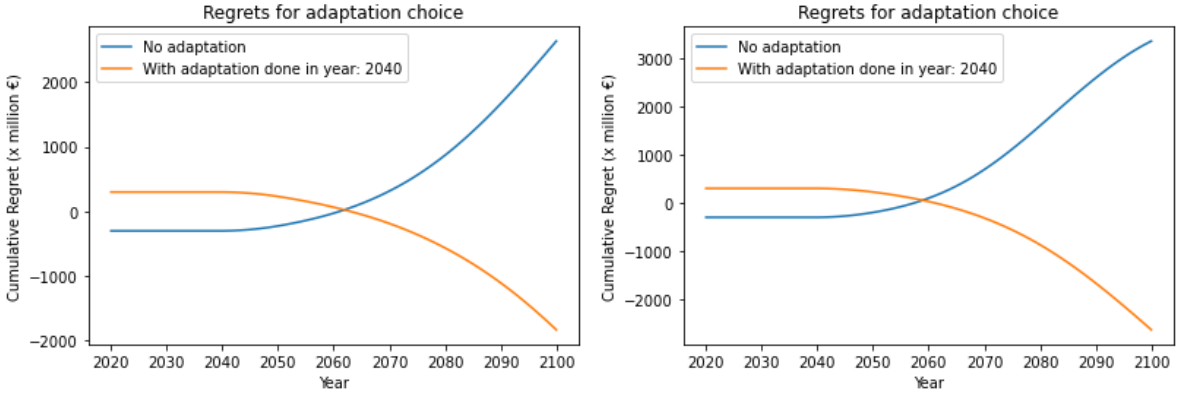

(a) Regrets when assuming RCP4.5 scenario

(b) Regrets when assuming RCP8.5 scenario

Figure 5.23: Regrets for RCP4.5 and 8.5 scenarios

5.4.3 Expected regrets

It is not possible to calculate the errors of RCP scenarios since they are projections and not extrapolations of existing measured trends. Which scenario will happen is unknown at the moment because it depends on human activities more than anything else. As time goes by, it might become more evident which scenarios are more likely than others. In this case, the different scenarios could be given weights to reflect the likelihood of the scenario happening. This makes the regrets more meaningful, although it would also introduce extra uncertainty due to the assumptions made when defining the weights.

The results from the RCP8.5 unlikely and likely scenario are shown in Figure 5.24.

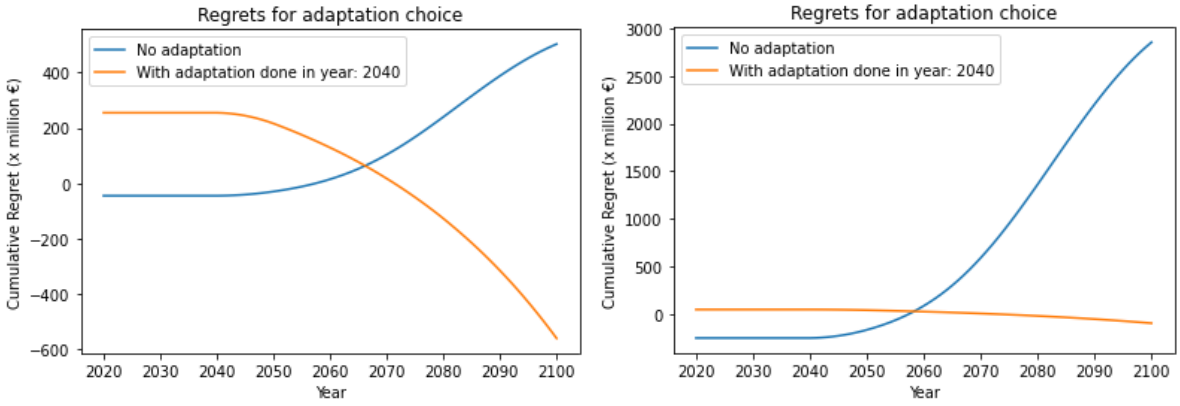

(a) Regrets when RCP8.5 scenario is unlikely (b) Regrets where RCP8.5 scenario is likely

Figure 5.24: Comparison regrets for RCP8.5 scenario unlikely or likely

The results from the RCP4.5 unlikely and likely scenario are shown in Figure 5.25.

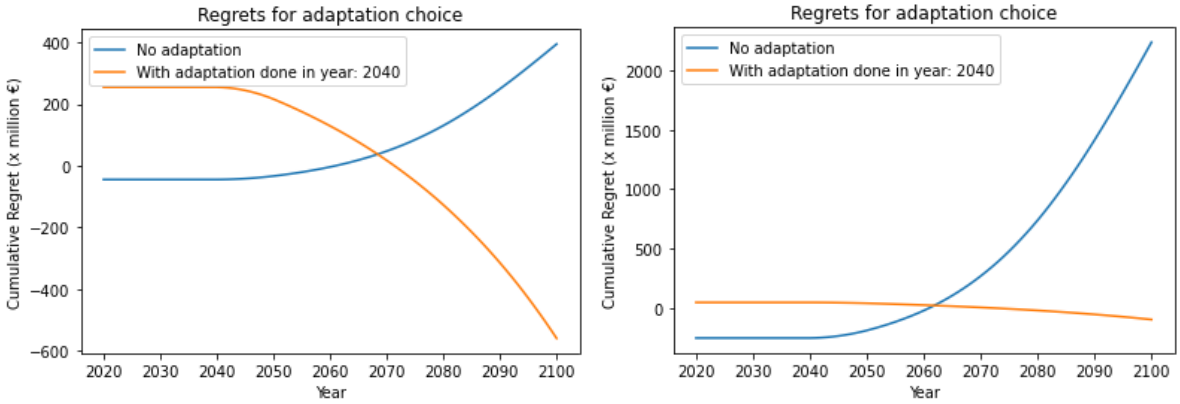

(a) Regrets when RCP4.5 scenario is unlikely (b) Regrets where RCP4.5 scenario is likely

Figure 5.25: Comparison regrets for RCP4.5 scenario unlikely or likely

5.4.4 Framework with uncertainties

Figure 5.26 compares the regrets for RCP scenario 8.5 being likely or unlikely. When the scenario is unlikely, the regret of adapting is still lower than not adapting. This is the case because the damages from the scenario are extremely high and the costs of adapting low. So even for a small chance, the loss of adaptation money compared to the potential damages from the case where the RCP8.5 scenario happens is low.

When the scenario is likely, the regret of no adaptation is a lot larger than adapting, leading to a more profound preference for the adapt option.

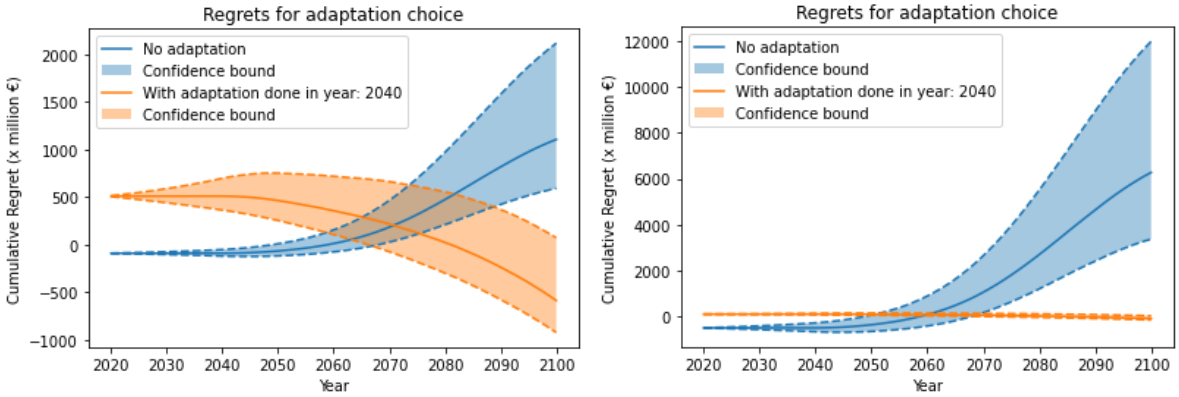

(a) Regrets when RCP8.5 scenario is unlikely

(b) Regrets where RCP8.5 scenario is likely

Figure 5.26: Comparison regrets for RCP8.5 scenario unlikely or likely

The choice gets less evident when the adaptation is postponed. Let us say the adaptation is done in 2070 and the costs have risen to 1 billion euros due to inflation. In Figure 5.27 can be seen that the uncertainty bounds overlap almost entirely. The regret from the adaptation strategy is very uncertain in this case due to the RCP8.5 scenario being unlikely.

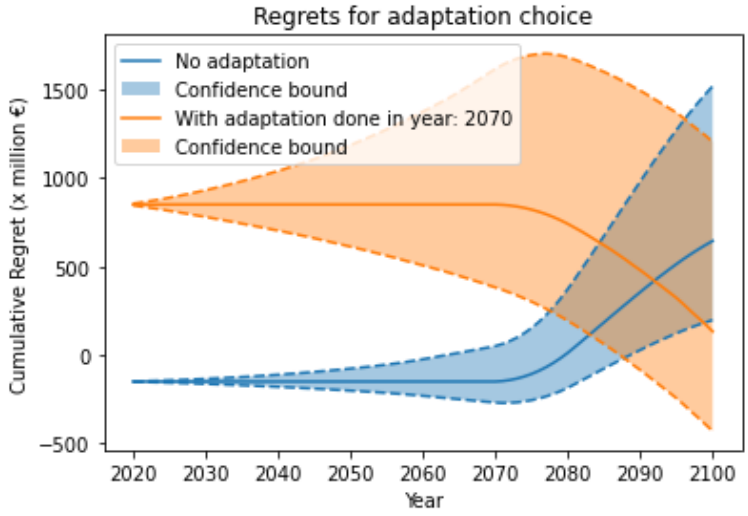

Figure 5.27: Regrets when RCP8.5 is unlikely, and the adaptation is done in 2070

The benefits resulting from an adaptation pathway are large enough to make this the preferable option when RCP8.5 is both likely and unlikely. Table 5.4 shows the benefit does become smaller when the scenario is unlikely and if the adaptation is built at a later moment.

Scenario	Regret RCP8.5 unlikely (mil. euros)	Regret RCP8.5 likely (mil. euros)	Regret, late adaptation RCP8.5 unlikely (mil. euros)
No adaptation	1076	6104	673
Adaptation	-414	-71	-43
Benefit	1490	6175	716

Table 5.4: Regrets in 2100 compared for RCP8.5 likely or unlikely

6 Discussion

6.1 Extreme Value Analysis

The non-stationary GEV distribution fitted the detrended maxima better than the stationary GEV distribution. This could imply a trend in the data since the linear time varying parameter improved the fit more than the penalty in the AIC. However, the Mann-Kendall test did not find a significant trend in the detrended maxima. Therefore, a non-stationary fit would traditionally not be considered after detrending, and a stationary approach would be adopted. The difference between the return periods is large and would have implications on the design of the protection measure. (Luke et al., 2017) argued against the use of non-stationary methods since their behaviour when extrapolated in the future could be wrong. When a quadratic time varying parameter was fitted, the AIC results were still better than the stationary approach. However, when this was extrapolated into the future, the results became psychically impossible, demonstrating the fit was only suited for the historical data and could not be used for future predictions. This makes non-stationary methods difficult to imply. However, falsely disregarding a trend could lead to insufficient designs which could lead to large damages.

When comparing different methods to fit a non-stationary distribution to water level data, the transformed stationary method (TS) showed a jump in the return level of a 1/100-year event. This changed the oscillation of the TS method around the stationary fit to the non-stationary fit. The jump is caused by a change in measurement frequency and the effect that has on the standard deviation on the dataset. Why it follows the stationary line and then follows the non-stationary line is not known.

6.2 Method for estimating future closures

The method used to calculate future closings is limited to water levels observed in the past, which means that the effects causing these high-water levels are not considered. High water levels are caused by waves and set-up due to wind speed, as well as precipitation levels. The depth of the Adriatic Sea and the Venice lagoon also affects set-up and wave heights. Mean sea level rise is considered the main contributor to the larger number of closures expected in the future. While the data is randomly shuffled to create variance, the peaks are assumed to be the same, with only the mean sea level changing. However, changes in wind speeds, precipitation levels, and depth-influenced effects are not considered. These contributors could vary due to climate change and could increase water levels in the city, leading to more closures than predicted here, or could lead to fewer closures, depending on how these contributors change in the future.

The MOSE barrier is closed before the safeguarding level of 110 cm + ZMPS is reached, and that decision is based on various components and predictions, as described in Appendix A. The method chosen in this research, counting events where the barrier should have closed, does not consider closure scenarios where the safeguarding level was not reached. Predictions may suggest closing the barrier because the water level is expected to reach 110 cm + ZMPS, but it does not actually reach this level. This could increase the number of actual closures.

6.3 Damages

To calculate the damage per flood event, the INSYDE model computes damages based on the water level present at or in the building. However, this water level is assumed to be the same in every place within the city. In reality, the wind, water flow velocity, and narrowness of streets will have an impact on how high the water levels are in front of specific buildings. There will be differences in actual damage costs between different buildings.
The water level present during closures is assumed as 110cm + ZMPS since this is the level the barrier

closes for. During actual closures, the barrier will close at a lower water level and the water depth in the city is likely lower than 110 cm + ZMPS. However, the barrier blocks water from flowing out into the sea, leading to higher water levels inside the lagoon due to river inflow and rainfall. This could lead to an increase in water level in the city. Once again hydrodynamic models could make a better predication of water levels inside the lagoon during a closure event.

The costs are calculated from insurance claims collected from previous flood events. These were larger floods than 110cm + ZMPS, so it is questionable how well these figures can be applied to low-level floods.

The damages are added cumulatively for every closure event per year. If these events occur in short succession, parts of the damage figure will change. Damages to buildings may not be repaired in time for the next event, so the damage cannot occur again. This causes damages to be overestimated. On the other hand, if parts of the building get wet repeatedly, the damage could be larger than the damage from just one flood.

The cost of maintenance is not considered for the damages because it is hard to specify the cost for a single closure in terms of extra maintenance. It can be assumed that these costs will increase for more frequent closures since the gates will take more load and thus need more checks and repairs. This could be a considerable amount of money since the maintenance budget is around 60 million euros per year from 2020 to 2030. This causes an underestimation of the damages for more frequent closing.

6.4 Sea level rise projections

The projections from the (NASA, 2022) are very uncertain, and the actual sea level rise level for 2100 is hard to estimate. The modified framework does allow for comparing different scenarios and assigning probabilities to them. The adaptation of raising the city provides benefits, even for small sea level rise. In this situation, the result is useful even if the uncertainties are large. The tool is, however, unreliable when the projections are closer together. The uncertainties are too large to make a clear adaptation choice in that scenario.

6.5 Possible alternative adaptions

In Section 3.2, the distribution of closures throughout the year is analysed for various levels of sea level rise. As sea levels rise beyond 20cm, the barrier is required to close all year round, leaving no extended periods for maintenance.

In all scenarios, the barrier will have to close for days on end by the end of the 21st century. In these moments, the barrier will function more like a dam than a barrier since it does not open anymore. The first option is to delay this process by the proposed adaptation in this research. Raising the city decreases the number of closures and for lower SLR projections the barrier will still be open most of the time in 2100. For more severe SLR projections the barrier loses its function however, it happens years later than without the adaptation.

When SLR exceeds 45cm compared to 2020, the barrier will be closed more than it is open, necessitating an alternative solution. One possibility is to replace the barrier with a closed dam, which could protect the city from SLR up to the height of the dam. However, this option would have significant ecological impacts on the lagoon, making it an unpopular choice.

To preserve the ecology of the lagoon, another option could be to dam the city itself, protecting it from high water levels while allowing water to flow in and out of the lagoon to the Adriatic Sea. However, this would require the construction of visible dams and the implementation of lock systems and in/out flow systems to maintain water quality.

The costs of these measures vary and need to be evaluated to determine their feasibility, based on the budget allocated for ensuring the safety of the city. No matter which option is chosen, the lagoon ecosystem will be affected to some extent, but MOSE has been designed to minimize its impact. However, if closures become more frequent, the lagoon system will be increasingly disturbed. Additionally, if MOSE were to be closed for extended periods, a system would have to be developed to dispose the water that flows into the lagoon, ensuring good water quality and lowering the water levels inside the lagoon.

7 Conclusion

The main research question will be answered by the answers to the sub-questions. The main research question is:

How to implement the (Rosner et al., 2014) adaptation framework for sea-level rise in Venice?

Answers to the sub-questions:

- How do stationary and non-stationary extreme value analysis results compare when applied to historical water level data in Venice?

  When comparing the different methods of extreme value analysis, the return levels are similar for the different non-stationary analysis. However, the stationary approach results in lower return levels, and the difference between the stationary and non-stationary approaches increases over time. The Transformed Stationary (TS) approach follows the stationary values for the years with less frequent measurements and a smaller standard deviation in the data. As the measurement frequency increases and the standard deviation of the data increases, the transformed stationary approach leads to return values like the other non-stationary methods. When the fits are extrapolated to 2100, the stationary analysis has a return level that matches the expected sea level rise (SLR) scenario based on historical trends. On the other hand, the non-stationary methods match the return level of the RCP4.5 SLR scenario, while the TS method matches the RCP8.5 SLR scenario.

- Does the barrier have to close more in the future due to sea-level rise and if so, how much more?

  It is expected that the barrier will need to close more frequently in the future due to sea level rise. The amount of increase in closures depends on the sea level rise scenario. For SLR increases of up to 10 cm, the closure interval ranges from 2 to 18 closures with a median of 10 closures per year. This is more than double the expected number of closures for 2020, which is 4.3. Therefore, it is expected that there will be more closures, but it is also possible that the number could be lower or remain unchanged. If the historical trend in sea level rise continues for Venice, 10 cm SLR is expected by 2060. However, for increased SLR scenarios like the ones suggested in RCP4.5 and RCP8.5, 10 cm SLR is projected to occur as early as 2040.

  For SLR scenarios arising from RCP4.5, RCP7.0, and RCP8.0, the number of closures will increase to over 100 per year before 2100. This means that the barrier will need to remain closed for consecutive months.

- Which costs are related to the more frequent and longer closures?

  The costs considered in this research include the damage to the city caused by more frequent high-water levels, direct costs of closing the barrier, and loss of income for the harbour. These effects combined lead to a cost of 972,200 euros per closure. When the barrier must close, the water level in the city reaches 110 cm, and the cost of structural damage from this water level is calculated to be 602,700 euros. The direct costs of closing are 300,000 euros, and the loss of income for the harbour is 60,000 euros per closure. The total costs are the product of the number of closures and costs per closure.

- How large are the damages for the different scenarios?

  The total cumulative damage in 2100 ranges from 100 million euros to over 10 billion euros, depending on the SLR scenario and the choice of adaptation. For the scenario where SLR is expected to follow the trend in annual maxima on top of the historic trend in SLR, the damage with the adaptation executed is 266 million euros. Without the adaptation in place, the damage will be 2,538 million euros in 2100.

For the RCP8.5 scenario, the damage with adaptation in place by 2040 is 3,328 million euros. When no adaptation is in place, the damage accumulates to 11,294 million euros. Damages are smaller in 2100 when the adaptation is done sooner.

- What are the regrets for the different scenarios?

  The regrets related to over-adapting, which occur when the adaptation is built without the trend being present, are lower than the regrets relating to over-preparedness in all cases. This means the adaptation path is economically favourable compared to the non-adapting path. The reason for the economic benefit of adaptation is due to the large damages that will occur without adaptation, combined with the low costs of adapting. The inexpensive adaptation will save expensive damages. The benefit of adapting increases for higher SLR scenarios. Only when the increase in SLR is assumed small and the adaptation costs are high, the regrets of adapting are larger than the regrets resulting from not adapting.

  The benefit of adapting in the scenario where SLR is taken as the trend in annual maxima is 785 million euros. If the RCP8.5 scenario is assumed unlikely, the benefit is 1,490 million euros in 2100. If the scenario is assumed likely, the benefit is 6,175 million euros. In both cases, the benefit is large enough to justify adapting even if the scenario is unlikely.

- What conclusions can be drawn from the framework?

  The option to adapt appears to be the favourable choice for all SLR scenarios. This is due to the significant benefits of raising the city and reducing the number of closures. These benefits also hold when there is no increase in SLR. Therefore, adapting for increasing SLR will always result in lower regrets than not adapting. Only if the cost of adaptation is assumed to be higher, at 800 million euros instead of 300 million euros, and the increase of SLR is limited to the trend in annual maxima alone, the adaptation path can lead to larger regrets than the non-adaptation path. In conclusion, even though there is considerable uncertainty regarding regrets, adapting to SLR is the recommended approach. This is under the assumption that the adaptation of lifting the city is technically achievable, which was not investigated in this thesis.

- Is the MOSE barrier the right adaptation if sea-level rise increases?

  The MOSE barrier can protect the city against SLR up to 60 cm. However, it would mean that the barrier must be closed throughout the year and would lose its function as a storm surge barrier. Additionally, the barrier is not designed to remain closed for extended periods, and hence an adaptation is required. The time it takes to reach 60 cm of SLR will again depend on the various scenarios, but it will result in a more closed than open situation by 2100. To provide more time for alternatives, the city could be lifted. This way, the barrier can still function as a storm surge barrier until 2100, and if SLR follows a mild scenario, an alternative might not be required.

- Which alternatives are there?

  Alternatives include the complete closure of the Venice lagoon, which would cause large ecological damage, and building dams around the city, which is another possibility. In both alternatives, either the lagoon sustains ecological damage, or the sights around Venice are affected.

8 Recommendations

- Calculate the number of closures with hydrodynamic models.

  In this research, the method for calculating the number of closures is based only on previously observed water levels and when the barrier would have closed. Multiple factors influence the closure of the barrier. This could lead to closures even though the 110 cm water level is never reached. A hydrodynamic model that takes wind speed and river inflow into account can more accurately calculate the number of closures for various levels of SLR.

- Adaptations are required to keep MOSE functional for as long as possible.

  The adaptation of lifting the city by injecting seawater into soil layers underneath the city of Venice should be considered. Research will have to be done on the feasibility of this adaptation, including evaluation of the costs, expected settling differences, and the risks that it poses to the structures. It is also important to investigate how much the city can rise with this method and the timeline of the project.

- Different adaptation scenarios should be worked out to deal with various levels of SLR.

  Depending on the level of SLR, alternatives to MOSE are required. This can include damming the entire lagoon, constructing a dam around the city, or implementing measures within the city to prevent flood damage. The best-suited adaptation depends on the city's preferences, the water levels present and expected, and the costs of the different measures. The framework proposed by (Rosner et al., 2014) can be used to assess trends in the water level over the coming years and compare the effects of different adaptations. This may lead to different pathways, where the chosen path is decided based on new SLR observations and projections in Venice.

- When conducting an Extreme Value Analysis (EVA), compare stationary and non-stationary methods even if trend tests suggest there is no significant trend present.

  If there is no significant trend present, a stationary EVA is the best fit, and non-stationary methods are not considered. However, in this research, it was found that non-stationary fits yielded a better fit than the stationary method. There was a significant difference in design return value, which is why the non-stationary fit should be considered.

References

Bank, W. (2023). *European Union Inflation Rate 1960-2023.* Macrotrends.

Buckley, J. (2022). The flood barriers that might save venice. *CNN.*

Carbonaro, G. (2019). *What's happened to Venice's MOSE flood defences?* CGTN News.

Cavallaro, L., Iuppa, C., and Foti, E. (2017). *Effect of Partial Use of Venice Flood Barriers.* J. Mar. Sci. Eng. 2017, 5, 58.

Coles, S. (2001). *An Introduction to Statistical Modeling of Extreme Values.* Springer-Verlag London limited.

Coles, S. and Pericchi, L. (2006). Extreme value analysis in civil engineering: An overview. *Journal of Structural Engineering, ASCE.*

Fontinia, F., Umgiesser, G., and Vergano, L. (2010). *The role of ambiguity in the evaluation of the net benefits of the MOSE system in the Venice lagoon.* Ecological Economics, Volume 69, Issue 10, 15 August 2010, Pages 1964-1972.

Glavovic, B., Dawson, R., Chow, W., Garschagen, M., Haasnoot, M., Singh, C., and Thomas, A. (2022). *Cross-Chapter Paper 2: Cities and Settlements by the Sea.* Climate Change 2022: Impacts, Adaptation and Vulnerability. Contribution of Working Group II to the Sixth Assessment Report of the Intergovernmental Panel on Climate Change [H.-O. Pörtner, D.C. Roberts, M. Tignor, E.S. Poloczanska, K. Mintenbeck, A. Alegría, M. Craig, S. Langsdorf, S. Löschke, V. Möller, A. Okem, B. Rama (eds.)]. Cambridge University Press, Cambridge, UK and New York, NY, USA, pp. 2163–2194.

Gumbel, E., Hwang, S., and Albrecht, P. (2009). Application of extreme value analysis for design of wind turbine structures. *Journal of Solar Energy Engineering, ASME.*

Haigh, I. et al. (2014). Non-stationary extreme value analysis for design of coastal structures in a changing climate. *Coastal Engineering.*

Handwerk, B. (2012). *Injections Could Lift Venice 12 Inches, Study Suggests.* National Geographic News.

Harlan, C. and Pitrelli, S. (2022). *An engineering marvel just saved Venice from a flood. What about when seas rise?* The Washington Post.

Hausfather, Z. (2018). *Explainer: How 'Shared Socioeconomic Pathways' explore future climate change.* CarbonBrief.

Jordà, G., Gomis, D., and Marcos, M. (2011). *Comment on "Storm surge frequency reduction in Venice under climate change" by Troccoli et al.* Springer Science+Business Media B.V.

Katz, R., Parlange, M., and Naveau, P. (2002). Design of water resources systems using extreme value analysis. *Water Resources Research.*

Kolbus, C. (2019). *MOSE: The Future of Venice.* Engineering Rome.

Li, D. et al. (2020). Non-stationary extreme value analysis for bridge design in a changing hydroclimate. *Journal of Hydrologic Engineering, ASCE.*

Lionello, P. (2005). *Extreme storm surges in the Gulf of Venice: present and future climate.* Cambridge University Press.

Luke, A., Vrugt, J. A., AghaKouchak, A., Matthew, R., and Sanders, B. F. (2017). *Predicting non-stationary flood frequencies: Evidence supports an updated stationarity thesis in the United States.* Water Resources Research volume 53, issue 7, pages 5469-5494.

Melchers, R. (2010). Extreme value analysis for design of offshore structures. *Journal of Offshore Mechanics and Arctic Engineering, ASME.*

Mentaschi, L., Vousdoukas, M., Voukouvalas, E., Sartini, L., Feyen, L., Besio, G., and Alfieri, L. (2016). *The transformed-stationary approach: a generic and simplified methodology for non-stationary extreme value analysis.* Hydrol. Earth Syst. Sci., 20, 3527–3547.

Milly, P. et al. (2008). Stationarity is dead: Whither water management? *Science magazine, AAAS.*

MOSEVenezia (2022). Mose system, the mobile barriers for the protection of venice from high tides.

NASA (2022). *Projected Sea-Level Rise Under Different SSP Scenarios.* Sea Level Projection Tool.

Nauels, A., Gütschow, J., Mengel, M., and Schleussner, C.-F. (2019). *Attributing long-term sea-level rise to Paris Agreement emission pledges.* PROCEEDINGS OF THE NATIONAL ACADEMY OF SCIENCES Vol. 116 — No. 47.

O'Neill, A. (2023). *Inflation rate in EU and Euro area 2027.* Statista.

Renard, B. et al. (2016). Non-stationary extreme value analysis for design of river flood defenses. *Water Resources Research.*

Rogelj, J., Pop, A., Calvin, K. V., Luderer, G., and et al. (2018). *Scenarios towards limiting global mean temperature increase below 1.5 °C.* Nature Climate Change volume 8, pages 325–332.

Rosner, A., Vogel, R. M., and Kirshen, P. H. (2014). *A risk-based approach, to flood management decisions in a nonstationary world.* Water Resour.Res., 50, 1928–1942.

Schlumberger, J., Ferrarin, C., Jonkman, S. N., Loaiza, M. A. D., Antonini, A., and Fatorić, S. (2022). *Developing a framework for the assessment of current and future flood risk in Venice, Italy.* Nat. Hazards Earth Syst. Sci., 22, 2381–2400.

Teatini, P., Ferronato, M., Gambolati, G., Baù, D., and Putti, M. (2010). *Anthropogenic Venice uplift by seawater pumping into a heterogeneous aquifer system.* Water Resources Research, Volume 46, Issue 11.

Umgiesser, G. (2020). *The impact of operating the mobile barriers in Venice (MOSE) under climate change.* Journal for Nature Conservation, Volume 54.

Umgiesser, G. and Matticchio, B. (2006). *Simulating the mobile barrier (MOSE) operation in the Venice Lagoon, Italy: global sea level rise and its implication for navigation.* Ocean Dynamics volume 56, pages320–332.

Vergano, L., Umgiesser, G., and Nunes, P. A. (2010). *An economic assessment of the impacts of the MOSE barriers on Venice port activities.* Transportation Research Part D.

Zanchettin, D., Bruni, S., Raicich, F., Lionello, P., Adloff, F., Androsov, A., Antonioli, F., Artale, V., Carminati, E., Ferrarin, C., Fofonova, V., Nicholls, R. J., Rubinetti, S., Rubino, A., Sannino, G., Spada, G., Thiéblemon, R., Tsimplis, M., Umgiesser, G., Vignudelli, S., Wöppelmann, G., and Zerbini, S. (2021). *Sea-level rise in Venice: historic and future trends (review article).* Nat. Hazards Earth Syst. Sci., 21, 2643–2678.

A MOSE barrier closure decision process

If this forecast exceeds 100 cm + ZMPS, a process called potential flood monitoring begins. The forecast is then improved by adding different parameters, such as wind, rain, and river discharge predictions (Cavallaro et al., 2017). Six hours before the 100 cm + ZMPS threshold is expected to be exceeded, a prediction is made for the first time. If the expected maximum water level exceeds 150 cm + ZMPS, the closure immediately starts when the water level in the city is measured to be 55 cm + ZMPS. If such a high water level is not expected, the decision to close is based on the combination of wind and rainfall. These combinations lead to a different action threshold that lies between 65 and 100 cm + ZMPS. When this level is measured, the barrier starts closing (Umgiesser and Matticchio, 2006). A diagram of different wind and rain situations leading to different closure levels is shown in Figure A.1.

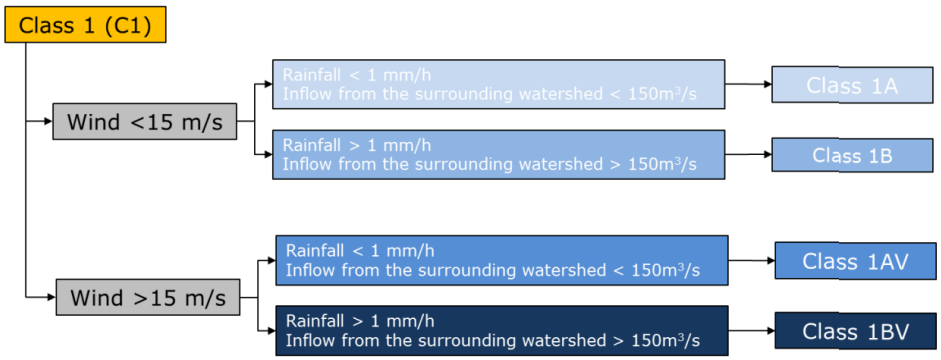

Figure A.1: Different wind and rain scenarios for the different classes (Cavallaro et al., 2017)

The closing water levels per class are (Cavallaro et al., 2017):
1.00 m MZPS (Mareographic Reference of Punta della Salute) for the C1-1A class
0.90 m MZPS for the C1-1B class
0.80 m MZPS for the C1-1AV class
0.75 m MZPS for the C1-1BV class

The safeguarding level is always set at 110 cm + ZMPS. However, the closure levels are set lower because it is expected that the water level will reach 110 cm + ZMPS under different wind and rainfall situations for the different classes.

B Peak over Threshold method

A peak over threshold method allows for multiple extreme points in one year. In theory this leads to a more precise fit of an EVA distribution. The data is detrended for annual means. After the detrending the data is analysed through a mean residual plot Figure B.1a. The mean excess should have linear behaviour for higher thresholds than the selected threshold since the distribution will be applied to the values higher than the threshold. The threshold should be as low as possible to allow for more data points and thus less variance.

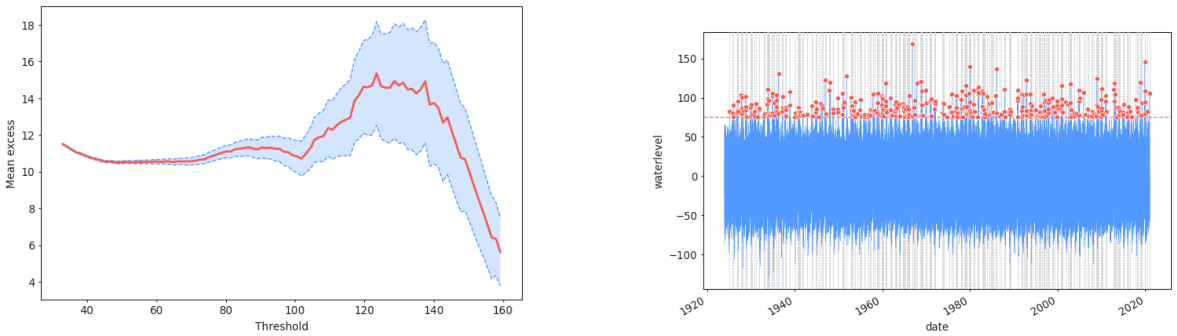

(a) Mean residual plot water levels

(b) Peaks over a threshold of 75 cm

Figure B.1: Peak over threshold

Higher thresholds values have only got a few excesses leading to irregular behaviour in the plot. From a threshold of 75cm, there is linear behaviour in the plot. 75 cm is therefore a good threshold. The next step is finding the water levels that exceed this value. When a high-water event occurs, the water level will rise and fall. The analyses will only need the peak of every excess. The peaks are found by deciding on a minimum time spacing between the exceedances of the threshold. In this way, the high-water level events can be considered unique. The time spacing chosen is 72 hours. This time spacing has been used for Venice in the past (Lionello, 2005). The isolated peaks are shown in Figure B.1b. There are 408 extremes. This is more than the 97 annual maxima and could therefore produce a better fit in the EVA. Pareto function:

$$H(y) = 1 - \left[1 + \frac{X - \mu}{\sigma}\right]^{-1/\xi}$$

In this function, μ is the threshold selected. X can only consist of water levels higher than the threshold and are the exceedances.

The summarised results from the Pareto fit are found in Figure B.2.

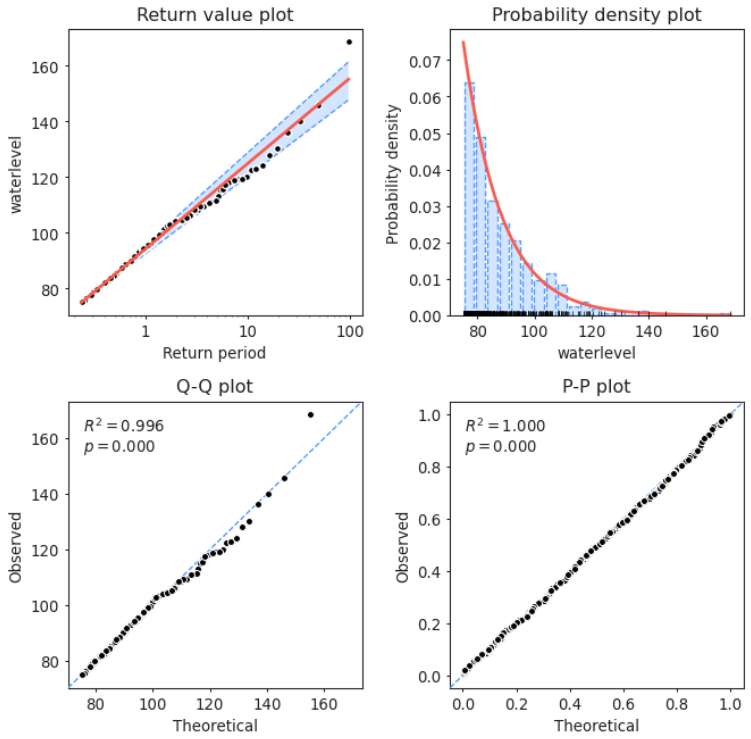

Figure B.2: Peak over threshold Pareto distribution fit results

To create randomness in the number of closures per year, a GP distribution is fitted to the annual maxima after which the the extremes can be regenerated from the distribution. Doing this a 1000 times leads to a 1000 different number of closures for every level of SLR. The issue with this method is the ideal threshold being close to the closure safe guarding level (ideal threshold is around a 100cm, safe guarding level is 110cm) and the selected threshold has major influence for the number of closures. The extremes were fitted for different thresholds, the results from this fit are displayed in Figures B.3 to B.6. The resulting number of closures differ for every threshold, leading to the conclusion that creating randomness in this way is very unreliable and threshold selection depended. An extra problem is the threshold needing to be raised by the same amount as the water levels when different SLR scenarios want to be explored.

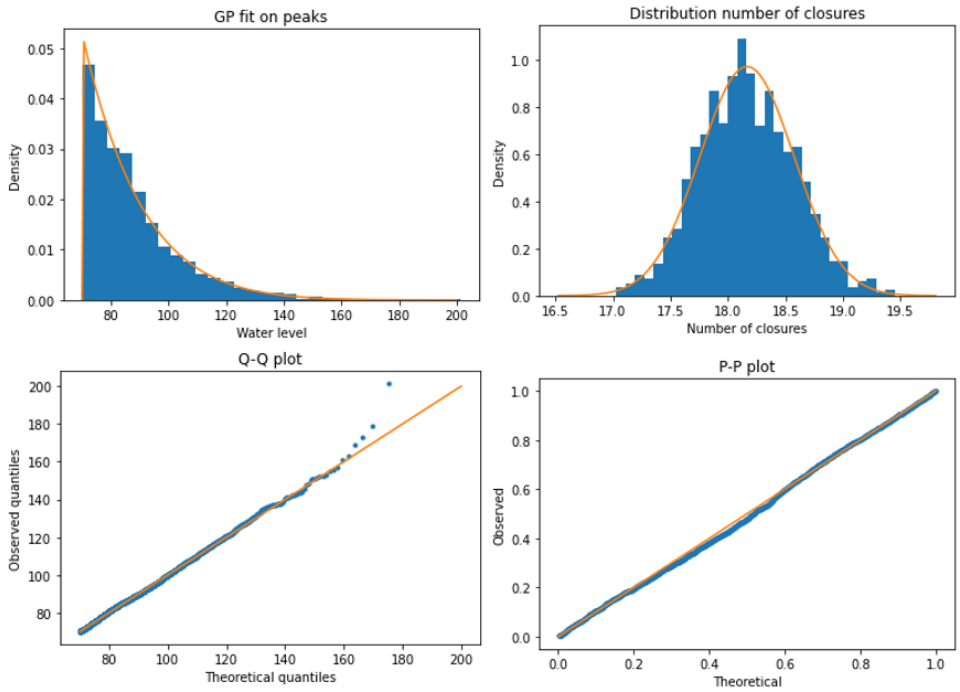

Figure B.3: Peak over 70cm threshold Pareto distribution fit results

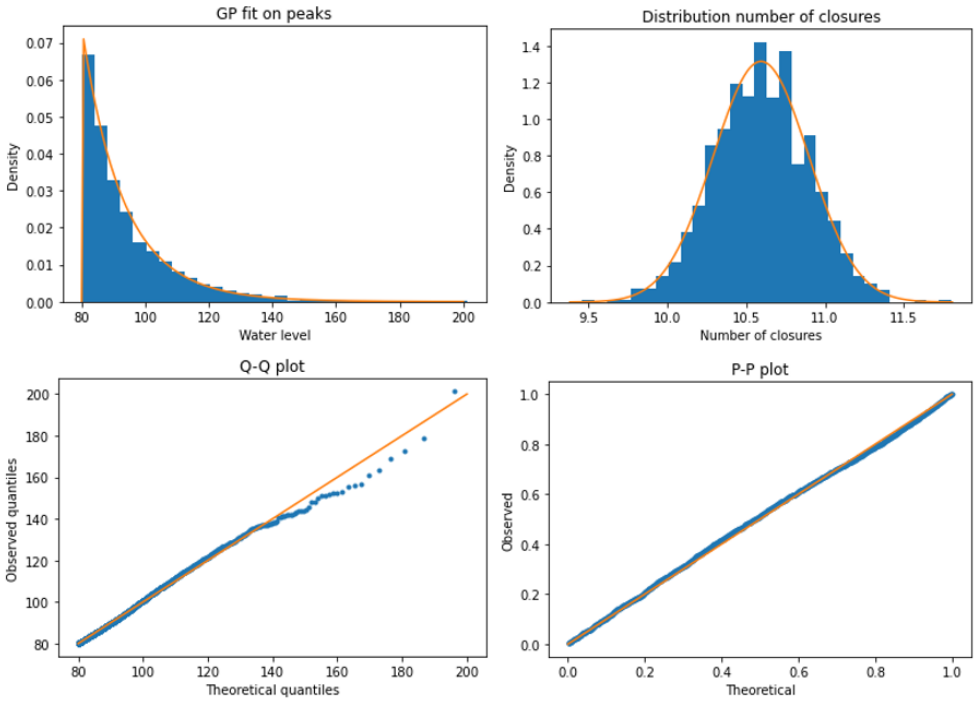

Figure B.4: Peak over 80cm threshold Pareto distribution fit results

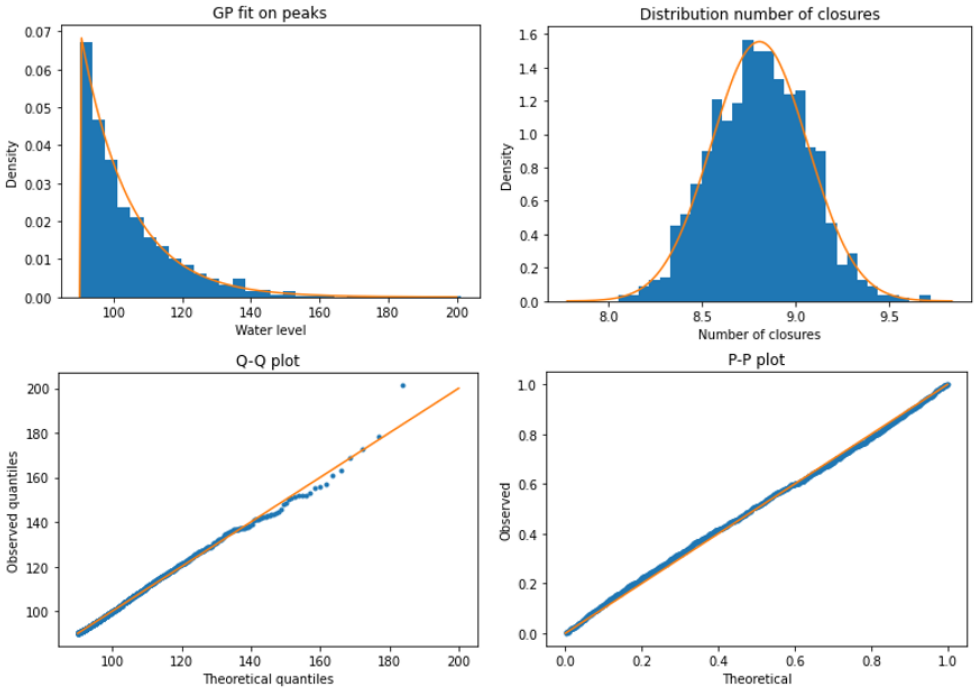

Figure B.5: Peak over 90cm threshold Pareto distribution fit results

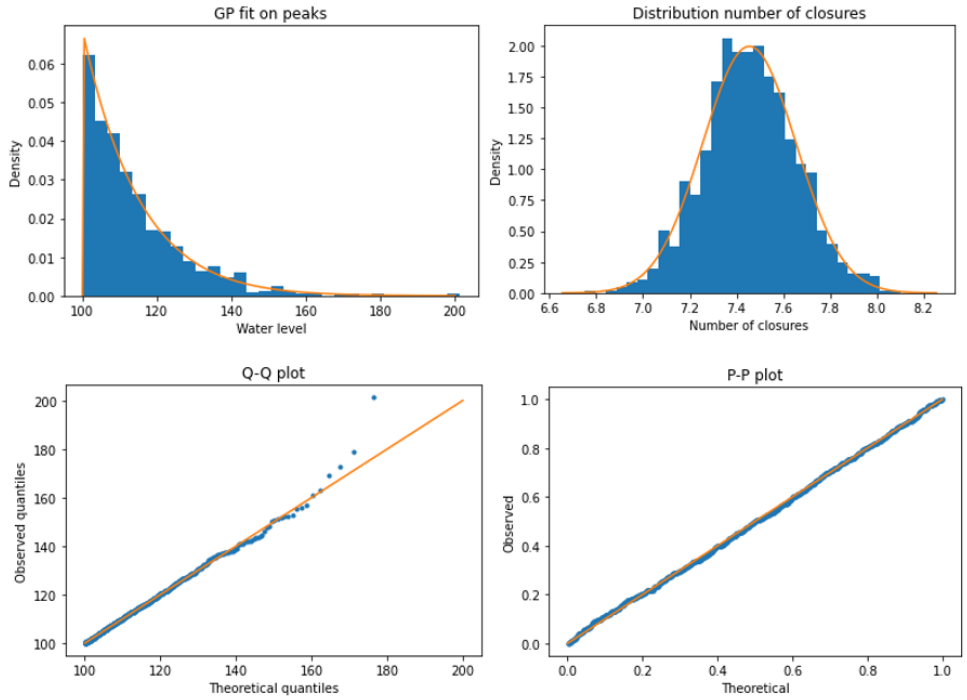

Figure B.6: Peak over 100cm threshold Pareto distribution fit results

C INSYDE Model

Table S6: Parameters to describe the flood characteristics

	explanation	used value
he	water depth $[m]$	D3DFM result
v	velocity $[m/s]$	$0.3\frac{m}{s}$
s	sediment concentration [-]	0.05
d	flood duration [h]	2
q	presence of pollutants	yes

Figure C.1: Input parameters used in the INSYDE model

Table S5: Parameters to describe the exposed building types in the study area. BEA: 'building with economic activity on ground floor'.

	explanation	used default values	
		residential	BEA
FA	Footprint area $[m^2]$	cadastral data	
IA	Internal area $[m]$	$0.9 * FA$	
BA	Basement area $[m^2]$	0	
EP	External perimeter $[m]$	cadastral data	
IP	Internal perimeter $[m]$	2.5 * EP	1.5 * EP
IH	Interstorey height $[m]$	$3.5m$	
BH	Basement height $[m]$	0	
BP	Basement perimeter $[m]$	0	
GL	Groundfloor level $[m]$	0.1 m	0.0 m
NF	Number of floors	1	
BT	Building type	4	5
BS	Building structure	Census data	
PD	Plant distribution	1- Centralized	
PT	Heating system type	1- Radiator	
FL	Finishing Level	1- medium	
YY	Year of construction	Census data	
LM	Level of maintenance	Census data	
additional			
EP_{eff}	effective external perimeter	Cadastral data	
SH	surface elevation of building	City of Venice [10]	
CH	Cultural heritage status	Cultural Heritage office Venice	

Figure C.2: Definition of different parameters used in the model

```
# Unit prices are expressed in €/...
UnitPrice

# Clean-up
pumping           2.58   #m3
disposal          36.15  #m3
cleaning          2.48   #m2
dehumidification  5.2    #m3

# Removal
screedremoval        12.18  #m2
parquetremoval       6.40   #m2 (parquet)
pavementremoval      12.50  #m2 (ceramic)
baseboardremoval     0.65   #m
partitionsremoval    15.39  #m2
plasterboardremoval  12.18  #m2
extplasterremoval    7.33   #m2
intplasterremoval    7.33   #m2
doorsremoval         21.76  #m2
windowsremoval       21.76  #m2
boilerremoval        0.26   #m2

# Non-structural
partitionsreplace    69.41  #m2
screedreplace        19.31  #m2
plasterboardreplace  47.00  #m2

# Structural
soilconsolidation   299.55  #m3
localrepair         38.73   #m2
pillarretrofitting  330.54  #m2

# Finishing
extplasterreplace  28.4   #m2
intplasterreplace  26.1   #m2
extpainting        10.63   #m2
intpainting        8.37    #m2
pavementreplace    46.48   #m2 (ceramic)
parquetreplace     116.72  #m2 (parquet)
baseboardreplace   2.48    #m

# Windows and doors
doorsreplace    201.42  #m2
windowsreplace  277.34  #m2

# Building systems
boilerreplace             18.38 #m2
radiatorpaint             64.04 #n
underfloorheatingreplace  74.37 #m2
electricalsystreplace     44.31 #m2
plumbingsystreplace       29.85 #m2
```

Figure C.3: Unit costs for calculating the damages

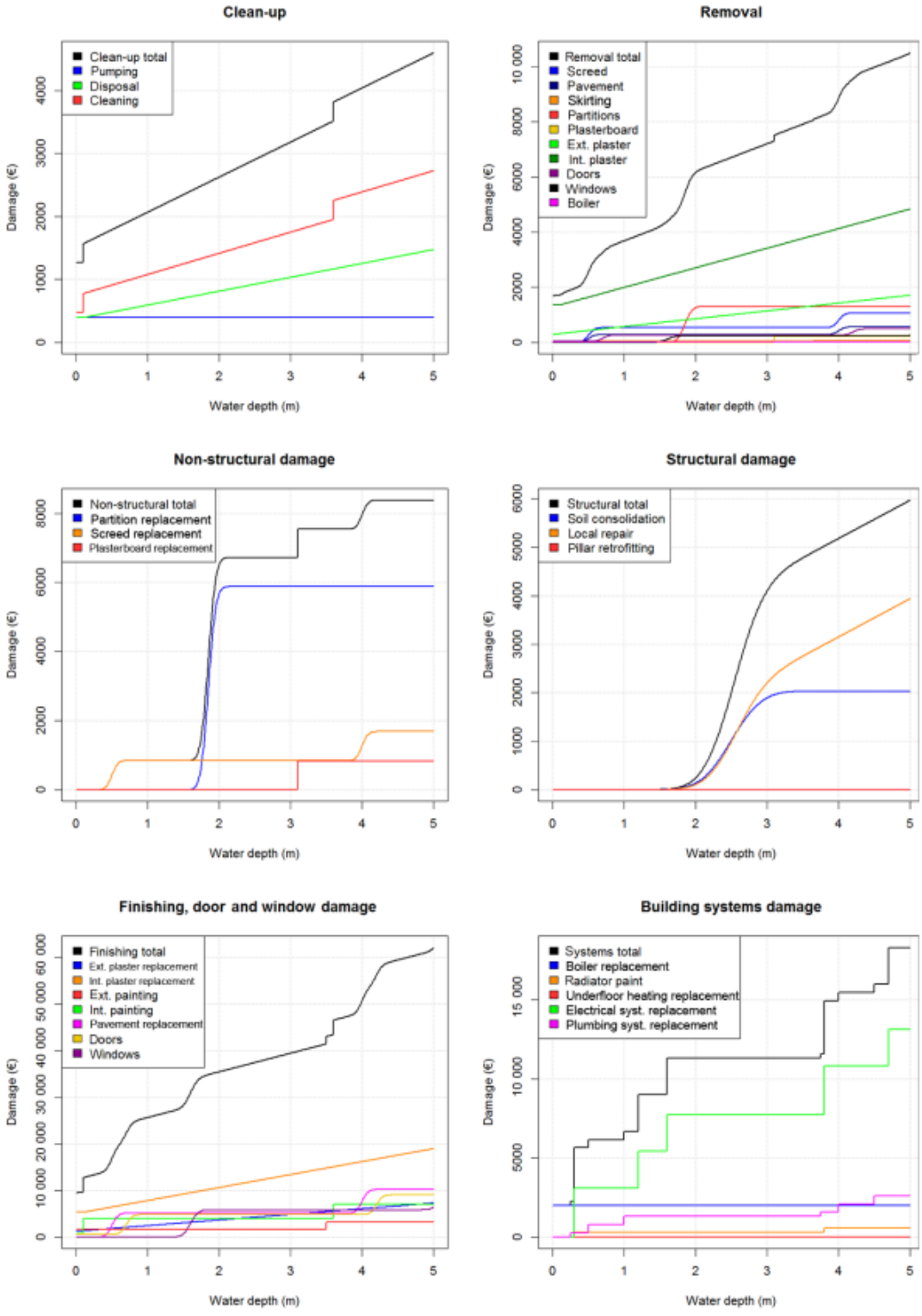

Figure C.4: Fragility functions for the different damage components

D Analyses of raw data

The data used in the analysis is originally measured data at the gauge station in Venice, which was then extrapolated to have water level data for every 15 minutes. The effect of this process was checked after it was found that the results of the Transformed Stationary (TS) method had a jump in the data.

The number of actual measurements is shown in Figure D.1. There is a jump in the frequency of measurements in the year 1983. Although Figure D.2 displays a decrease in standard error, the filled-up data has a higher standard deviation after 1983. The reason why the standard error of the raw data is lower is due to the number of observations. The standard deviation is smaller when the number of data points is large. After filling up the raw data, the number of data points is the same for all years. The data after 1983 has a higher standard deviation since it is more scattered due to the higher number of raw data points. This higher standard deviation causes the return levels to be larger when using the TS method.

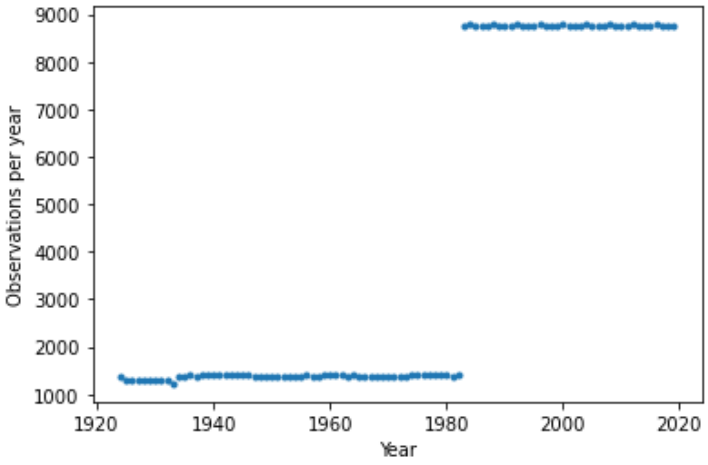

Figure D.1: Number of observations per year

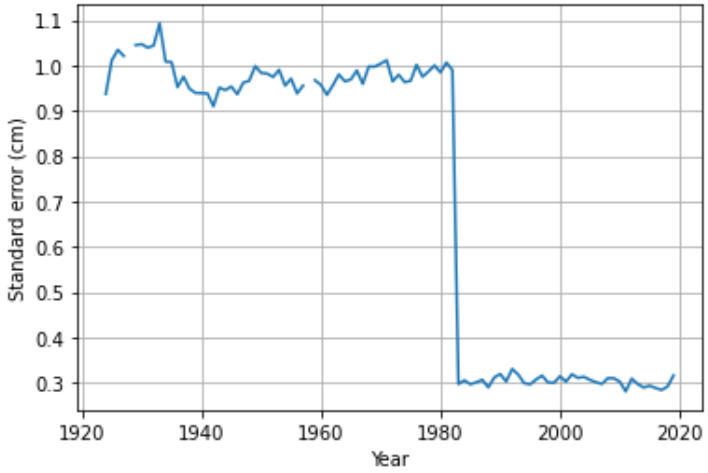

Figure D.2: Standard Error over the years

E Python Code

```python
#%%
import numpy as np
import matplotlib.pyplot as plt
import pandas as pd
from scipy.signal import find_peaks
#%% Data Loading

data = pd.read_csv('out.csv')
dta = pd.read_csv('DataVenicePuntaSaluteFinal.txt', header=None, skipinitialspace=True, delim_whitespace=True, parse_dates=True)
dta.columns = ["number", "year", "month", "day", "hour", "minute", "second", "waterlevel"]
dates = pd.to_datetime(dta[['year', 'month', 'day', 'hour', 'minute', 'second']])
dates = pd.DataFrame(dates)
dates['waterlevel'] = data['waterlevel']
dates.columns = ["date", "waterlevel"]
dates2 = dates
dates = dates.set_index('date')

series = dates.squeeze()
series = series.sort_index(ascending=True)
series = series.loc[pd.to_datetime("1924"):pd.to_datetime("2020")]
series = series + 32.74
#%% SELECTION TOOL - FUNCTIONS

def closures(closures2050,closures2100):
    riselvls = np.linspace(0,closures2050,30)
    counts2050 = np.zeros(len(riselvls))
    for i in range(len(riselvls)):
        series = dates.squeeze()
        series = series.sort_index(ascending=True)
        series = series.loc[pd.to_datetime("1924"):pd.to_datetime("2020")]
        series = series + 32.74 + riselvls[i]
        peaks,_ = find_peaks(series,height=110,distance=192)
        counts2050[i] = len(peaks)/96
    riselvls = np.linspace(closures2050+((closures2100-closures2050)/51),closures2100,51)
    counts2100 = np.zeros(len(riselvls))
    for i in range(len(riselvls)):
        series = dates.squeeze()
        series = series.sort_index(ascending=True)
        series = series.loc[pd.to_datetime("1924"):pd.to_datetime("2020")]
        series = series + 32.74 + riselvls[i]
        peaks,_ = find_peaks(series,height=110,distance=192)
        counts2100[i] = len(peaks)/96
    closuresoveryears = np.concatenate((counts2050,counts2100))
    return closuresoveryears

def closures30(closures2050,closures2100):
    riselvls = np.linspace(0,closures2050,30)
    counts2050 = np.zeros(len(riselvls))
    for i in range(len(riselvls)):
        series = dates.squeeze()
        series = series.sort_index(ascending=True)
        series = series.loc[pd.to_datetime("1924"):pd.to_datetime("2020")]
        series = series + 32.74 + riselvls[i]
        peaks,_ = find_peaks(series,height=140,distance=192)
        counts2050[i] = len(peaks)/96
```

```
    riselvls = np.linspace(closures2050+((closures2100-closures2050)/51),closures2100,51)
    counts2100 = np.zeros(len(riselvls))
    for i in range(len(riselvls)):
        series = dates.squeeze()
        series = series.sort_index(ascending=True)
        series = series.loc[pd.to_datetime("1924"):pd.to_datetime("2020")]
        series = series + 32.74 + riselvls[i]
        peaks,_ = find_peaks(series,height=140,distance=192)
        counts2100[i] = len(peaks)/96
    closuresoveryears = np.concatenate((counts2050,counts2100))
    return closuresoveryears

def damage(clos,clos30,adapt,yearofadapt,coc):
    years=np.linspace(2020,2100,81)
    costclosure = 1
    damageperyear = np.zeros(81)
    cumdamage = 0
    cumdamageperyear = np.zeros(81)
    if adapt == 0:
        for i in range(len(years)):
            damageperyear[i] = costclosure * clos[i] * (1+i * coc)
            cumdamage += damageperyear[i]
            cumdamageperyear[i] = cumdamage
    if adapt == 1:
        for j in range(len(years)):
            if yearofadapt == years[j]:
                for k in range(len(years)):
                    if k <= j:
                        damageperyear[k] = costclosure * clos[k] * (1+k * coc)
                        cumdamage += damageperyear[k]
                        cumdamageperyear[k] = cumdamage
                    elif k > j and k < j+11:
                        damageperyear[k] = (costclosure * (clos[k] -
                        ((clos[j+11] - clos30[j+11]) / 11) * (k-j))) * (1+k * coc)
                        cumdamage += damageperyear[k]
                        cumdamageperyear[k] = cumdamage
                    else:
                        damageperyear[k] = costclosure * clos30[k] * (1+k * coc)
                        cumdamage += damageperyear[k]
                        cumdamageperyear[k] = cumdamage
    return cumdamageperyear

def closureplot(clos,clos30,adapt,yearofadapt):
    years=np.linspace(2020,2100,81)
    closureplotperyear = np.zeros(81)
    if adapt == 0:
        for i in range(len(years)):
            closureplotperyear[i] = clos[i]
    if adapt == 1:
        for j in range(len(years)):
            if yearofadapt == years[j]:
                for k in range(len(years)):
                    if k <= j:
                        closureplotperyear[k] = clos[k]
```

```
                    elif k > j and k < j+11:
                        closureplotperyear[k] = (clos[k] -
                        ((clos[j+11] - clos30[j+11]) / 11) * (k-j))
                    else:
                        closureplotperyear[k] = clos30[k]
    return closureplotperyear
#%% SELECTION TOOL - REGRET FUNCTIONS

def regret(adaptationbudget,sealevelrise2050,sealevelrise2100,adapt,yearofadapt,alpha,beta,coc):
    if adapt == 0:
        regrets = (damage(sealevelrise2050, sealevelrise2100, 0, yearofadapt,coc) - damage(sealevelrise2050,sealevelrise2100,1,yearofadapt,coc)
        - adaptationbudget) * beta
    else:
        regrets = (adaptationbudget + damage(sealevelrise2050,sealevelrise2100,1,yearofadapt,coc)
       - damage(sealevelrise2050,sealevelrise2100,0,yearofadapt,coc)) * alpha
    return regrets

def regretCI(adaptationbudget,slvrise2050min95,slvrise2100min95,sealevelrise2050,sealevelrise2100,adapt,yearofadapt,alpha,beta,coc):
    if adapt == 0:
        regrets = (damage(sealevelrise2050, sealevelrise2100, 0, yearofadapt,coc) - damage(slvrise2050min95,slvrise2100min95,1,yearofadapt,coc)
        - adaptationbudget) * beta
    else:
        regrets = (adaptationbudget + damage(sealevelrise2050,sealevelrise2100,1,yearofadapt,coc)
       - damage(slvrise2050min95,slvrise2100min95,0,yearofadapt,coc)) * alpha
    return regrets
#%% SELECTION TOOL - PLOTTER

def plotter():
    #Sea level rise in 2050:
    #Assumed increase:
    slvrise2050s1 = 10.2
    #Baselevel:
    slvrise2050s2 = 7.14

    #Sea level rise in 2100:
    #Assumed incease:
    slvrise2100s1 = 27.2
    #Baselevel:
    slvrise2100s2 = 19

    #Error probabilities:
    #Type I error (alpha):
    alpha = 1
    #Type II error (Beta):
    beta = 1

    #Year of adaptation:
    yearofadapts1 = 2060

    #Cost of closure:
    coc = 0

    #Adaptation budget:
    adaptationbudgets1 = 300

```

```
    #Print money saved:
    printmonsav = 1

    #Print CI:
    printci = 0

    #randomnnumbers:
    rand = 0

    #Inflation:
    inf = 0

    #Calculating interval coc:
    if inf == 1:
        coc = 0.02
        cocmin95 = 0.01 #- coc*0.3*1.35
        cocplus95 = 0.04 #+ coc*0.3*1.35
    elif inf == 0:
        coc = 0.0
        cocmin95 = 0.0 #- coc*0.3*1.35
        cocplus95 = 0.0 #+ coc*0.3*1.35

    cl = closures(slvrise2050s1,slvrise2100s1)
    cl30 = closures30(slvrise2050s1,slvrise2100s1)
    cls2 = closures(slvrise2050s2,slvrise2100s2)
    cl30s2 = closures30(slvrise2050s2,slvrise2100s2)

    clos = cl
    clos30 = cl30
    closs2 = cls2
    clos30s2 = cl30s2

    if rand == 1:
        closm95 = cl[1]
        closp95 = cl[2]
        closm95s2 = cls2[1]
        closp95s2 = cls2[2]
        closm9530 = cl30[1]
        closp9530 = cl30[2]
        closm95s230 = cl30s2[1]
        closp95s230 = cl30s2[2]
    elif rand == 0:
        closm95 = cl[0]
        closp95 = cl[0]
        closm95s2 = cls2[0]
        closp95s2 = cls2[0]
        closm9530 = cl30[0]
        closp9530 = cl30[0]
        closm95s230 = cl30s2[0]
        closp95s230 = cl30s2[0]

    years=np.linspace(2020,2100,81)

    plt.figure('closuresperyear')
    plt.plot(years,closureplot(clos,clos30,0,yearofadapts1),label='No adapation')
```

```
    output = pd.DataFrame(closureplot(clos,clos30,0,yearofadapts1))
    output.to_csv('oldmethod_output.csv',index=False, index_label=None, header=False)
    if printci == 1:
        plt.plot(years,closureplot(closm95,closm9530,0,yearofadapts1),'--',color='tab:blue')
        plt.plot(years,closureplot(closp95,closp9530,0,yearofadapts1),'--',color='tab:blue')
        plt.fill_between(years,closureplot(closm95,closm9530,0,yearofadapts1),
                         closureplot(closp95,closp9530,0,yearofadapts1),alpha=0.4,label='Confidence bound')
    plt.plot(years,closureplot(clos,clos30,1,yearofadapts1),label='Adaptation done in year: '+ str(yearofadapts1))
    if printci == 1:
        plt.plot(years,closureplot(closm95,closm9530,1,yearofadapts1),'--',color='tab:orange')
        plt.plot(years,closureplot(closp95,closp9530,1,yearofadapts1),'--',color='tab:orange')
        plt.fill_between(years,closureplot(closm95,closm9530,1,yearofadapts1),
                         closureplot(closp95,closp9530,1,yearofadapts1),alpha=0.4,label='Confidence bound')
    plt.plot(yearofadapts1,closureplot(clos,clos30,0,yearofadapts1)[yearofadapts1-2020],'o',color='tab:red')
    plt.xlabel('Year')
    plt.ylabel('Number of closures per year')
    plt.title('Closures for sea level rise 2050: '+ str(slvrise2050s1) + 'cm in 2100: '+ str(slvrise2100s1) + 'cm')
    plt.legend()

    plt.figure('Damages')
    plt.plot(years,damage(clos,clos30,0,yearofadapts1,coc),label='No adapation')
    if printci == 1:
        plt.plot(years,damage(closm95,closm9530,0,yearofadapts1,cocmin95),'--',color='tab:blue')
        plt.plot(years,damage(closp95,closp9530,0,yearofadapts1,cocplus95),'--',color='tab:blue')
        plt.fill_between(years,damage(closm95,closm9530,0,yearofadapts1,cocmin95),
                         damage(closp95,closp9530,0,yearofadapts1,cocplus95),alpha=0.4,label='Confidence bound')
    plt.plot(years,damage(clos,clos30,1,yearofadapts1,coc),label='Adaptation done in year: '+ str(yearofadapts1))
    if printci == 1:
        plt.plot(years,damage(closm95,closm9530,1,yearofadapts1,cocmin95),'--',color='tab:orange')
        plt.plot(years,damage(closp95,closp9530,1,yearofadapts1,cocplus95),'--',color='tab:orange')
        plt.fill_between(years,damage(closm95,closm9530,1,yearofadapts1,cocmin95),
                         damage(closp95,closp9530,1,yearofadapts1,cocplus95),alpha=0.4,label='Confidence bound')
    plt.plot(yearofadapts1,damage(clos,clos30,0,yearofadapts1,coc)[yearofadapts1-2020],'o',color='tab:red')
    plt.xlabel('Year')
    plt.ylabel('Cumulative Damage (x million €)')
    plt.title('Damages for sea level rise 2050: '+ str(slvrise2050s1) + 'cm in 2100: '+ str(slvrise2100s1) + 'cm')

    #Money saved through adaptation
    if printmonsav == 1:
        yearadap = np.linspace(2020,2100,81)
        dam0=damage(clos,clos30,0,yearofadapts1,coc)
        dam1=damage(clos,clos30,1,yearofadapts1,coc)
        moneylost = np.zeros(len(yearadap))
        for i in range(len(yearadap)):
            moneylost[i] = dam0[i] - dam1[i]
        plt.plot(yearadap,moneylost,'--',color='tab:green',label='Money saved by adapting')
    plt.legend()

    plt.figure('Regrets')
    plt.plot(years,regret(adaptationbudgets1,clos,clos30,0,yearofadapts1,alpha,beta,coc),label= 'No adaptation')
    if printci == 1:
        plt.plot(years,regretCI(adaptationbudgets1,closp95,closp9530,closm95,closm9530,0,yearofadapts1,alpha,beta,cocmin95),'--',color='tab:blue')
        plt.plot(years,regretCI(adaptationbudgets1,closm95,closm9530,closp95,closp9530,0,yearofadapts1,alpha,beta,cocplus95),'--',color='tab:blue')
        plt.fill_between(years,regretCI(adaptationbudgets1,closp95,closp9530,closm95,closm9530,0,yearofadapts1,alpha,beta,cocmin95),
                         regretCI(adaptationbudgets1,closm95,closm9530,closp95,closp9530,0,yearofadapts1,alpha,beta,cocplus95),
                         alpha=0.4,label='Confidence bound')
    plt.plot(years,regret(adaptationbudgets1,closs2,clos30s2,1,yearofadapts1,alpha,beta,coc),
             label='With adaptation done in year: '+ str(yearofadapts1))
    if printci == 1:
        plt.plot(years,regretCI(adaptationbudgets1,closp95s2,closp95s230,closm95s2,closm95s230,1,yearofadapts1,alpha,beta,cocmin95),
                 '--',color='tab:orange')
        plt.plot(years,regretCI(adaptationbudgets1,closm95s2,closm95s230,closp95s2,closp95s230,1,yearofadapts1,alpha,beta,cocplus95),
                 '--',color='tab:orange')
        plt.fill_between(years,regretCI(adaptationbudgets1,closp95s2,closp95s230,closm95s2,closm95s230,1,yearofadapts1,alpha,beta,cocmin95),
                         regretCI(adaptationbudgets1,closm95s2,closm95s230,closp95s2,closp95s230,1,yearofadapts1,alpha,beta,cocplus95),
                         alpha=0.4,label='Confidence bound')
    plt.legend()
    plt.title('Regrets for adaptation choice')
    plt.xlabel('Year')
    plt.ylabel('Cumulative Regret (x million €)')
    plt.show()
    return
plotter()
```

F Q-Q and P-P plots

For the stationary GEV fit, the Q-Q and P-P plots are given in Figure F.1.

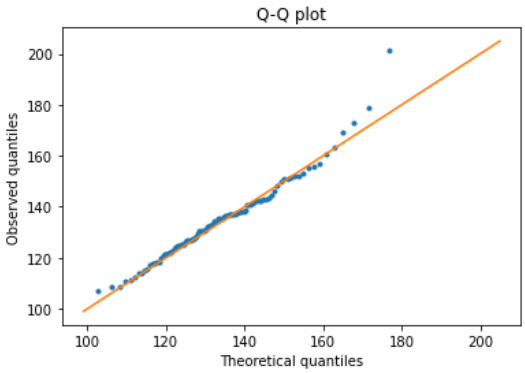

(a) Q-Q plot

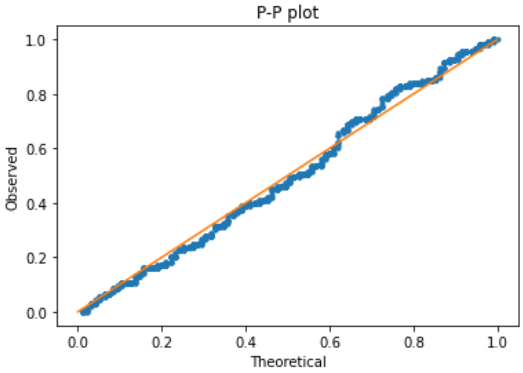

(b) P-P plot

Figure F.1